IDENTIFICATION AND CHARACTERIZATION OF *APP1*-ENCODED PHOSPHATIDATE PHOSPHATASE IN *SACCAROMYCES CEREVISIAE*

by

MINJUNG CHAE

A dissertation submitted to the

Graduate School-New Brunswick

Rutgers, the State University of New Jersey

in partial fulfillment of the requirements

for the degree of

Doctor of Philosophy

Graduate Program in Food Science

written under the direction of

Dr. George M. Carman

and approved by

_____

_____

_____

_____

_____

New Brunswick, New Jersey

January 2013

ABSTRACT OF THE DISSERTATION

Identification and Characterization of *APP1*-encoded Phosphatidate Phosphatase in *Saccharomyces cerevisiae*

By MINJUNG CHAE

Dissertation Director:
Dr. George M. Carman

Phosphatidate phosphatase (PAP) catalyzes the dephosphorylation of phosphatidate to yield diacylglycerol. In the yeast *Saccharomyces cerevisiae*, PAP activity is encoded by *PAH1*, *DPP1*, and *LPP1*. The presence of PAP activity in the *pah1*Δ *dpp1*Δ *lpp1*Δ triple mutant indicated another gene(s) encoding the enzyme. I purified PAP activity from the *pah1*Δ *dpp1*Δ *lpp1*Δ triple mutant by salt-extraction of mitochondria, followed by chromatography with DE52, Affi-Gel Blue, phenyl-Sepharose, MonoQ, and Superdex 200. Liquid chromatography/tandem mass spectrometry analysis of a PAP-enriched sample revealed multiple putative phosphatases. By analysis of PAP activity in mutants lacking each of the proteins, I found that *APP1*, a gene whose molecular function has been unknown, confers ~30 % PAP activity of wild type cells. The overexpression of *APP1* in the *pah1*Δ *dpp1*Δ *lpp1*Δ mutant exhibited a 10-fold increase in PAP activity. The PAP activity shown by App1p that was heterologously expressed in *Escherichia coli* confirmed that *APP1* is the structural gene for the enzyme. Introduction of the *app1*Δ mutation into the *pah1*Δ *dpp1*Δ *lpp1*Δ mutant resulted in a complete loss of PAP activity, indicating that the enzyme in *S. cerevisiae* is encoded by *APP1*, *PAH1*, *DPP1*, and *LPP1*.

Protein A-tagged App1p PAP was expressed and purified from *S. cerevisiae*. The App1p PAP activity followed saturation kinetics with respect to the molar concentration of phosphatidic acid (PA) (K_m = 0.5 mM) but followed positive cooperative (Hill number of ~2.3) kinetics with

respect to the surface concentration of PA (K_m = 2.0 mol %) in Triton X-100/PA mixed micelles. The App1p also exhibited lysoPA phosphatase and diacylglycerol pyrophosphate phosphatase activities. The order of substrate preference was phosphatidic acid> diacylglycerol pyrophosphate > lysoPA. The maximum PAP activity was dependent on Mg^{2+} ions at pH 7.5 at 30 ^{0}C. The activation energy for the reaction was 16.5 kcal/mol, and the enzyme was labile above 40 ^{0}C. The App1p PAP activity was inhibited by Ca^{2+}, Mn^{2+}, Zn^{2+}, *N*-ethylmaleimide, propranolol, nucleotides, diacylglycerol, phosphatidylethanolamine, phosphatidylcholine, and sphinganine, while lysoPA, cardiolipin, phosphatidylglycerol, phosphatidylserine, sphingosine and sphingosine 1-phosphate stimulated the activity. Lipid analysis of cells lacking the PAP genes, singly or in combination, showed that Pah1p is the only PAP involved in the synthesis of triacylglycerol as well as in the regulation of phospholipid synthesis. App1p, which shows interactions with endocytic proteins, may play a role in vesicular trafficking through its PAP activity.

ACKNOWLEDGEMENTS

Pursuing Ph. D. degree was an enduring process, not only training my knowledge and skills, but also reflecting on myself. I am delighted to finish a long journey with enormous efforts that I've never devoted before. I can't wait to explore a new stage of my life after all the work and experience that I have gained. There are many people I'd like to express my appreciation.

First, I want to deliver my sincere appreciation to my major advisor, Dr. George Carman, for providing the opportunity of pursuing Ph. D. degree and guiding me through my study with effort and patience. It was a great pleasure to work with him. I will always remember his passion for science. He made me strong and wise as a good mentor.

I'd like to thank the faculty, staff, and colleagues in the department of Food Science at Rutgers, who helped me by providing a great environment for research. Also, I want to express my appreciation to my committee members, Dr. Han, Dr. Chikindas, Dr. Quadro and Dr. Dixon for their time, comments and suggestions on my dissertation. Special thank goes to Dr. Han for guidance on all the experiments and also for performing the lipid analysis of all PAP mutants.

I am grateful to my present and former lab members, Hyeon-Son Choi, Anibal Soto, Jeanelle Morgan, Florencia Pascual, Wen-Min Su, Stylianos Fakas, Zhi Xu, Chris Konstantinou, Yeon-Hee Park, Yixuan Qiu, Lu-Sheng Hsieh, and Leticia Aquio. My daily life in the lab wasn't lonely because of them. They made my life rich and fun all the time.

Special thank to my friends. It was a pleasure to meet friends in New York all of whom I've known from Korea. Also, friends I've met here were other treasures I've gained during Ph. D. program. HeeSeung Nahm, who was my former classmate, insisted I mention her name on my thesis. My life in New Jersey was full of joy because of her.

Finally, Thanks to my father, mother, sister, and brother for endless support and encouragement throughout my journey. I am so happy I can finally settle down around them.

TABLE OF CONTENTS

LIST OF TABLES

LIST OF FIGURES

LIST OF ABBREVIATIONS

CDP-DAG	cytidine diphosphate diacylglycerol
CL	Cardiolipin
CMP	cytidine monophosphate
CTP	cytidine triphosphate
DAG	Diacylglycerol
DGK	diacylglycerol kinase
DGPP	diacylglycerol pyrophosphate
EDTA	ethylenediaminetetraacetic acid
ER	endoplasmic reticulum
GTP	guanosine triphosphate
HAD	haloacid dehalogenase
Ins	Inositol
kDa	kilo Daltons
LPA	lysoPA
LPP	lipid phosphate phosphatase
NEM	*N*-ethylmaleimide
PA	phosphatidic acid
PAP	phosphatidate phosphatase
PC	phosphatidylcholine
PE	phosphatidylethanolamine
PG	phosphatidylglycerol
PI	phosphatidylinositol

Pi	inorganic phosphate
PL	Phospholipid
proPr	propranolol
PS	phosphatidylserine
PVDF	polyvinylidene difluoride
SC	synthetic complete
SDS	sodium dodecyl sulfate
TAG	Triacylglycerol
TTP	thymidine triphosphate
UAS_{INO}	upstream activating sequence, inositol responsive element
UTP	uridine triphosphate

INTRODUCTION

Biological membranes are an essential component of cells (1). They consist of lipid bilayers where proteins are associated by noncovalent interactions to form a flexible and hydrophobic layer around the cell and their organelles (1). Cell membrane functions as selective barriers by protecting the cells from the external environment and maintaning the cell integrity (2, 3). Communications between cells through the transduction of molecular signals by proteins embedded on the cell surface are other important functions of membranes (2, 3). The budding yeast *Saccharomyces cerevisiae* has been extensively studied for cellular membranes because of its similarity to higher eukaryotes (4, 5, 6). Moreover, feasibility of genetic manipulation (recombination) was a strong advantage of using the yeast as a model organism (2, 7). Of course, another advantage of yeast is its ease of growth and short time of generation, thus allowing the isolation of large amounts of cells for biochemical studies (5, 8).

Phospholipids are the most abundant class of membrane lipids, and, therefore, intimately linked to cellular growth (1). Phospholipid functions as macromolecule precursors, protein-membrane associations, molecular chaperones and reservoirs of lipid signaling molecules (9, 10, 11, 4). The crucial roles of phospholipids in cells are highly conserved from bacteria to humans (5). Phospholipids are essential amphipathic molecules composed of a glycerol molecule, two fatty acyl chains, and a hydrophilic head group (2, 3). The most abundant phospholipid found in yeast membranes are PC, PE, PS, and PI (Fig. 1) (2, 5, 6, 10, 12, 13). These phospholipids contain the head groups choline, ethanolamine, serine, and inositol, which are attached to the phosphate group of the third carbon of the glycerol backbone (2, 3, 11). All phospholipids share a common structure, where the common fatty acids esterified to the glycerol backbone are palmitic acid (16:0), palmitoleic acid ($16{:}1\Delta^{9,10}$), stearic acid (18:0) and oleic acid ($18{:}1\Delta^{9,10}$) in yeast (10).

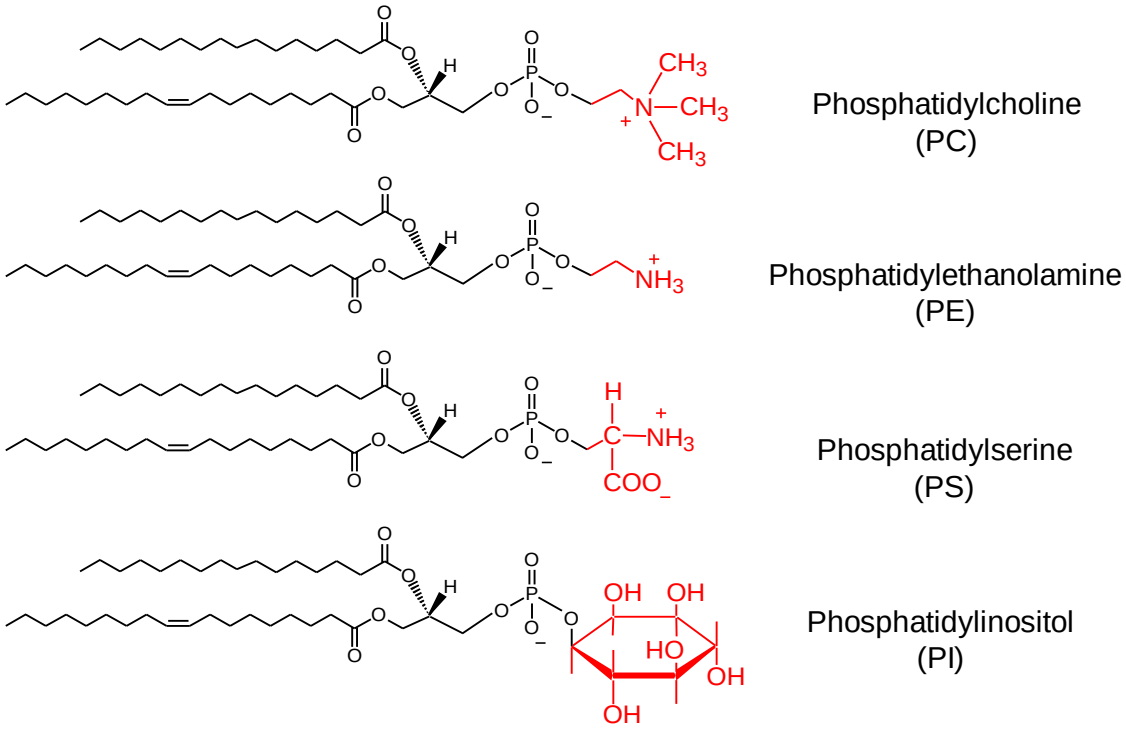

FIGURE 1. **Major Phospholipids in *S. cerevisiae.***

Phospholipid Biosynthetic Pathways

There are two pathways involved in the synthesis of the major phospholipid in yeast, the CDP-DAG pathway and the Kennedy pathway (Fig. 2) (10, 11). The major phospholipids PS, PE and PC are synthesized from PA via the CDP- DAG pathway (Fig. 2). In the CDP-DAG pathway, Cds1p CDP-DAG synthase catalyzes the formation of energy-rich intermediate CDP-DAG from PA and CTP (14, 15). The CMP in CDP-DAG is replaced by serine to form PS by Cho1p PS synthase (16-19). After decaboxylating reactions catalyzed by Psd1p and Psd2p PS decarboxylase, PS is converted to PE (16, 20-23). PC is finally synthesized through three sequential methylations of PE, catalyzed by the Pem1p/Cho2p PE methyltransferase and Pem2p/Opi3p phospholipid methyltransferase (24-27).

DAG generated from PA by the PAP reaction is utilized for the synthesis of PE and PC via the CDP-choline and CDP-ethanolamine branches of the Kennedy pathway (Fig. 2). Choline (28) and ethanolamine (29) are first phosphorylated by Cki1p choline kinase and Eki1p ethanolamine kinase to form PC and PE, respectively. These intermediates are activated by CTP to form CDP-choline and CDP-ethanolamine, which are catalyzed by Pct1p phosphocholine cytidyltransferases and Ect1p phosphoethanolamine cytidyltransferases, respectively (30, 31). The reactions of phospholipid synthesis in yeast are very similar to those in higher eukaryotes except the synthesis of PS. The PS is synthesized from CDP-DAG and serine in yeast, while, in higher eukaryotes, PS is formed via exchange reaction between PE and serine or PC or between PC and serine (32).

CDP-DAG is a key branch point in phospholipid biosynthesis (14, 15). The CDP-DAG pathway is used for the synthesis of PE and PC when yeast cells are grown in the absence of ethanolamine or choline, respectively (5, 12). When the cell is supplemented with exogenous choline and ethanolamine, PC and PE are primarily synthesized by the Kennedy pathway (5, 12).

FIGURE 2. **Phospholipid Biosynthesis in *S. cerevisiae*.** The CDP-DAG, CDP-choline, and CDP-ethanolamine pathways are shown for the synthesis of phospholipids, and include the relevant steps discussed throughout. The genes that are known to encode enzymes catalyzing individual steps in the lipid synthesis pathway are indicated. UAS_{INO}-containing genes that are subject to inositol regulation are highlighted in blue. P-Etn, phosphoethanolamine; P-Cho, phosphocholine. Taken from Carman and Han 2009 (33).

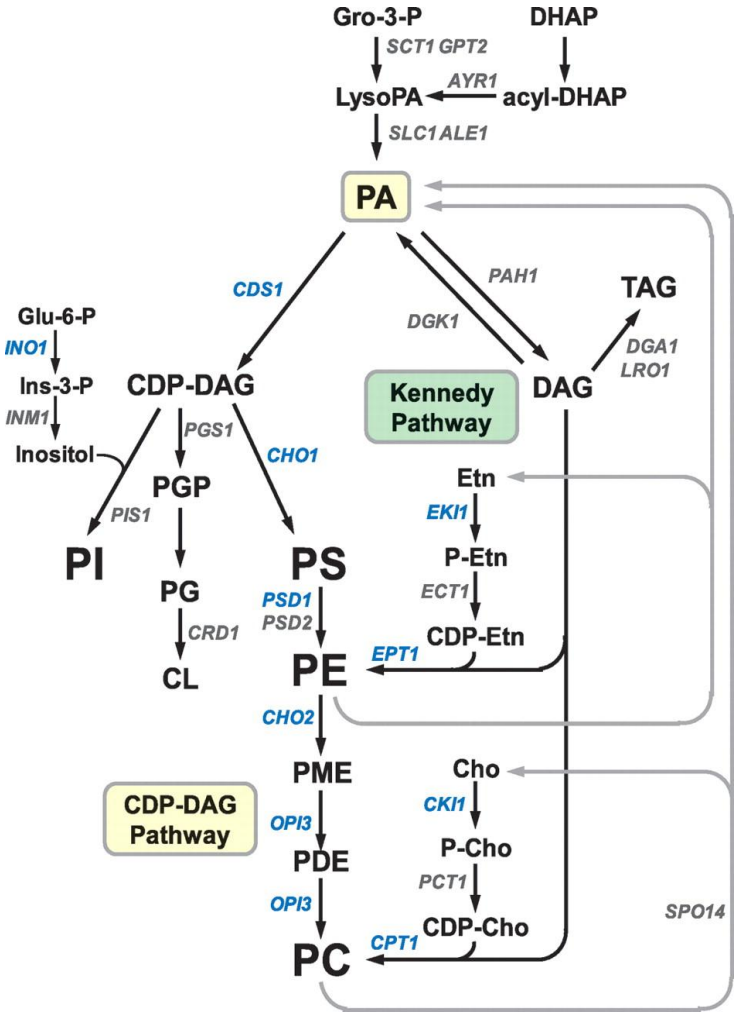
Gro-3-P
DHAP
SCT1 GPT2
AYR1
LysoPA
acyl-DHAP
SLC1 ALE1
PA
CDS1
PAH1
TAG
DGK1
DGA1
LRO1
Glu-6-P
INO1
Ins-3-P
CDP-DAG
Kennedy Pathway
DAG
INM1
PGS1
CHO1
Inositol
PGP
Etn
EKI1
PIS1
PI
PS
P-Etn
PG
PSD1
PSD2
ECT1
CRD1
CDP-Etn
EPT1
CL
PE
CHO2
PME
Cho
CDP-DAG Pathway
CKI1
OPI3
P-Cho
PDE
PCT1
OPI3
SPO14
CDP-Cho
CPT1
PC

However, the Kennedy pathway still can contribute to the synthesis of PE and PC in the absence of ethanolamine or choline, because they can be generated through the phospholipase D-mediated turnover of PE and PC synthesized via CDP-DAG (34-37). The Kennedy pathway shows a critical role in PC synthesis in mutants defective in enzymes involved in the CDP-DAG pathway (6, 12, 34, 38, 39). Mutants in this pathway require choline or ethanolamine for growth (38, 39). However, Kennedy pathway mutants do not exhibit any auxotrophic requirements, unlike mutants defective in the CDP-DAG pathway (21, 26, 27, 37).

CDP-DAG is also used for the synthesis of PI, PG and CL (Fig. 2) (6, 40). The CMP of CDP-DAG can be replaced by inositol to form PI by Pis1p PI synthase. The inositol used for the PI synthase is derived from glucose-6-phosphate, which is converted to inositol-3-phosphate by Ino1p inositol-3-phosphate synthase, and subsequently to inositol by Inm1p inositol phosphatase (11, 40-43). PG and CL are confined to the mitochondrial membranes (6, 40). The synthesis of CL is catalyzed by the Pgs1p PGP synthase, which synthesizes PGP by displacement of the CMP of CDP-DAG with glycerol-3-phosphate (44, 45). PGP is then dephosphorylated by PGP phosphatase to synthesize PG (39), which is further catalyzed by Crd1p CL synthase to form CL (1).

Importance of PAP in Yeast

PAP catalyzes the dephosphorylation of PA, yielding DAG and inorganic phosphate (Fig. 3) (12, 46, 47). PA is the simplest membrane phospholipid that serves as a central intermediate for the synthesis of membrane lipids and storage lipids (3, 48). PA is produced from glycerol-3-phosphate by two successive acyltransferase reactions, and also generated by the action of phospholipase D from PC (3, 49). PA serves as a precursor for the formation of CDP-DAG by CDP-DAG synthase and DAG by PAP (Fig. 3) (11).

FIGURE 3. **Roles of PAP in Lipid Synthesis.** The reaction catalyzed by the Pah1p PAP enzyme is highlighted and its roles in lipid synthesis depicted. Taken from Carman and Han 2008 (50).

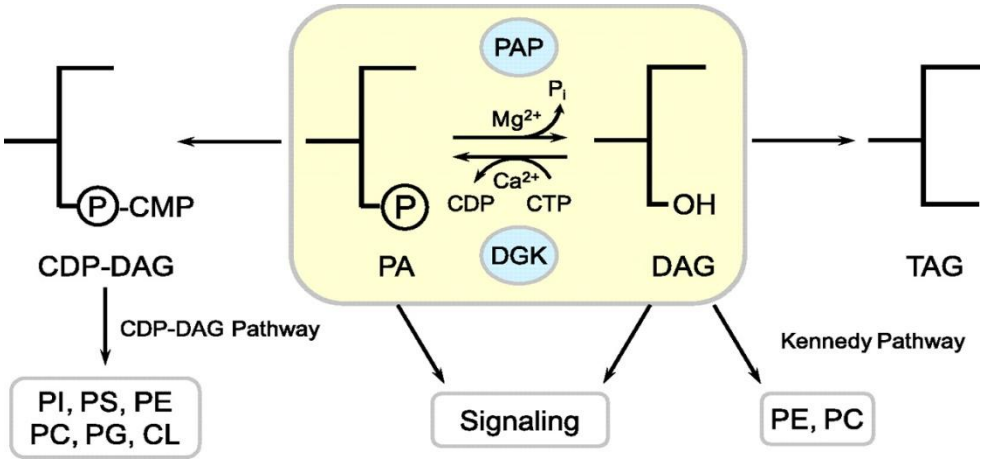
PAP
Pi
Mg2+
Ca2+
CDP CTP
DGK
P-CMP
CDP-DAG
P
PA
OH
DAG
TAG
CDP-DAG Pathway
Kennedy Pathway
PI, PS, PE
PC, PG, CL
Signaling
PE, PC

As discussed above, DAG is a precursor for membrane phospholipids such as PC and PE by the Kennedy pathway and it is also used to make TAG (28-32, 50, 51). In addition, CDP-DAG pathway also serves in the synthesis of all membrane phospholipids through the intermediate CDP-DAG (14, 15). Thus, regulation of PAP activity is important to determine whether the cells make storage lipids through DAG or phospholipids through CDP-DAG (50, 51).

PAP enzymes have roles in the generation or degradation of lipid signaling molecules in eukaryotic cells, as well as the synthesis of lipids (49-54). In the lipid signaling, PAP generates a pool of DAG used for protein kinase C activation (52-54). In addition, PAP activity can attenuate the signaling function of PA, which includes promoting cell growth and proliferation, vesicular trafficking, secretion and endocytosis (32, 50-53). In addition, PAP is involved in the transcriptional regulation of phospholipid synthesis (50, 51). Genetic and biochemical studies in yeast and mammalian cells have revealed PAP as a major regulator of lipid metabolism and cell physiology (33, 50, 51)

Importance of PA and DAG in Lipid Signaling on the Vesicle Formation

Although the bulk of cellular PA is synthesized via acylation pathways, PA is also generated via other types of lipid-modifying enzymes on a much faster time scale, which pathway serves to produce PA that functions in a signaling molecule controlling cell biological processes. There are two major families of enzymes involved in generation of PA during signaling events — Phospholipase D hydrolyzes PC to yield choline and PA, and DAG kinase (DGK) phosphorylates DAG to generate PA (55). Conversely, PA can be converted into DAG through dephosphorylation, via the action of PAP.

Both in yeast and in mammals, DAG is a simple and small sized signal-transducing lipid which is required for protein transport from the Golgi complex to the cell surface. DAG acts in the *trans*-Golgi network as a membrane acceptor for the protein kinase D, mediated by the

binding of its C1 domain (56). DAG also promotes the Golgi membrane targeting and activation of other C1 domain-containing signaling molecules such as other protein kinase C isoforms (57-59). The structure of DAG has a pronounced cone shape due to an electrically neutral polar head, explaining its capacity to undergo rapid transbilayer movement. Thus, DAG may induce membrane bending and facilitate the formation of highly curved membrane intermediates, thereby enhancing membrane constriction (60) and fusion (61). PA has special biophysical properties by providing a docking site for interfacial insertion of positively charged membrane protein domains (62, 63). Thus, a PA-DAG interconversion cycle could be crucial for final membrane constriction/fission of coated/noncoated transport vesicles.

Importance of PA Levels in Transcriptional Regulation of Phospholipid Synthesis

PAP is involved in the transcriptional regulation of phospholipid synthesis by controlling the PA levels on the nuclear/ER membrane (64). The UAS_{INO} element, which contains a 10 base pair consensus sequence (5'-CATGTGAAAT-3'), has been identified by sequence inspection of the promoter of several genes that are responsive to inositol and choline (5, 65). This sequence is known as inositol-sensitive upstream activating sequence (UAS_{INO}) or an inositol choline responsive element (ICRE). The regulation of phospholipid synthesis genes is dependent on the transcriptional regulatory proteins Ino2p, Ino4p, Opi1p, and UAS_{INO} elements present in the promoters of the phospholipid synthesis genes (Fig. 4) (66, 67). Ino2p-Ino4p heterodimer complex activates the transcription of phospholipid synthesis genes by binding to the UAS_{INO} elements (6, 10, 68). The first 6 bases of UAS_{INO} elements serves as the binding site of the Ino2p-Ino4p heterodimer, and substitution of these sites can completely eliminate or severely reduce the transcriptional activation (69, 70). The activation of transcription by Ino2p-Ino4p is repressed by Opi1p, which binds to Ino2p (Fig. 4) (64). Opi1p binds PA and the Scs2p protein at the nuclear/endoplasmic reticulum (ER) membrane, which block its repressor function in the nucleus

FIGURE 4**. Model for the Opi1p-Mediated Regulation of Phospholipid Biosynthetic Genes.** (A) In exponential phase and/or inositol depleted conditions under which the levels of PA are relatively high, the Opi1p repressor is tethered to the nuclear/ER membrane, and UAS_{INO}-containing genes are maximally expressed (boldface arrow) by the Ino2p-Ino4p activator complex. (Inset) Localization of Opi1p, fused with GFP at its C-terminal end and integrated into the chromosome, being expressed under its own promoter in live cells growing logarithmically in synthetic complete medium lacking inositol (−Ins) and analyzed by fluorescence microscopy. (B) In stationary phase and/or inositol supplementation under which the levels of PA are reduced, Opi1p dissociates from the nuclear/ER membrane, and enters into the nucleus where it binds to Ino2p and attenuates (thin arrow) transcriptional activation by the Ino2p–Ino4p complex. (Inset) Localization of Opi1p, as described in A, except that the cells are growing logarithmically in medium containing 75 μM inositol. PA level decreases by the stimulation of PI synthesis in response to inositol (+Ins) supplementation. The regulation in response to stationary phase occurs without inositol supplementation. Pah1p and Dgk1p play important roles in controlling PA content and transcriptional regulation of UAS_{INO}-containing genes. Taken from Henry and Carman 2012 (66).

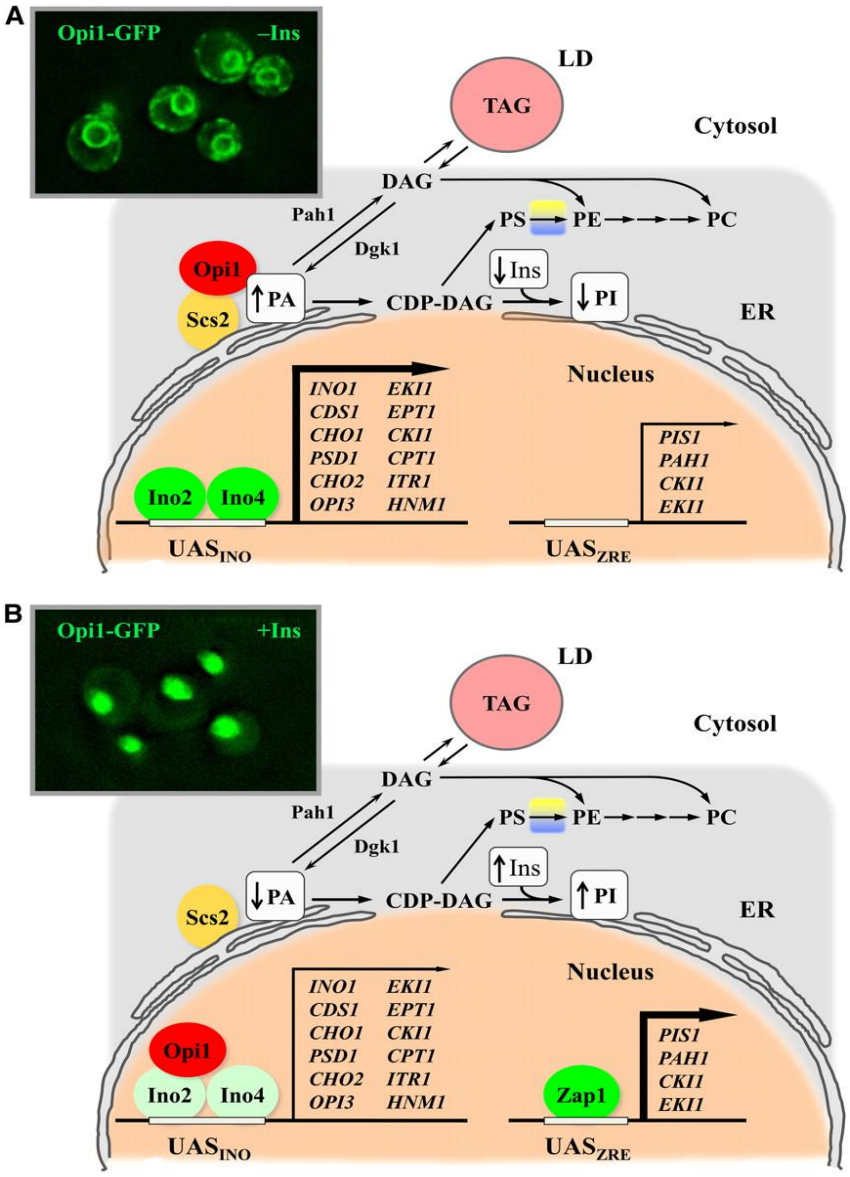
A
Opi1-GFP
–Ins
LD
TAG
Cytosol
DAG
Pah1
Dgk1
PS
PE
PC
Opi1
Scs2
↑PA
CDP-DAG
↓Ins
↓PI
ER
Nucleus
INO1 EKI1
CDS1 EPT1
CHO1 CKI1
PSD1 CPT1
CHO2 ITR1
OPI3 HNM1
PIS1
PAH1
CKI1
EKI1
Ino2
Ino4
UASINO
UASZRE
B
Opi1-GFP
+Ins
LD
TAG
Cytosol
DAG
Pah1
Dgk1
PS
PE
PC
↓PA
Scs2
CDP-DAG
↑Ins
↑PI
ER
Nucleus
INO1 EKI1
CDS1 EPT1
CHO1 CKI1
PSD1 CPT1
CHO2 ITR1
OPI3 HNM1
PIS1
PAH1
CKI1
EKI1
Opi1
Ino2
Ino4
Zap1
UASINO
UASZRE

(71-73). Upon reduction of PA levels, Opi1p is released from the nuclear/ER membrane and enters the nucleus (72), where it interacts with Ino2p and represses transcription. Since the PAP activity controls PA levels at the nuclear/ER membrane, its regulation is an important factor that controls the Opi1p-mediated regulation of UAS_{INO}-containing genes.

The maximal expression of UAS_{INO}-containing genes occurs during exponential phase in the absence of inositol and choline, while they are repressed in the stationary phase, even, in the absence of inositol (74). This repression leads to a decrease in the activities of the phospholipid biosynthetic enzymes in the route PA to PC, leading to divert PA to TAG at the expense of total phospholipid synthesis (74, 75). When the inositol is supplemented to the growth medium, the level of PA is reduced through the utilization of CDP-DAG to synthesize PI (76) because inositol exhibits allosteric inhibition of the Cho1p PS synthase (77), leading to the activation of the Pis1p PI synthase (73). The decreased PA levels cause Opi1p to be released from the nuclear/ER membrane and its translocation into the nucleus and consequently repress UAS_{INO}–containing genes (72).

Differentiation of PAP Enzymes

PAP was first described in chickens by Smith *et al.* in 1957 (78). The discovery of PAP completed the well-known scheme of glycerolipids biosynthetic pathway by providing a link between the neutral lipids and phospholipid synthesis pathways in mammalian cells. Due to the instability of the mammalian enzyme, the isolation of PAP remained elusive for more than three decades. The enzymes knowns for PAP are differentiated by their cofactor requirement for its catalytic activity. Besides the difference in their cofactor requirement, these enzymes are distinguished by NEM sensitivity and catalytic motifs.

Cofactor Requirement

Mg^{2+}-independent PAP

One of the Mg^{2+}-independent PAP activities in yeast was purified 33,333-fold from *S. cerevisiae* as an enzyme that catalyzes the dephosphorylation of DGPP (79). Its purification procedure included Triton X-100 solubilization of microsomal membranes, followed by chromatography with DE53, Affi-Gel Blue, hydroxylapatite, and MonoQ (79). The procedure resulted in the isolation of an apparent homogeneous protein with a subunit molecular mass of 34 kDa. The enzyme catalyzed the dephosphorylation of the β-phosphate of DGPP to form PA, and subsequently dephosphorylation of PA to produce DAG. Thus, the enzyme was termed DGPP phosphatase (79). Although the DGPP phosphatase enzyme utilized PA as substrate in the absence of DGPP, DGPP was the preferred substrate for the enzyme with a specificity constant (V_{max}/K_m) 10-fold greater than that for PA (80). Amino acid sequence information derived from DGPP phosphatase was used to identify and isolate the *DPP1* (diacylglycerol pyrophosphate phosphatase) gene encoding the enzyme (80). *LPP1* (lipid phosphate phosphatase) gene has been identified by the sequence information of *DPP1* (80).

Dpp1p (80) and Lpp1p (81) PAP enzymes are integral membrane proteins with six transmembrane spanning regions (80, 81), and the majority of PAP activity in yeast is attributed to the Dpp1p enzyme (82). Dpp1p and Lpp1p PAP enzymes have the molecular mass of 34 and 32 kDa, respectively, and are localized in the vacuole and Golgi, respectively (80, 81). Dpp1p and Lpp1p PAP enzymes have broad substrate specificity. In addition to PA, the Dpp1p and Lpp1p PAP enzymes use various lipid phosphate substrates, including DGPP, LPA, sphingoid base phosphates and isoprenoid phosphates (80, 81). However, only DGPP and PA have shown to be substrates *in vivo* (81). The Dpp1p enzyme shows a preference for DGPP as a substrate (80), whereas the Lpp1p enzyme has similar substrate specificity for both PA and DGPP (81). The substrate specificity of the Dpp1p and Lpp1p suggests that these enzymes are involved in

signaling events rather than in phospholipid synthesis (49, 83). Moreover, Dpp1p and/or Lpp1p, which localize in the vacuole and Golgi, respectively, are not responsible for the *de novo* synthesis of phospholipid and TAG that occurs presumably in the ER (51). The mutant lacking *DPP1* and *LPP1* genes shows normal growth and morphology without any defects, indicating that the Dpp1p and Lpp1p PAP are not required for cell viability (82).

Mg^{2+}-dependent PAP

Hosaka *et al*. (84) reported that Mg^{2+}-dependent PAP was first identified and partially purified from the soluble fraction about 600-fold in yeast. The purification procedure included $(NH_4)_2SO_4$ fractionation, poly (ethylene glycol) 6000 fractionation and chromatography on DEAE-Sepharose, Sephadex G-100 and Blue-Sepharose. The purified enzyme was dependent on Mg^{2+} ions for the activity. The molecular mass of the enzyme was estimated to approximately 75 kDa by analytical gel filtration on Sephadex G-100. The enzyme is specific for PA with an apparent K_m for 0.05 mM (84).

In 1989, the purification of the membrane associated PAP in yeast was reported the procedure included sodium cholate solubilization of total membranes followed by chromatography with DE53, Affi-gel Blue, hydroxylapatite, MonoQ, and Superose 12 (7). The purification resulted in the isolation of a homogeneous protein with a subunit molecular mass of 91 kDa (7). PAP activity was dependent on Mg^{2+} ions and Triton X-100 at pH 7, and was sensitive to thioreactive reagents. The K_m for PA was 50 μM, and the V_{max} was 30 μmol/min/mg (7). Additionally, immunoblot analysis of cell extracts using antibodies specific for the 91 kDa form of membrane-associatd PAP revealed the existence of 45-kDa form of PAP, and the study also showed that the 91 kDa form of PAP is the proteolytic product of a 104 kDa protein (85). The 45 and 104 kDa enzymed were isolated from mitochondria and microsome, respectively (85).

In 2006, a gene, *PAH1*, encoding Mg^{2+}-dependent PAP in yeast was identified through a reverse genetic approach by mass spectrometry analysis of the amino acid sequence derived from a purified preparation of the 91 kDa enzyme (86). The deduced sequence matched that of previously known as *SMP2*, which has been implicated in plasmid maintenance and respiration (87). Upon identification of the protein product as a PAP, the gene was renamed *PAH1* (phosphatidic acid phosphohydrolase). The *PAH1* is localized on chromosome XIII and does not have any sequence motifs suggesting introns in the gene (86). The Pah1p PAP shows that the enzymological properties of recombinant Mg^{2+}-dependent PAP predicted size of 95 kDa are very similar to those of 91 kDa Mg^{2+}-dependent enzyme previously purified from yeast (7, 86).

Pah1p found in the cytosolic and membrane fractions of the cell, and the membrane bound form of the enzymes is salt extractable, indicating its peripheral nature (51, 86). The monomeric Pah1p is a 95 kDa protein that migrates upon SDS–PAGE as a 124 kDa protein (51, 86). Smaller molecular mass forms (e.g., 91 kDa) of PAP purified from yeast appear to be proteolytic products of the enzyme (86). Unlike the Dpp1p and Lpp1p PAP, the Pah1p PAP is specific for PA, The Pah1p PAP has been identified to contribute a major regulation of PA content among the enzymes (eg., LPA acyltransferase, CDP-DAG synthase, PAP, DAG kinase, phospholipase D) that control the metabolism of PA (51). Lipid analysis shows that the mutant lacking *PAH1* (*pah1*Δ mutant) accumulates PA and has reduced amounts of DAG and its acylated derivative TAG (86). In addition, the *pah1*Δ mutation affects the contents of the major phospholipids, PC, PE and PI, sterol esters, and fatty acids, indicating PAP controls the regulation of overall lipid synthesis (86). The effects of the *pah1*Δ mutation on phospholipid composition are most pronounced in exponential phase, but its effect is not as great in stationary phase. Interestingly, the effects on the contents of TAG and other neutral lipids are more dramatic in stationary phase (86). The loss of PAP activity in stationary phase cells resulted in more than a 90% decrease in TAG content (86). Along with the change in lipid synthesis, the *pah1*Δ mutant

exhibits the massive expansion of the nuclear/ER membrane and abnormally high expression of key phospholipid biosynthetic genes (i.e., *INO1* involved in PI synthesis, and *OPI3* involved in PC synthesis) (88). In the *pah1*Δ mutant, PA levels are elevated and tethers Opi1p at nuclear/ER membrane along with Scs2 and prevents its translocation into the nucleus, where it functions to repress transcription of phospholipid synthesis genes (14). Thus, PA content at the nuclear/ER membrane is an important factor that controls the Opi1p-mediated regulation of UAS_{INO}-containing gene expression (14). In addition, the *pah1*Δ mutant presents slow growth (86), temperature sensitivity (86), respiratory deficiency (86, 89), defects in lipid droplet formation (90) and morphology (91), vacuole homoeostasis and fusion (92), and fatty acid induced lipotoxicity (93).

Thioreactive Sensitivity and Catalytic Motifs

The study of sensitivity to the thioreactive compound NEM indicates that the Dpp1p and Pah1p enzyme is insensitive to NEM (80) while the Lpp1p enzyme is sensitive to NEM (81, 86). Sequence information indicates that NEM-sensitive enzymes have more cysteine residues than NEM-insensitive one. For example, Lpp1p contains ten cysteine residues, while Dpp1p and Pah1p contain only three (51).

The catalytic motifs that govern the phosphatase reactions of these enzymes are different. The Pah1p PAP enzyme has a D*X*D*X*T catalytic motif present in a haloaid dehalogenase (HAD)-like domain, which is found in a superfamily of Mg^{2+}-dependent phosphatase enzymes (94, 95). Its first aspartate residue is responsible for binding the phosphate moiety in the phosphatase reaction (33). However, the Dpp1p and Lpp1p enzymes have a three domain lipid phosphatase motif that is localized to the hydrophilic surface of the membrane (96). A superfamily of Mg^{2+}-independent LPP have conserved motifs consisting of the consensus sequence K*XXXXXX*RP (domain 1), PSGH (domain 2), and SR*XXXXX*H*XXX*D (domain 3) (96). The conserved arginine

residue in domain 1 and the conserved histidine residue in domain 2 and 3 are critical for the catalytic activity of the Dpp1p and Lpp1p enzymes (97).

Regulation of PAP Enzymes

PAP enzymes have roles in the synthesis of lipids and the generation or degradation of lipid signaling molecules in eukaryotic cells (51). In addition, PAP is involved in the transcriptional regulation of phospholipid synthesis (64). As discussed on the *pah1*Δ mutant phenotype, accumuulation of PA and reduction of DAG is toxic to cell. A balanced level of PA and DAG mediated by the Pah1p PAP activity must be achieved to maintain lipid homeostasis and normal cell physiology. In view of the variety of cellular processes in which PA and DAG play a role, the regulation of PAP activity is crucial and complex, being controlled by genetic and biochemical mechanisms.

Genetic Regulation of PAP

The expression of the Pah1p PAP activity is affected by intracellular levels of zinc (98). Since zinc serves as a cofactor for numerous enzymes (99, 100) and structural component of many proteins (99, 101, 102), the tight control of intracellular zinc levels is accomplished by the action of zinc transporters located in the plasma, vacuole, ER, and mitochondrial membranes (102-112). A deficiency in zinc changes the phospholipid composition mediated by an induction in the expression of many of zinc transporters, which is a result from the transcriptional regulation of various phospholipid synthesis genes (64, 113-115). The *PAH1* expression is induced in response to zinc depletion in a Zap1p-dependent manner through its interaction with zinc-responsive upstream activating (UAS_{ZRE}) sequences in the *PAH1* promoter (99). This induction correlates with an increase in Pah1p PAP activity and elevated TAG levels (99).

Biochemical Regulation of PAP

Maximum Pah1p PAP is dependent on $MgCl_2$ (1 mM) and non-ionic detergent Triton X-100 at pH 7.5 (86, 116). The Triton X-100 forms a mixed micelle which provides a favorable environment for catalysis (7, 117, 118). Thus, PAP activity is dependent on the molar (e.g., number of micelles containing substrate) and surface (e.g., number of PA molecules on the micelle surface) concentration of PA (116), which is indicative of surface dilution kinetics (116). By this mechanism, PAP binds to micelle surface before binding its substrate and catalyzes its dephosphorylation, which is relevant *in vivo* since PAP is presumed to associate with PA at the ER/nuclear membrane. The PAP enzyme is specific for PA, and exhibits positive cooperative kinetics with respect to the surface concentration of PA (50, 86).

Phospholipid synthesized through CDP-DAG, including CDP-DAG, PI and CL, which act as mixed competitive activators of PAP activity, stimulates the Pah1p PAP activity (50, 118). Since PA is partitioned between CDP-DAG and DAG, and CDP-DAG is precursor for PI and CL, the activation of PAP activityby CDP-DAG, PI and CL, would favor PE and PC synthesis and TAG synthesis through DAG. Simultaneously, the activation of PAP activity lowers PA content, leading to repression of UAS_{INO}-containing genes that encode enzymes for phospholipid synthesis via CDP-DAG (33, 64). On the other hand, PAP activity is inhibited by the sphingoid bases sphingosine, phytosphingosine, and sphinganine (119) in parabolic competitive manner, indicating that more than one inhibitor molecule contribute to the exclusion of PA from the enzyme (50). This inhibition causes an increased PA contents, stimulating phospholipid synthesis through the activation of UAS_{INO}-containing genes (50).

Cellular ATP and CTP levels are correlated with synthesis of phospholipid and TAG. The nucleotide ATP and CTP, which are precursors for the synthesis of phospholipid, inhibit PAP activity (42, 66). Kinetic studies show that ATP and CTP are competitive inhibitors with respect to Mg^{2+} ions, indicating that the mechanism is based on the chelation of the cofactor (120).

Moreover, cellular ATP and CTP levels correlate with synthesis of phospholipids and TAG (120). A high level of ATP resulted in an increased level of PA and phospholipid synthesis, while low level of ATP favored a reduced level of PA and an increase in the synthesis of TAG (120). A high level of CTP caused an increase of PA and thus resulted in derepression of UAS_{INO}-containing phospholipid synthesis genes (121).

Regulation of PAP by Phosphorylation/Dephosphorylation

A reversible covalent modification of a protein by phosphorylation is a common posttranslational modification to regulate its biological function (3). Phosphorylation is catalyzed by protein kinases, which recognize a specific consensus motif and transfers the γ-phosphate group from ATP to the target proteins (48, 122). The addition of a bulky and charged phosphate group in an enzyme could change its activity, subcellular localization, protein stability, as well as its interaction with other proteins (48, 123-125)

Biochemical analysis showed that the phosphorylated PAP is a substrate for Nem1p-Spo7p protein phosphatase complex (88). Since Nem1p-Spo7p protein complex is localized in the nuclear/ER membrane, phosphorylated PAP is recruited to membrane for its dephosphorylation. Cells lacking either Nem1p or Spo7p phosphatase complex resulted the same aberrant nuclear/ER membrane expansion phenotype exhibited by the *pah1*Δ mutation (88, 126), indicating that physiological functions of PAP require this protein phosphatase complex.

PAP is subject to the covalent modification of phosphorylation (127). Mass spectrometry analysis of purified PAP has identified multiple (i.e.) 14 sites of phosphorylation (126). Of theses, seven sites (Ser^{110}, Ser^{114}, Ser^{168}, Ser^{602}, Thr^{723}, Ser^{744}, and Ser^{748}) are contained within the minimal Ser/Thr-Pro motif that is a target for Pho85p-Pho80p phosphorylation (128) and three of the sites (Ser^{602}, Thr^{723}, and Ser^{744}) are also targets of Cdc28p-cyclin B (129). Phosphorylation by pho85p-Pho80p results in a 6-fold reduction in the catalytic efficiency of PAP (V_{max}/K_m), while

activity was not affected by phosphorylation via Cdc28p-cyclin B (129). Recent study shows Pah1p was a *bona fide* substrate for protein kinase A, and five sites (Ser^{10}, Ser^{677}, Ser^{773}, Ser^{774}, and Ser^{788}) are targets for phosphorylation (130). Protein kinase A-mediated phosphorylation of Pah1p inhibits its PAP activity by decreasing catalytic efficiency (1.8-fold), and the inhibitory effect was primarily conferred by phosphorylation at Ser-10 (130). The protein kinase A-mediated phosphorylation of Ser-10 functions in conjunction with the phosphorylations mediated by Pho85p-Pho80p and Cdc28p-cyclin B and that phospho-Ser-10 should be dephosphorylated for proper PAP function (130). The remaining sites are putative targets for protein kinases, such as protein kinases C, casein kinases I and II, and MAPK, indicating that the regulation of PAP by phosphorylation is complex.

The localization of PAP is affected by phosphorylation of Pho85p-Pho80p and Cdc28p-cyclin B kinase (128, 129). Subcellular fractionation analysis shows that PAP enzyme of the phosphorylation-deficient 7A mutant, where all seven sites within the Ser/Thr-Pro motif are mutated to a nonphosphorylatable alanine, is enriched in the membrane fractions and exhibits elevated PAP activity (129). *In vivo*, expression of the 7A mutant enzyme complements the *pah1*Δ *nem1*Δ double mutant phenotypes that include temperature sensitivity, nuclear/ER membrane expansion, and derepression of phospholipid synthesis genes (127, 129). Cells lacking the Nem1p-Spo7p complex exhibit reduced TAG due to loss of PAP function, thus indicating lack of phosphorylation of the seven sites renders Pah1p capable of bypassing the Nem1p-Spo7p requirement for *in vivo* function (129).

Lipin Connection

The identification of *PAH1* gene in yeast revealed that its mammalian homologs *Lpin 1*, *2*, and *3* encode PAP activity in mammalian cells (50, 86). The Pah1p PAP protein has sequence homology with the lipin-1 in evolutionarily conserved N-terminal domain (NLIP) and HAD-like

domain (50, 86). In addition to its PAP activity, lipin-1 functions as a transcriptional coactivator in the regulation of lipid metabolism gene expression (65). This transcriptional coactivator function is dependent on an L*XX*IL motif found near the D*X*D*X*(T/V) motif but independent of PAP activity (65).

LPIN1, identified by positional cloning, is the gene mutated in the fatty liver dystrophy (*fld*) mouse (131). At that time, the function of lipin-1 was linked to fat metabolisim, as lipin-1 deficiency leads to lipodystrophy and insulin resistance, otherwise excess of lipin-1 results in obesity and insulin sensitivity (131-133). In addition, the mice lacking lipin-1 exhibit peripheral neuropathy that is characterized by myelin degradation, Schwann cell differentiation and proliferation, and reduction in nerve conduction velocity (132, 135, 136). The phenotypes are caused by the degradation of myelin through the MEK/ERK signaling pathway that is activated by elevated levels of PA (136). Mutations in the *LPIN1* gene in human are associated with metabolic syndrome, type 2 diabetes, and recurrent acute myoglobinuria in children, whereas mutations in the *LPIN2* gene cause Majeed syndrome associated with anemia and inflammatory disorders (138-140). *LPIN1* expression is required for adipocyte differentiation with the stimulation by glucocorticoids (138-141), otherwise *LPIN2* expression is repressed during adipogenesis. This elucidates that *LPIN1* and *LPIN2* have distinct functions in adipocytes (138). In addition, alternative splicing of mouse *LPIN1* mRNA results in two lipin 1 isoforms (α and β) that may play distinct functions in adipogenesis (134).

Phosphorylation of lipin-1, which influences cellular location, is stimulated by insulin and mediated by the mTOR signaling pathway (141). Lipin-1 is also phosphorylated during the mitotic phase of the cell cycle (138). Phosphorylated forms of lipin-1 are enriched in the cytosolic fraction, whereas the dephosphorylated forms are enriched in the membrane fraction (7, 138, 142). The translocation of lipin-1 from the cytosol to the membrane is essential to its function as a PAP enzyme.

Specific Aims of the Study

In the *pah1*Δ *dpp1*Δ *lpp1*Δ mutant, there is still a remaining Mg^{2+}-dependent PAP in the cytosol and membrane fractions (86). The residual activity is NEM sensitive and salt extractable (86). These data indicate that an additional gene other than *PAH1*, *DPP1*, and *LPP1* encodes a Mg^{2+}-dependent PA phosphatase enzyme in *S. cerevisiae*. The studies into its mode of action and regulation require the identification of the gene and purification of the enzyme. Thus, the specific aim of my study was to identify the gene encoding PAP through a reverse genetics approach using protein sequence information derived from the purified PAP enzyme preparation from the *pah1*Δ *dpp1*Δ *lpp1*Δ triple mutant. Using genetic information, the PAP enzyme was expressed and purified to characterize the enzymological and kinetic properties. Furthermore, the effects of this PAP on the synthesis of TAG and lipid metabolism was examined, leading to define the the role of this PAP in the cells.

EXPERIMENTAL PROCEDURES

Materials

All chemicals were reagent grade. Growth medium supplies were purchased from Difco. Polyvinylidene difluoride membrane, the enhanced chemifluorescence Western blotting detection kit, phenyl-Sepharose CL-4B, MonoQ, Superdex 200 columns, Sepharose Fast-Flow and IgG Sepharose were purchased from GE Healthcare. DE52 (DEAE-cellulose) was purchased from Whatman. Affi-Gel Blue, protein assay reagents, electrophoretic reagents, and protein standards were purchased from Bio-Rad. Radiochemicals were purchased from PerkinElmer Life Sciences. Bovine serum albumin, phenylmethylsulfonyl fluoride, benzamidine, aprotinin, leupeptin, pepstatin, isopropyl-β-D-thiogalactoside, sodium cholate, Triton X-100, Nucleotides, oligonucleotides, ammonium molybdate and molecular mass standards for gel filtration were purchased from Sigma. Lipids were obtained from Avanti Polar Lipids. Silica gel thin layer chromatography plates were from EM Science. Restriction endonucleases, modifying enzymes, and recombinant Vent DNA polymerase were purchased from New England Biolabs. Plasmid isolation and gel extraction kits, Ni^{2+}-NTA agarose resin, spin column were purchased from Qiagen. Invitrogen was the source of the DNA size standards, the yeast deletion consortium strain collection and His_6-tagged tobacco etch virus protease. The Yeast Maker yeast transformation kit was purchased from Clontech. Stratagene supplied the QuickChange site-directed mutagenesis kit. Malachite green was from Fisher. Protease inhibitor mixture tablets, Mouse monoclonal anti-HA and anti-His_6 antibodies were from Roche Applied Science. Anti-App1p antibodies were prepared in rabbits against the C-terminal portion (residues 490-502) of the protein at EZBiolab. Alkaline phosphatase-conjugated goat anti-rabbit IgG antibodies and alkaline phosphatase-conjugated goat anti-mouse IgG antibodies were from Thermo Scientific

and Pierce, respectively. Scintillation counting supplies were purchased from National Diagnostics.

Strains and Growth Conditions

The strains used in this work are listed in Table 1. Yeast cells were grown in YEPD medium (1% yeast extract, 2% peptone, 2% glucose) or in synthetic complete (SC) medium containing 2% glucose at 30 ℃ as described previously (143, 144). For selection of yeast cells bearing plasmids, appropriate amino acids were omitted from SC medium. Plasmid maintenance/amplifications (strain DH5α) and App1p expression (strain BL21(DE3)pLysS) were performed in *Escherichia coli*. The bacterial cells were grown in LB medium (1% tryptone, 0.5% yeast extract, 1% NaCl, pH 7.4) at 37°C, and ampicillin (100 µg/ml) was added to select for the cells carrying plasmid. For growth on solid media, agar plates were prepared with supplementation of either 2% (yeast) or 1.5% (*E. coli*) agar. For App1p PAP purification in yeast, *pah1Δ dpp1Δ lpp1Δ* mutant cells were grown to late exponential phase in YEPD medium at 30 ^{o}C. Uracil was omitted from the growth medium to select for cells carrying plasmid pMC104, and 2 % agar was included for growth on plates. For App1p PAP purification, yeast cells were grown in 2 liters of synthetic complete medium with 2 % raffinose as the carbon source. To induce expression of protein A-tagged App1p PAP, the growth medium was supplemented with 2 % galactose. Maximum expression, as confirmed by immunoblot analysis using anti-protein A antibodies, was obtained after 6 hours of growth. For heterologous expression of His_6-tagged App1p, *E. coli* BL21(DE3)pLysS cells bearing pMC101 were grown to $A_{600\ nm}$ = 0.5 at 30 ^{0}C in 1 L of LB medium containing ampicillin (100 µg/ml) and chloramphenicol (34 µg/ml). The culture was then incubated for 3 h with 1 mM isopropyl-B-D-thiogalactoside to induce the expression of the PAP enzyme.

DNA Manipulations, Cloning of *APP1*, and Construction of Plasmids

Standard methods were used to isolate plasmid and genomic DNA and for manipulation of DNA using restriction enzymes, DNA ligase, and modifying enzymes (144) Transformations of *S. cerevisiae* (145) and *E. coli* (144) with DNA/plasmids, and PCR reactions (146) followed the standard protocols. The plasmids used in this work are listed in Table 1. The *S. cerevisiae APP1* gene was cloned by PCR. A 3,024-bp DNA fragment that contains the entire coding sequence (1,764 bp) of *APP1*, the 5'-untranslated region (824 bp) and the 3'-untranslated region (436 bp) was amplified from W303-1A genomic DNA (forward, 5'-GATTATAAGCTTAACTGACACCCATATCGCTTGACCC-3'; reverse, 5'-GGTCAATATACGTGCATCTAGAAGGCCTTTCCCGAC-3'). The *APP1* DNA fragment was digested with HindIII/XbaI and inserted into plasmid YEp351 at the same restriction enzyme sites. The multicopy plasmid containing *APP1* was named pMC102. The *APP1* gene was used to construct $APP1^{HA}$, in which the sequence for the HA epitope (YPYDVPDYA) was located after start codon. The 854-bp (forward, 5'-GATTATAAGCTTAACTGACACCCATATCGCTTGACCC-3'; reverse, 5'-AGCGTAGTCTGGGACGTCGTATGGGTACATCTTTTTATTCCTTCTCCAAAGCAATTTTTTCCCCC-3') and 2,224-bp (forward, 5-TACCCATACGACGTCCCAGACTACGCTAATAGTCAAGGTTACGATGAAAGCTCTTCCTCTACTGC-3'; reverse, 5'- GGTCAATATACGTGCATCTAGAAGGCCTTTCCCGAC-3') *APP1* DNA fragments that contain the HA tag at the 3' and 5' ends, respectively, were amplified by PCR. These PCR products containing 27 bp overlapping ends were combined by overlap-extension PCR. The combined 3,051 bp DNA was then amplified followed by digestion with HindIII and XbaI and inserted into YEp351 at HindIII/XbaI sites. The multicopy plasmid containing $APP1^{HA}$ was named pMC103. Plasmids pMC102-D281E and pMC103-D281E were

TABLE 1. Strains and Plasmids Used in This Work

Strain or plasmid	Relevant characteristics	Source or Ref
Strains		
E. coli		
DH5α	F$^-$ ϕ80d*lacZ*ΔM15 Δ*lacZYA-argF*)U169 *deoR recA endA1 hsdR17*(r_k^- m_k^+) *phoA supE44* λ$^-$ *thi-1 gyrA9 relA1*	(144)
BL21(DE3)pLysS	F$^-$ *ompT hsdS$_B$* ($r_B^-m_B^-$) *gal dcm* (DE3) pLysS	Novagen
S. cerevisiae		
BY4741	*MAT***a** *his3Δ1 leu2Δ0 met15Δ0 ura3Δ0*	(147)
BY4741-*app1*Δ	*app1*Δ::*KanMX4* derivative of BY4741	Deletion consortium
W303-1A	*MAT***a** *ade2-1 can1-100 his3-11,15 leu2-3,112 trp1 -1 ura3-1*	(148)
GHY63	*app1*Δ*::natMX4* derivative of W303-1A	This study
GHY57	*pah1*Δ*::URA3* derivative of W303-1A	(86)
GHY64	*app1*Δ*::natMX4 pah1*Δ*::URA3* derivative of W303-1A	This study
TBY1	*dpp1*Δ*::TRP1/Kan^r lpp1*Δ*::HIS3/Kan^r* derivative of W303-1A	(97)
GHY65	*app1*Δ*::natMX4 dpp1*Δ*::TRP1/Kan^r lpp1*Δ*::HIS3/Kan^r* derivative of W303-1A	This study
GHY58	*pah1*Δ*::URA3 dpp1*Δ*::TRP1/Kan^r lpp1*Δ*::HIS3/Kan^r* derivative of W303-1A	(86)
GHY66	*app1*Δ *::natMX4 pah1*Δ*::URA3 dpp1*Δ*::TRP1/Kan^r lpp1*Δ*::HIS3/Kan^r* derivative of W303-1A	This study
Plasmids		
YEp351	Multicopy *E. coli*/yeast shuttle vector with LEU2	(149)
pMC102	*APP1* gene inserted into YEp351	This study
pMC102-D281E	*APP1*(D281E) derivative of pMC102	This study
pMC103	*APP1*^{HA} gene inserted into YEp351	This study
pMC103-D281E	*APP1*(D281E) derivative of pMC103	This study
pYES2	Yeast protein expression vector with a galactose-inducible promoter (GAL1) , 2μ origin and a *URA3* gene as selectable marker, Ampr	Invitrogen
pMC104	*APP1*-PtA gene inserted into pYES2	This study
pET-15b	*E. coli* expression vector with N-terminal His_6-tag fusion	Novagen
pMC101	*APP1* coding sequence inserted into pET-15b	This study

produced by PCR-mediated site-directed mutagenesis with the codon change of GAT to GAA. The nucleotide change in the *APP1* and *APP1*^{HA} alleles was confirmed by DNA sequencing. The 1.8-kb *APP1* coding sequence with a 30-bp linker at the 3' end was amplified from pMC102 (forward, 5'-TGGAGAGAGCTCAAAAAAATGAATAGTCAAGG-3'; reverse, 5'-ATACAGGTTTTCGGTCGTTGGGATGGATCCGTTTGAATACTTCTCCCTAATTCTGCG-3'), and the 0.45-kb *Staphylococcus aureus spa* coding sequence with a 30-bp linker at the 5' end was amplified from YCplac111-*PAH1*-PtA (forward, 5'-GGATCCATCCCAACGACCGAAAACCTGTAT-3'; reverse, 5'-ATAACACTCGAGTTAGCATGCTGAATTCGCG-3'). The *APP1* and *spa* coding sequences were combined through the common 30-bp linker by overlap-extension PCR. The 2.2-kb *APP1-spa* sequence was digested with SacI and XhoI, and inserted into plasmid pYES2 at the same restriction sites. The recombinant plasmid for galactose-inducible overexpression of protein A-tagged App1p was named pMC104. For expression of *APP1* in *E. coli*, the entire coding sequence of *APP1* (except the first adenosine because the blunted (Klenow) NdeI site of pET-15b starts with adenosine) was amplified by PCR from genomic DNA template (forward, 5'-TGAATAGTCAAGGTTACGATGAAAGCTCTTCC-3'; reverse, 5'-TAATCCTCGAGTTAGTTTGAATACTTCTCCCTAATTCTGCG-3'). The PCR product (~1.8 kb) was digested with XhoI, and the vector was digested with NdeI, filled with Klenow, and digested with XhoI. The blunt-cohesive end PCR products were inserted into pET-15b at NdeI (Klenow)/XhoI sites. The plasmid bearing His_6-tagged *APP1* was named pMC101.

Construction of the *app1*Δ Mutant and Its Derivatives

The *app1*Δ mutation in the wild type strain W303-1A and in the *dpp1*Δ *lpp1*Δ mutant strain TBY1 was generated by one-step gene replacement (68). The strains were transformed with the 1,219-bp disruption cassette (*app1*Δ*::natMX4*) that had been amplified from pAG25 (Euroscarf)

using the primers APP1-natMX-F (5'-AGTTCCGTCAAA GGGGGAAAAAATTGCTTTGGAGAAGGAATAAAAAGATGACATGGAGGCCCAGAATA CCC-3') and APP1-natMX-R (5'-TATACAATTTTTAAACTCCCTCCCGATGTATATAAATAACAGTGTATTTACAGTATAG CGACCAGCATTCA C-3'). Yeast transformants were selected on YEPD medium containing 100 μg/ml nourseothricin, and the *app1*Δ mutation in the nourseothricin-resistant cells was confirmed by PCR amplification of the 1,217-bp fragment from genomic DNA using the primers APP1-F-36 (5'-AGGGGGAAAAAATTGCTTTGGA-3') and APP1-R-46 (5'-ATACAATTTTTAAACTCCCTCCCG-3'). The *pah1*Δ mutation in the *app1*Δ mutant strain GHY63 and the *app1*Δ *dpp1*Δ *lpp1*Δ mutant strain GHY65 was generated by one-step gene replacement as described previously (86). These experiments were performed by Gil-Soo Han.

Partial Purification of App1p PAP from *S. cerevisiae*

The *pah1*Δ *dpp1*Δ *lpp1*Δ mutant strain GHY58 (86) was used for purification to eliminate the PAP activities encoded by the *PAH1* (84) *DPP1* (80), and *LPP* (81) genes. All steps were performed at 8 °C.

Step 1: Preparation of Cell Extract

The cell extract was prepared from 200 g (wet weight) of *pah1*Δ *dpp1*Δ *lpp1*Δ mutant cells by disruption with glass beads (0.5 mm diameter) using a Biospec Products Bead Beater as described previously (150) using buffer A (50 mM Tris-HCl (pH 7.5), 0.3 M sucrose, 10 mM 2-mercaptoethanol, 1 mM Na_2 EDTA, 0.5 mM phenylmethanesulfonyl fluoride, 1 mM benzamide, 5 μg/ml aprotinin, 5 μg/ml leupeptin, 5 μg/ml pepstatin). Unbroken cells and glass beads were removed by centrifugation at 1,500 x *g* for 10 min.

Step 2: Preparation of Crude Mitochondria

Crude mitochondria were collected from the cell extract by centrifugation at 32,000 x *g* for 10 min (151).

Step 3: Preparation of NaCl Extract

Mitochondria were suspended in buffer A containing 1 M NaCl to a final protein concentration of 10 mg/ml. The suspension was centrifuged at 32,000 x *g* for 10min to remove non-salt extractable proteins from mitochondrial membranes. The supernatant containing the salt-extractable proteins was then dialyzed overnight against buffer B (50 mM Tris-HCl (pH 7.5), 1mM $MgCl_2$, 10 mM 2-mercaptoethanol, 1 mM PMSF) containing 0.5% sodium cholate. Sodium cholate was included in buffer B to prevent the precipitation of PAP that occurred after the removal of salt from the enzyme preparation.

Step 4: DE52 Chromatography

A DE52 column (1.5 x 7 cm) was equilibrated with buffer B containing 0.5% sodium cholate. The enzyme preparation from the previous step was applied to the column at a flow rate of 40 ml/h, and the column was washed with 5 column volumes of buffer B plus 0.5% sodium cholate., followed by elution of the enzyme in 5-ml fractions with 10 column volumes of a linear NaCl gradient (0-0.5 M) in the same buffer. The peak of PAP activity eluted at 0.2 M NaCl.

Step 5: Affi-Gel Blue Chromatography

An Affi-Gel Blue column (1.5 x 5 cm) was equilibrated with buffer B containing 0.2 M NaCl and 0.5% sodium cholate. The DE52-purified enzyme was applied to the column at a flow rate of 60 ml/h. The column was washed with 5 column volumes of buffer B containing 0.5 M NaCl and 0.5% sodium cholate. PAP activity was then eluted in 3-ml fractions with 12 column volumes of a linear gradient of NaCl (0.5 – 3.0 M) in buffer B and 0.2% sodium cholate. The peak of activity eluted at a NaCl concentration of 1.3 M.

Step 6: Phenyl-Sepharose Chromatography

A phenyl-Sepharose (0.8 x 2 cm) column was equilibrated with buffer B containing 3 M NaCl and 0.2% sodium cholate. The Affi-Gel Blue-purified enzyme was made to contain 3 M NaCl and then applied to the column under gravity flow. The column was first washed with 10 column volumes of buffer B containing 3 M NaCl and then washed with 10 column volumes of buffer B without NaCl. PAP activity was then eluted in 1-ml fractions with 10 column volumes of buffer B containing 1% Triton X-100.

Step 7: MonoQ Chromatography

A MonoQ column (0.5 x 5 cm) was equilibrated with buffer B containing 0.5% Triton X-100. The phenyl-Sepharose-purified enzyme was applied to the column; the column was then washed with 5 column volumes of buffer C containing 0.5% Triton X-100 followed by elution of PAP in 1-ml fractions with 20 column volumes of a linear NaCl gradient (0-1 M) at a flow rate 24 ml/h. The peak of activity was eluted at NaCl concentration of 0.5 M.

Step 8: Superdex 200 Chromatography

A gel filtration Superdex 200 column (1 x 30 cm) was equilibrated with buffer B containing 0.5 M NaCl and 0.5% Triton X-100. The MonoQ-purified enzyme was applied to the column at a flow rate of 40 ml/h. The enzyme was then eluted in 0.5-ml fractions with 1 column volume of the same buffer. The column was calibrated with molecular mass standards (β-amylase, 200 kDa; alcohol dehydrogenase, 150 kDa; bovine serum albumin, 66 kDa; carbonic anhydrase 29 kDa; cytochrome c, 12.4 kDa) under the same conditions used to purify PAP.

Purification of His_6-tagged App1p PAP from *E. coli*

All steps were performed at 8 °C. *E. coli* cells expressing His_6-tagged App1p were suspended in 20 ml of 20 mM Tris-HCl (pH 8.0) buffer containing 0.5 M NaCl, 5mM imidazole, and 1 mM phenylmethylsulfonyl fluoride. Cells were disrupted by a freeze-thawing cycle and by two passes through a French press at 20,000 pounds/square inch. Unbroken cells and cell debris

were removed by centrifugation at 12,000 *g* for 30 min at 4 ℃. The supernatant (cell lysate) was gently mixed with 2 ml of 50 % slurry of Ni^{2+}-NTA agarose for 2 h. The Ni^{2+}-NTA agarose/enzyme mixture was packed in a 10-ml column and washed with 20 ml of 20 mM Tris-HCl (pH 8.0) buffer containing 0.5 M NaCl, 45 mM imidazole, 10% glycerol, and 7 mM 2-mercaptoethanol. His_6-tagged App1p was eluted from the column in 1-ml fractions with 20 mM Tris-HCl (pH 8.0) buffer containing 0.5 M NaCl, 250 mM imidazole, 10% glycerol, and 7 mM 2-mercaptoethanol. Purified enzyme preparations were stored at -80 ℃.

Purification of Protein A-tagged App1p from *S. cerevisiae*

Yeast cells (~ 3 g wet weight) were disrupted with glass beads (0.5 mm diameter) using a Biospec Products Bead Beater in lysis buffer containing 20 mM Tris-HCl (pH 7.5), 150 mM KCl, 5 mM $MgCl_2$, 1% Triton X-100, and a cocktail of protease inhibitors. Unbroken cells and glass beads were removed by centrifugation at 1,500 x *g* for 10 min. The cell extract (supernatant) was precleared of contaminating proteins by incubation with 1 ml Sepharose Fast-Flow resin in a centrifuge tube. The enzyme sample was obtained by centrifugation at 1,500 x *g* for 10 min, and then it was passed through 0.2 ml IgG Sepharose resin packed in a Bio-Rad Poly-Prep chromatography column. The column was washed with 10 ml of lysis buffer followed by 10 ml of wash buffer containing 50 mM Tris-HCl (pH 8.0), 0.5 mM EDTA, 0.5 M NaCl. The resin was then transferred to a 1 ml spin column and incubated with an equal volume of elution buffer containing 50 mM Tris-HCl (pH 8.0), 0.5 mM EDTA, 0.5 M NaCl, 3 mM glutathione, 0.3 mM oxidized glutathione, and 100 units of tobacco etch virus protease. After incubation for 5 h, the column was subjected to a brief centrifugation and the eluted enzyme (supernatant) was transferred to another 1 ml spin containing a mixture of protein A-Sepharose resin (0.1 ml) and Ni^2 -NTA-agarose resin (0.1 ml) for the removal of contaminating IgG and tobacco etch virus protease. After 30 min incubation, the spin column was briefly centrifuged to obtain the purified

App1p PAP enzyme. The concentration of purified App1p was determined by the method of Bradford using bovine serum albumin as the standard. Enzyme concentration was also determined by ImageQuant analysis of App1p and bovine serum albumin standards in SDS-polyacrylamide gels stained with Coomassie Blue. Both methods of protein concentration determination yield similar results.

Native Molecular Mass Determination by Superdex 200 Chromatography

The native molecular mass of App1p was determined by gel filtration chromatography using a Superdex 200 HR 10/30 column attached to an Ä KTA fast protein liquid chromatography system. The buffer system used for the chromatography contained 50 mM Tris-HCl (pH 7.5) and 0.15 M NaCl, and the flow rate was 40 ml/h. The molecular mass standards were β-amylase (200 kDa), alcohol dehydrogenase (150 kDa), bovine serum albumin (66 kDa), carbonic anhydrase (29 kDa), and cytochrome c (12.4 kDa).

Preparation of [^{32}P]PA and Malachite Green-Molybdate Reagent

[^{32}P]PA was synthesized enzymatically from DAG and [γ-^{32}P]ATP using *E. coli* DAG kinase as described by Carman and Lin (152). A color reagent to detect inorganic free phosphate was prepared by modification of the procedure described by Mahuren *et al.* (153) and was composed of 3 volumes of 0.1 mm malachite green and 1 volume of 34 mm ammonium molybdate in 5 m HCl.

Preparation of Triton X-100/Lipid-mixed Micelles

PA in chloroform was transferred to a glass test tube, and the solvent was eliminated *in vacuo* for 1 h. Triton X-100 was added to PA to prepare Triton X-100/PA-mixed micelles. Micelles containing other lipids were prepared in the same manner. The mol % of a lipid in a

Triton X-100/lipid-mixed micelle was calculated using the following formula, mol $\%_{lipid}$ = 100 × [lipid (molar)]/([lipid (molar)] + [Triton X-100 (molar)]). The total lipid concentration in the Triton X-100/lipid-mixed micelles was kept below 15 mol % to ensure that the structure of the lipid-mixed micelles was similar to that of pure Triton X-100 micelles (154, 155)

PAP Assay and Protein Determination

PAP activity was measured for 20 min by following the release of water-soluble [^{32}P]P_i from chloroform-soluble [^{32}P]PA (~5,000 cpm/nmol) at 30 °C as described previously (151). The reaction mixture contained 50 mM Tris-HCl buffer (pH 7.5), 10 mM $MgCl_2$, 0.2 mM PA, 2 mM Triton X-100, 10 mM 2-mercaptoethanol, and enzyme protein in a total volume of 0.1 ml. For the characterization of App1p, a reaction mixture contained 50 mM Tris-HCl (pH 7.5) buffer, 1.0mM $MgCl_2$, 10 mM 2-mercaptoethanol, 2 mM dioleoyl [^{32}P]PA (5,00 cpm/nmol), 20 mM Triton X-100, and 1 ng of enzyme protein in a total volumer of 0.1 ml. Following phase separation, 0.5 ml of the aqueous (upper) phase was measured for radioactivity. In the assay with non-radioactive PA, the enzyme reaction was terminated as described above except that 1 m $MgCl_2$ was replaced with water. After phase separation, 1 volume of the upper phase was mixed with 2 volumes of malachite green-molybdate reagent, and the mixture was measured for absorbance at 650 nm. The same assay was used to examine the dephosphorylation of other nonradioactive lipid phosphate molecules. Enzyme assays were conducted in triplicate, and the average standard deviation of the assays was ± 5 %. All reactions were linear with time and protein concentration. A unit of enzyme activity was defined as the amount of enzyme that catalyzed the formation of 1 nmol or 1 μmol of product per minute. Protein concentration was estimated by the method of Bradford (156) using bovine serum albumin as the standard.

SDS-PAGE and Western Blot Analysis

SDS-PAGE (157) using 10 % slab gels and Western blotting (158, 159) using polyvinylidene difluoride membrane were performed as described previously. Proteins on polyacrylamide gels were visualized with Coomassie Blue R250. The anti-HA, anti-His_6, anti-Protein A and anti-App1p antibodies were used at a dilution of 1:5000. Alkaline phosphatase-conjugated goat anti-mouse IgG antibodies and goat anti-rabbit IgG antibodies were used at a dilution of 1:5,000. Immune complexes were detected using the enhanced chemifluorescence Western blotting detection kit. Fluorimaging was used to acquire images from Western blots.

Identification of Proteins by Tandem Mass Spectrometry

An SDS-polyacrylamide gel slice containing protein purified through the Superdex 200 chromatography step was subjected to trypsin digestion (160) followed by tandem mass spectrometry using a Thermo Fisher Scientific LTQ Obitrap Velos instrument (161) The spectra were searched against the Swiss-Prot yeast database using the MASCOT (V.2.3) search engine (160). The band on the gel containing purified from Protein A fusion App1p was digested with trypsin, and the peptides were analyzed by MALDI-TOF/TOF. This work was performed at the Center for Advanced Proteomics Research facility of the University of Medicine and Dentistry of New Jersey (Newark, NJ).

Labeling and Analysis of Lipids

Steady-state labeling of phospholipids and neutral lipids with $^{32}P_i$ and [2-^{14}C]acetate, respectively, were performed as described previously (86). Lipids were extracted from labeled cells by the method of Bligh and Dyer (162). Phospholipids were analyzed by two-dimensional thin-layer chromatography on silica gel plates using chloroform/methanol/ammonium hydroxide/water (45:25:2:3, v/v) as the solvent system for dimension one and chloroform/methanol/glacial acetic acid/water (32:4:5:1, v/v) as the solvent system for dimension two (163) Neutral lipids were

analyzed by one-dimensional thin-layer chromatography on silica gel plates using the solvent system hexane/diethyl ether/glacial acetic acid (40:10:1, v/v) (164). The identity of the labeled lipids on TLC plates was confirmed by comparison with standards after exposure to iodine vapor. Radiolabeled lipids were visualized by phosphorimaging analysis. The relative quantities of labeled lipids were analyzed using ImageQuant software. These experiments were performed by Gil-Soo Han.

Analyses of Data

Statistical analyses were performed with SigmaPlot software. Kinetic data were analyzed according to the Michaelis-Menten and Hill equations using the SigmaPlot enzyme kinetics module. Student's *t* test (SigmaPlot software) was used to determine statistical significance, and *p* values of <0.05 were taken as a significant difference.

RESULTS

PAP Activity is Purified from the *pah1*Δ *dpp1*Δ *lpp1*Δ Triple Mutant and is Identified as the Product of the *APP1* Gene

An NEM sensitive Mg^{2+}-dependent PAP activity is present *pah1*Δ *dpp1*Δ *lpp1*Δ mutant cells (86). This activity is found in both the soluble and membrane fractions of the cell, and its association with the membrane is peripheral in nature (86). The triple mutant was used to purify this PAP enzyme, and by doing so, we eliminated the activities encoded by *PAH1*, *DPP1*, and *LPP1* (80, 81, 86). PAP specific activity was enriched 5-fold in the mitochondrial fraction, and accordingly, this fraction was used as the source of enzyme. PAP activity was dissociated from the mitochondrial membranes with 1 M NaCl followed by chromatography with DE52 (Fig. 5), Affi-Gel Blue (Fig. 6), phenyl-Sepharose, MonoQ (Fig. 7), and Superdex 200 (Fig. 8). The Superdex 200 chromatography step afforded the greatest enrichment (4.5-fold) in specific activity (Table 2), and the peak fraction of activity emerged from the column at the position of the 66 kDa molecular mass standard (Fig. 8). An SDS-PAGE analysis indicated that the enzyme preparation was not homogeneous (Fig. 8). However, further attempts to purify the enzyme to homogeneity were unsuccessful, mainly because the PAP activity was labile. Overall, PAP was purified 2,143-fold over the cell extract to a final specific activity of 1,500 nmol/min/mg with an activity yield of 5 % (Table 2).

The peak of PAP activity that emerged from the Superdex 200 column correlated with the enrichment of a minor protein band that migrated near the size of the 50 kDa molecular mass marker (Fig. 8, fraction 27). An SDS-polyacrylamide gel slice containing this band was subjected to trypsin digestion followed by the analysis of peptides by liquid chromatography-tandem mass spectrometry. This analysis revealed that the minor band from the polyacrylamide gel contained 112 proteins (or proteolytic fragments thereof) (Table 3). We narorrowed down the list of

FIGURE 5. **Elution Profile of PAP Activity after DE52 Chromatography.** Salt extracts from mitochondrial membranes were subjected to the DE52 chromatography. Fractions (5 ml of each fraction) were collected and assayed for PAP activity (U = nmol/min/mg) (●) and protein (○) by Braford reagent. The NaCl gradient profile is indicated by the dashed line.

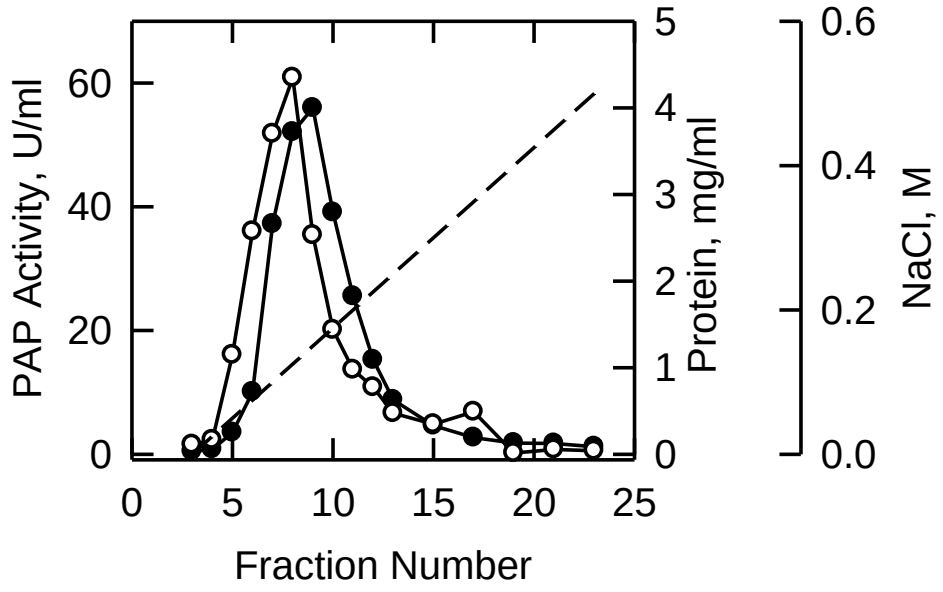
PAP Activity, U/ml
Protein, mg/ml
NaCl, M
Fraction Number
0
20
40
60
0
1
2
3
4
5
0.0
0.2
0.4
0.6
0
5
10
15
20
25

FIGURE 6. **Elution Profile of PAP Activity after Affi-gel Blue Chromatography.** The most active fractions from the DE52 chromatography were subjected to the Affi-Gel Blue chromatography. Fractions (3 ml of each fraction) were collected and assayed for PAP activity (●) and protein (○) by Braford reagent. The NaCl gradient profile is indicated by the dashed line.

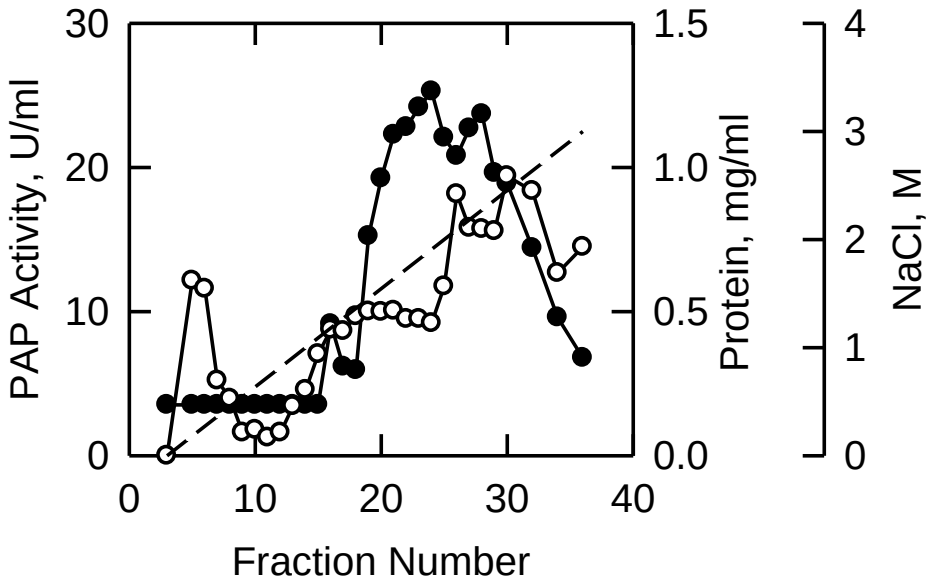
30
20
10
0
PAP Activity, U/ml
1.5
1.0
0.5
0.0
Protein, mg/ml
4
3
2
1
0
NaCl, M
0
10
20
30
40
Fraction Number

FIGURE 7. **Elution Profile of PAP activity after MonoQ Chromatography.** The active fractions from the phenyl-Sepharose chromatography were subjected to the Mono Q chromatography. Fractions (1 ml of each fraction) were collected and assayed for PAP activity (●) and protein (○) by the absorbance at 280 nm. The NaCl gradient profile is indicated by the dashed line.

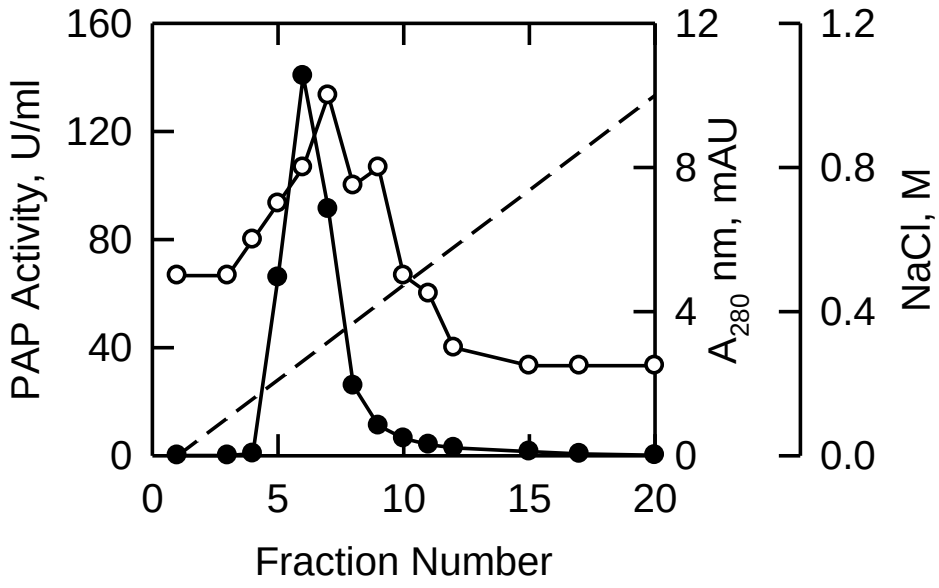
160
120
80
40
0
PAP Activity, U/ml
12
8
4
0
A_{280} nm, mAU
1.2
0.8
0.4
0.0
NaCl, M
0
5
10
15
20
Fraction Number

FIGURE 8. **Elution Profile of PAP activity after Superdex 200 Chromatography and SDS-PAGE of the Purified Enzyme.** The MonoQ-purified PAP enzyme preparation was subjected to Superdex 200 chromatography. Fractions (0.5 ml of each fraction) were collected and assayed for PAP activity (●) and protein (○). Fractions 24-30 were subjected to SDS-PAGE followed by staining with Coomassie Blue (*above plot*). The band derived from fraction 27 that was used for protein sequencing is indicated by the *asterisk*.

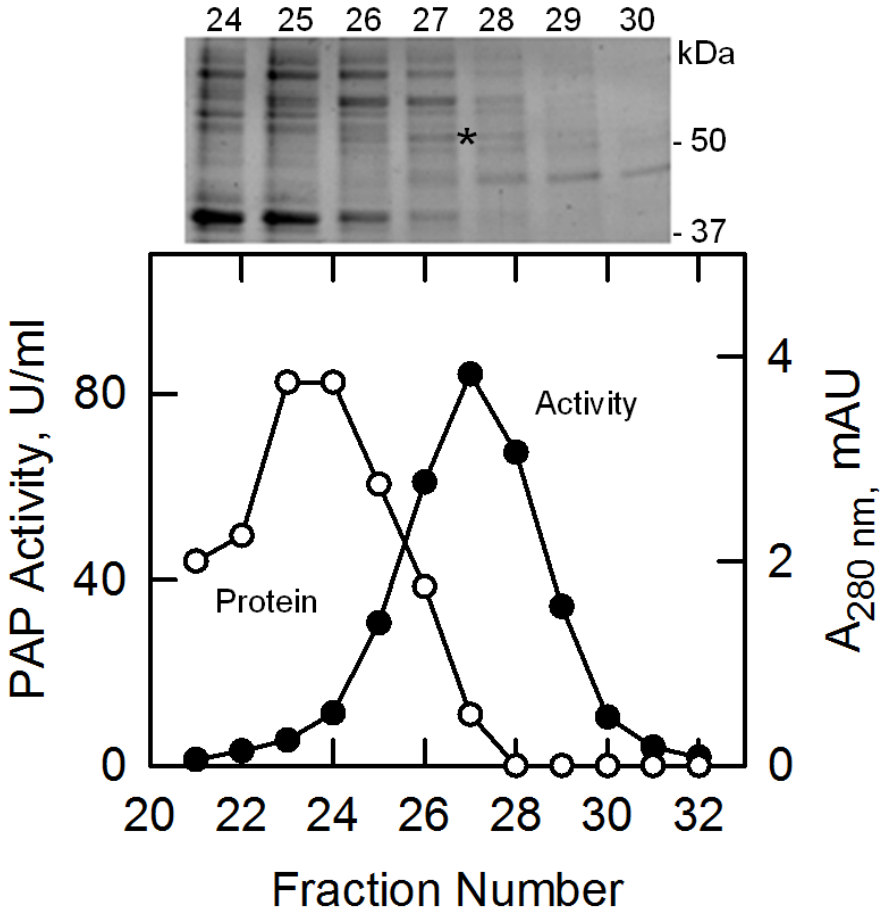
24 25 26 27 28 29 30
kDa
- 50
- 37
*
PAP Activity, U/ml
80
40
0
Activity
Protein
4
2
0
$A_{280\ nm}$, mAU
20 22 24 26 28 30 32
Fraction Number

TABLE 2. Partial Purification of PAP from *S. cerevisiae*.
PAP was purified from *pah1*Δ *dpp1*Δ *lpp1*Δ mutant cells as described under "Experimental Procedures." The data are based on starting with 200 g (wet weight) of cells.

Purification step	Total units	Protein	Specific activity	Yield	Purification
	nmol/min	*Mg*	*units/mg*	*%*	*-fold*
1. Cell extract	3237	4625	0.7	100	1
2. Mitochondria	2200	628	3.5	68	5
3. NaCl extract	1745	346	5	54	7
4. DE52	1053	65	16	33	23
5. Affi-Gel Blue	770	20	39	24	56
6. Phenyl-Sepharose	545	4	137	17	196
7. MonoQ	300	0.9	330	9	471
8. Superdex 200	150	0.1	1500	5	2143

TABLE 3. Mass Spectrometry Analysis.
Proteins containing a phosphatase motif were indicated in bold.

Standard Name	MM (kDa)	Standard Name	MM (kDa)	Standard Name	MM (kDa)	Standard Name	MM (kDa)	Standard Name	MM (kDa)	Standard Name	MM (kDa)	Standard Name	MM (kDa)	Standard Name	MM (kDa)
ORC1	104	*CBF1*	39	***GCD11***	58	*MDM20*	*55*	*SPO14*	195	*RSP5*	92	*TRP2*	54	*YFR006W*	62
GND1	54	*CCR4*	94	*SEC2*	85	*BLM3*	*75*	*ADE4*	57	***SAC1***	71	*UBP3*	102	*YGL004C*	46
SSK2	181	*CDC19*	56	***GLK2***	55	*LEU1*	*83*	*SER1*	43	***CDC3***	60	*UBP6*	57	*YGL110C*	72
ALA1	107	*VPS13*	358	*GLT1*	238	*DBF20*	*66*	*PAB1*	64	*SET3*	86	*VTC4*	75	*YGR266W*	81
ATF1	61	*RGR1*	123	*SEC12*	52	*KRE2*	*51*	*PHM1*	95	*FKS3*	207	*FOL1*	98	*YJL049W*	53
APP1	66	***YLR345W***	58	*DYN1*	238	*KTR7*	*61*	*YBR139W*	58	*SRO9*	52	*UTP7*	62	*YJR098C*	74
GGA2	64	*BNR1*	220	***HXK2***	54	*AI2*	*98*	*PTP2*	86	*SRP1*	49	*VTC3*	96	*YMR192W*	82
HOM3	58	***LAT1***	52	*SOK1*	101	*MDM38*	*65*	*PUB1*	51	***SSA2***	69	*YAR042W*	135	*YNL077C*	59
TRA1	433	*POL1*	60	*NRG2*	25	*SSC1*	*71*	*RAP1*	92	*ERG6*	43	*YBL004W*	288	*YOL098C*	118
ISW1	131	*YDR444W*	78	*HOS3*	79	*MVP1*	*60*	*ENP2*	82	***YNL209W***	67	*YCG1*	120	*YOR227W*	139
TUB2	51	***EMI2***	56	*UTR1*	60	*TRM1*	*64*	*REH1*	50	***TED1***	55	*YDR023W*	51	*YOR374W*	57
POB3	55	*ENT5*	45	*IMI1*	182	*PDC1*	*61*	*SRO9*	52	*GDB1*	175	*YDR432W*	35	*YPR031W*	86
BRE3	47	*ERG11*	52	*KEL1*	131	*PFK1*	*108*	*RPA190*	186	*TEF2*	31	*YDR485C*	92	*YTA12*	93
BRE5	58	*FRA1*	85	*CDC54*	105	*PFK2*	*105*	*RRP6*	84	*TRL1*	95	*YER166W*	178	*ZPR1*	55

of proteins that might be a product of a PAP gene by choosing those proteins without an identified molecular function and possessed a phosphatase motif. I also considered proteins whose genes showed genetic interactions with other genes involved in lipid metabolism. Based on these criteria, cell extracts derived from twenty mutants from the yeast deletion strain collection (mutants derived from BY4741) for a defect in PAP activity were examined. One of the mutants, namely *app1*Δ exhibited a decrease (50 %) in cytosolic PAP activity when compared with the wild type parental strain (Fig. 9). I then constructed the *app1*Δ mutation in the W303-1A genetic background so that all of our PAP mutants (see below) were isogenic (Table 1). This *app1*Δ mutant (strain GHY63) also exhibited a reduced (32 %) PAP activity in the cell extract. This result provided confidence that I might have identified *APP1* as the gene encoding the enzyme. The gene acronym stands for actin patch protein because its product App1p is a component of cortical actin patches (166-173). App1p is annotated in the *Saccharomyces* genome database as a protein of unknown function. Coincidently, App1p has a subunit molecular mass of 66.1 kDa (587 amino acids in length).

I used heterologous expression of the *S. cerevisiae APP1* gene in *E. coli* to further test the hypothesis that the gene encodes a PAP enzyme. The purified His_6-tagged App1p migrated upon SDS-PAGE at the expected size (Fig. 10A). In addition, the purified protein reacted with antibodies directed against the His_6 epitope and against a peptide sequence found at the C-terminal portion of App1p (Fig. 10A). Moreover, the purified protein exhibited PAP activity and this activity was almost completely inhibited by NEM (Fig. 10B). These data established that *APP1* is a *bona fide* structural gene encoding a PAP enzyme in *S. cerevisiae*.

PAP Activity is Affected by the *app1*Δ, *pah1*Δ, *dpp1*Δ, *lpp1*Δ Mutations and by the *APP1*(D281E) Mutation

The analysis of the *app1*Δ *pah1*Δ *dpp1*Δ *lpp1Δ* quadruple mutant indicated that all

FIGURE 9. **PAP Activity in Various Mutants.** Cytosols were prepared from the indicated cells at the exponential phase of growth and assayed for PAP activity. The data shown are means ± S.D. from triplicate enzyme determinations.

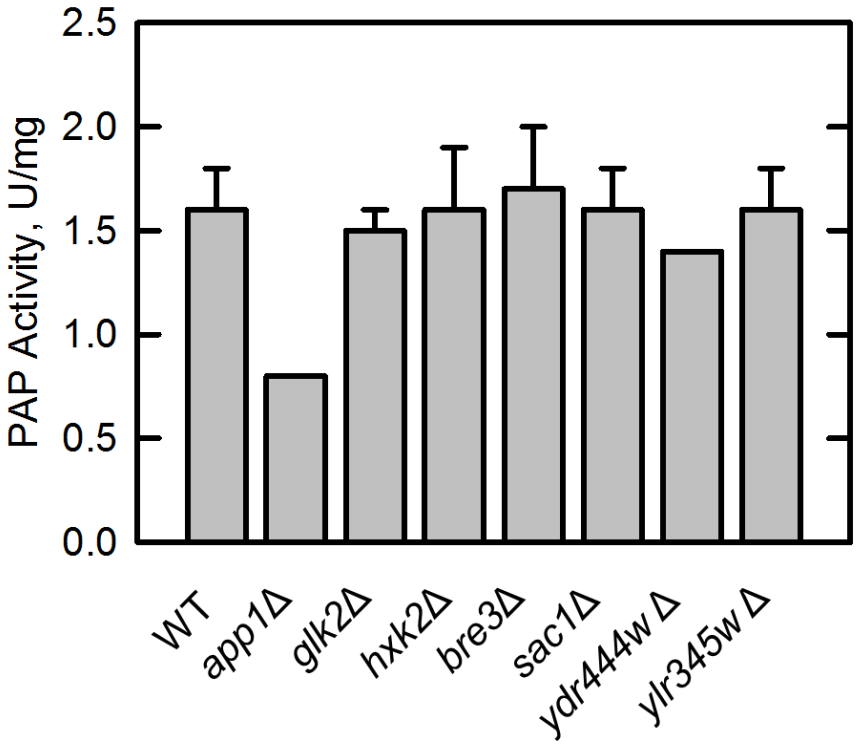
PAP Activity, U/mg
2.5
2.0
1.5
1.0
0.5
0.0
WT
app1Δ
glk2Δ
hxk2Δ
bre3Δ
sac1Δ
ydr444w Δ
ylr345w Δ

FIGURE 10. **SDS-PAGE and Western Blot Analysis of His_6-tagged App1p Purified from *E. coli* and the PAP Activity of the Purified Enzyme.** *A,* molecular mass standards (*Std*) and His_6-tagged App1p (1 µg) purified from *E. coli* were subjected to SDS-PAGE and stained with Coomassie Blue (*left*). The purified His_6-tagged App1p (samples of 1 µg and 1 ng, respectively) was subjected to Western blot analysis using a 1:5000 dilution of anti-His_6 (*αHis_6*) and anti-App1p (*αApp1p*) antibodies, respectively (*right*). *B,* PAP activity (U = µmol/min) of purified His_6-tagged App1p measured in the absence and presence of 20 mM *N*-ethylmaleimide (*NEM*). The data in *A* were representative of two experiments, whereas the data in *B* were the average of three experiments ± S.D. (*error bars*).

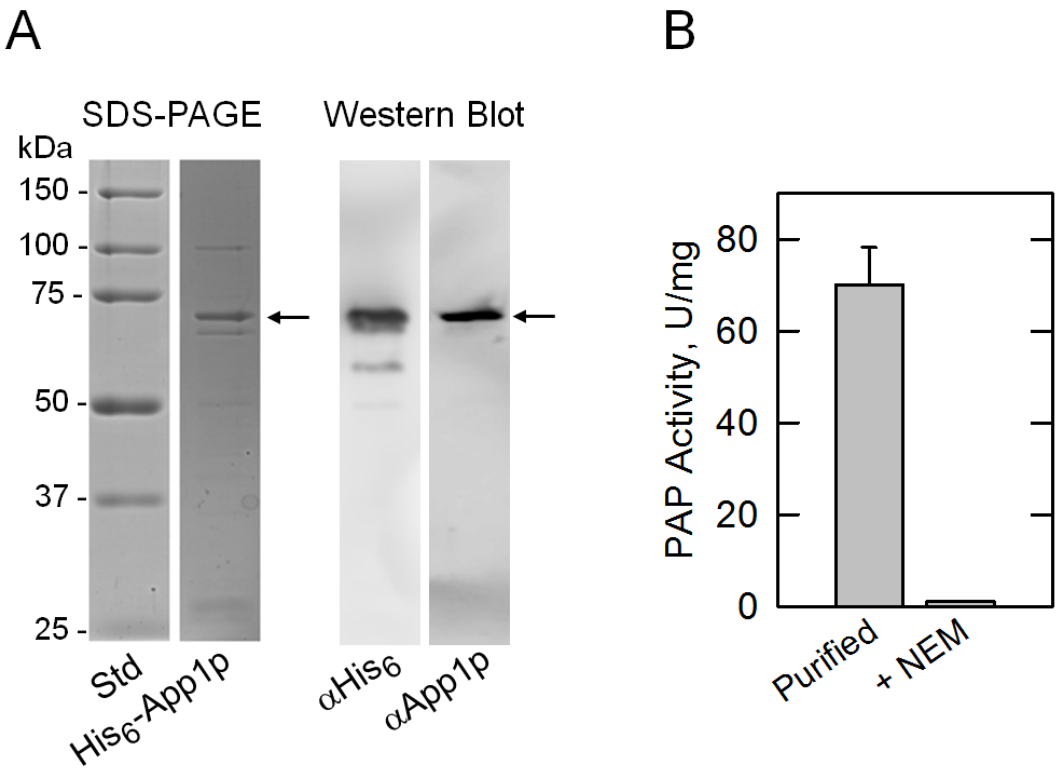
A
SDS-PAGE
Western Blot
kDa
150 -
100 -
75 -
50 -
37 -
25 -
Std
His6-App1p
αHis6
αApp1p
B
PAP Activity, U/mg
80
60
40
20
0
Purified
+ NEM

detectable PAP activity in *S. cerevisiae* was attributed to *APP1*, *PAH1*, *DPP1* and *LPP1* (Fig. 11). The *APP1* coding sequence along with its 5'- and 3'-flanking sequences was amplified by PCR using genomic DNA from strain W303-1A as the template. The fidelity of the gene sequence was confirmed by DNA sequencing. *APP1* and *HA-APP1* versions were expressed on a multicopy plasmid in the *app1*Δ *pah1*Δ *dpp1*Δ *lpp1Δ* quadruple mutant, cell extracts were prepared, and used for the measurement of PAP activity.Both plasmids directed the overexpression of PAP to specific activities of 6.8 ± 0.7 and 6.5 ± 0.6 nmol/min/mg, respectively (Fig. 11), indicating that the HA epitope did not compromise enzyme function. App1p contains a D*X*D*X*T/V (residues 281-285) motif found in the superfamily of Mg^{2+}-dependent phosphatase enzymes (95) that include the Pah1p PAP (86), but not the Dpp1p (80) and Lpp1p (81) PAP enzymes. The first conserved aspartate residue in the motif was mutated to glutamate by site-specific mutagenesis. Glutamate was chosen to replace aspartate to conserve the charge of the amino acid at this position, and thus, preserve enzyme structure. The D281E mutation abolished the overexpressed PAP activity directed by the *APP1* and *HA-APP1* genes (Fig. 11). An immunoblot analysis using anti-HA antibodies showed that the D281E mutation in the HA-tagged version of App1p did not affect the expression of the enzyme (Fig. 11, *inset*). These data indicated that the D*X*D*X*T/V catalytic motif in App1p is responsible for its PAP catalytic function.

Protein A-tagged App1p PAP was Purified from Yeast

We expressed App1p fused with Protein A sequence at the C terminus under *GAL1*-inducible promoter in yeast. A significant proteolysis of the expressed App1p-PtA in cell extracts was observed by probing with anti-Protein A antibody. However, SDS-PAGE anaylsis showed that affinity purification using IgG-Sepharose and TEV protease digestion resulted in highly purified enzyme preparation (Fig. 12). One single protein band at the predicted size of ~68 kDa was observed and sequence of the band was confirmed as App1p by mass spectrometry. Native

FIGURE 11. **PAP activity is Affected by the *app1*Δ, *pah1*Δ, *dpp1*Δ, *lpp1*Δ Mutations, the Overexpression of the *APP1* Gene, and the *APP1*(D281E) Mutation.** Cell extracts were prepared from the indicated cells at the exponential phase of growth and assayed for PAP activity. *Inset*, samples (50 μg protein) of the cell extracts were subjected to Western blot using anti-HA antibodies. *Lanes a*, *b*, and *c*correspond to the *app1*Δ, *pah1*Δ, *dpp1*Δ, *lpp1*Δ quadruple mutant (*QM*), and the QM mutant overexpressing *HA-APP1* and *HA-APP1*(D281E), respectively. The *arrow* indicates the position of HA-tagged App1p. The activity data shown in *A* and *B* were the average of three experiments ± S.D. (*error bars*), whereas the Western blot shown in *B* is representative of three experiments.

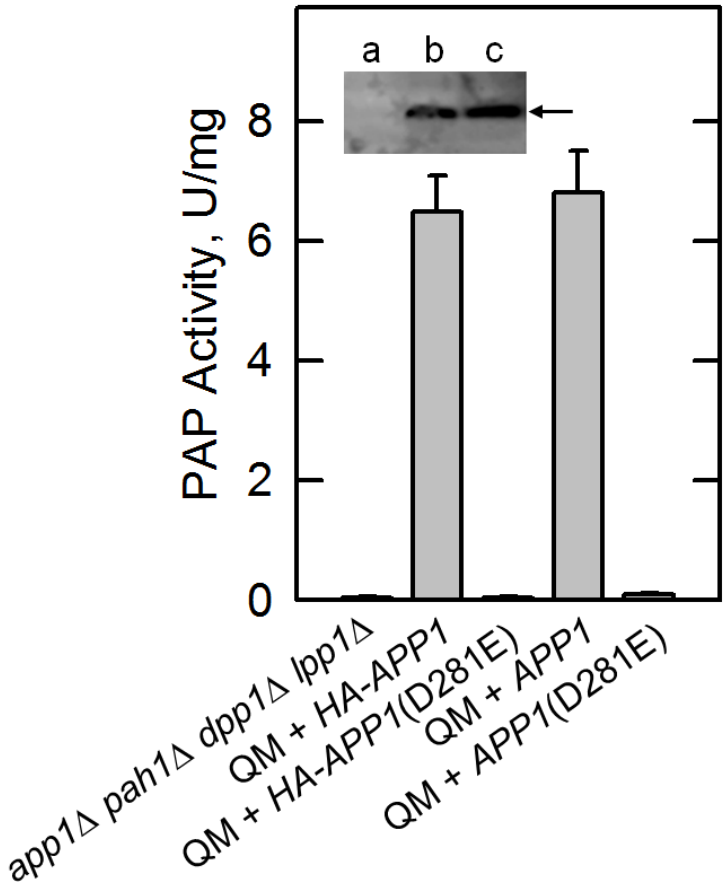
a
b
c
PAP Activity, U/mg
0
2
4
6
8
app1Δ pah1Δ dpp1Δ lpp1Δ
QM + HA-APP1
QM + HA-APP1(D281E)
QM + APP1
QM + APP1(D281E)

molecular mass was estimated as 66 kDa by Superdex 200 gel filtration (Fig 13).

Enzymological Properties of App1p PAP

The protein exhibited PAP activities in the range of the pH 6.5-8.5, with optimum activities at pH 7.5 (Fig. 14). The App1p PAP activities were dependent on either Mg^{2+} or Mn^{2+} ions, with Mg^{2+} being the preferred cofactor based on maximum activities (Fig. 15). The activity at optimum concentration of Mn^{2+} at 40 µM exhibited 58 % of the activity at optimum concentration of Mg^{2+} at 1 mM. Concentrations of Mg^{2+} or Mn^{2+} above their optimums resulted in the inhibition of PAP activity. With Mg^{2+} as the cofactor, the PAP activity was inhibited by the addition of 1mM concentration of Ca^{2+}, Mn^{2+} and Zn^{2+} by 81, 95 and 96 %, respectively (Fig. 16). The equilibrium constant for the App1p PAP reaction was determined using 2 mM PA allowing the reaction to come to equilibrium (Fig. 17). At equilibrium (45 min), the concentration of DAG and Pi was 1.8 mM. The equilibrium constant was calculated to be 16.2, indicating that the forward reaction was favored *in vitro*.

NEM sensitivity has been studied on Mg^{2+}-dependent PAP and Mg^{2+} -independent PAP. The Pah1p and Dpp1p enzymes are known to be NEM sensitive whereas the Lpp1p and residual PAP in *pah1*Δ *dpp1*Δ *lpp1*Δ enzymes are NEM-insensitive (79, 84). NEM inhibited the App1p PAP activity in a dose dependent manner (Fig. 18A). At a concentration of 10 mM, NEM inhibited the activity by 63%. In addition, the enzyme activity was stimulated (79%) by the addition of 10 mM β-ME to assay systems that did not contain NEM (Fig. 18B). The effect of general phosphatase inhibitors on the App1p PAP was examined. ProPr (non-selective β-blocker) at a concentration of 2.5 mM, and higher concentration of phenylglyoxal (an arginine reactive compound) at 20 mM inhibited the activity by about 90% (Fig. 19).

FIGURE 12. **SDS-PAGE Analysis of the Purified App1p from Yeast.** the App1p-PtA was purified by IgG-Sepharose and Protein A fusion was cleaved by tobacco etch virus (TEV) protease. Purified App1p (1.25 µg) was subjected to SDS-PAGE and stained with Coomassie Blue.

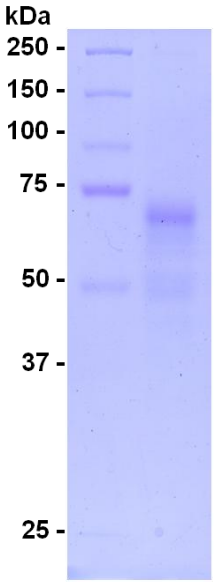
kDa
250 -
150 -
100 -
75 -
50 -
37 -
25 -

FIGURE 13. **Calibration Curve for the Determination of Native Molecular Mass of the App1p PAP**. Marker Protein β-amylase (200 kDa), alcohol dehydrogenase (150 kDa), bovine serum albumin (66 kDa), carbonic anhydrase (29 kDa) and cytocrome C (12.4 kDa) were applied on Superdex 200 column, and the values of ratio elution volume (Vo) to the void volume (Vo) were determined. The void volume was determined by the elution of blue dextran (2,000 kDa). The curve was plotted as log molecular mass (kDa) of protein standards *versus* Ve/Vo. The peak activity of App1p PAP was eluted out at the fraction where the 66 kDa albumin was eluted.

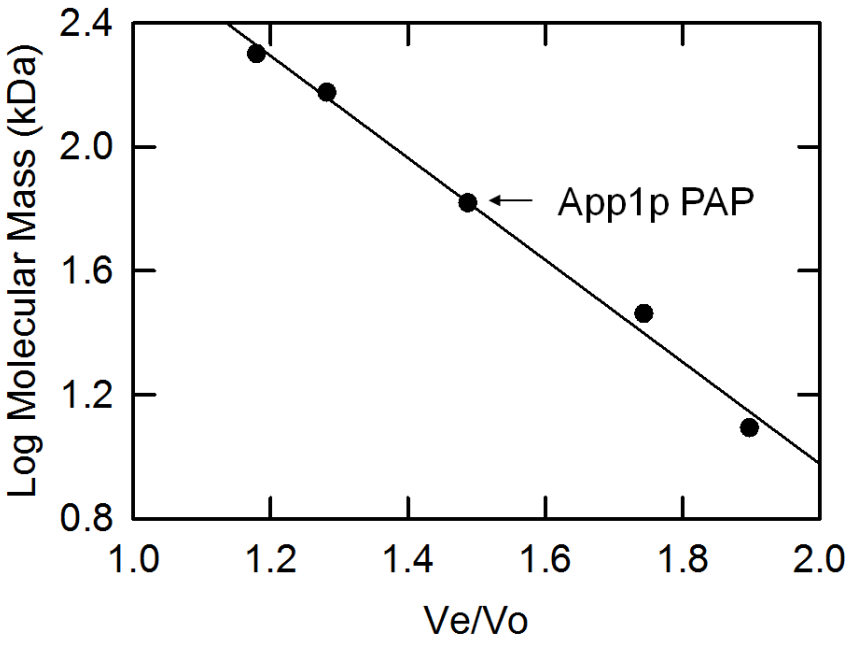
Log Molecular Mass (kDa)
2.4
2.0
1.6
1.2
0.8
1.0
1.2
1.4
1.6
1.8
2.0
Ve/Vo
App1p PAP

FIGURE 14. **Effects of pH on App1p PAP Activity.** PAP activity (U = µmol/min) was measured at the indicated pH values with 50mM Tris-maleate-glycine buffer. The data shown are means ± S.D. from triplicate enzyme determinations.

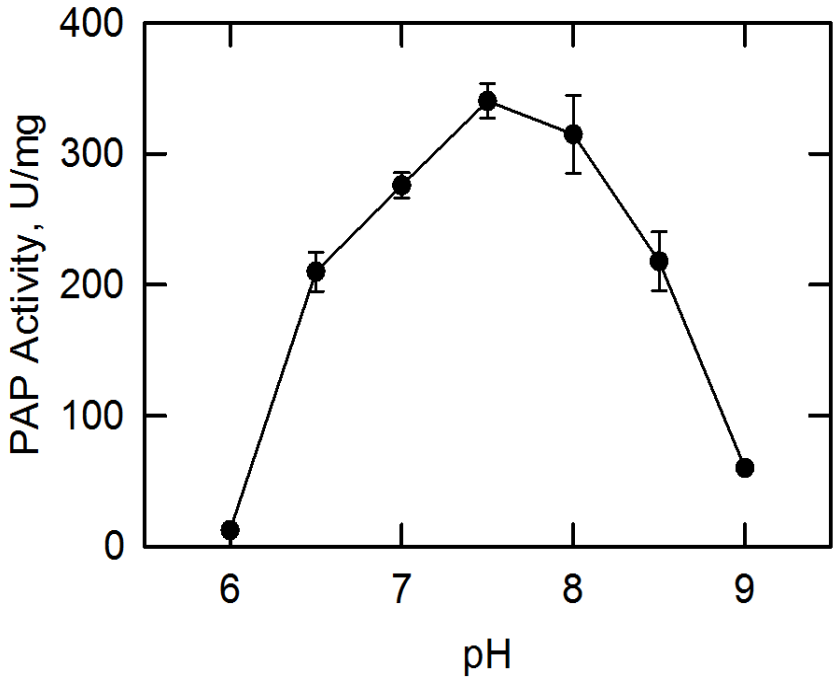
400
300
200
100
0
PAP Activity, U/mg
6
7
8
9
pH

FIGURE 15. **Effects of Mg^{2+} and Mn^{2+} on App1p PAP Activity.** PAP activity was measured in the absence and presence of the indicated concentration of $MgCl_2$ or $MnCl_2$.The data shown are means ± S.D. from triplicate enzyme determinations.

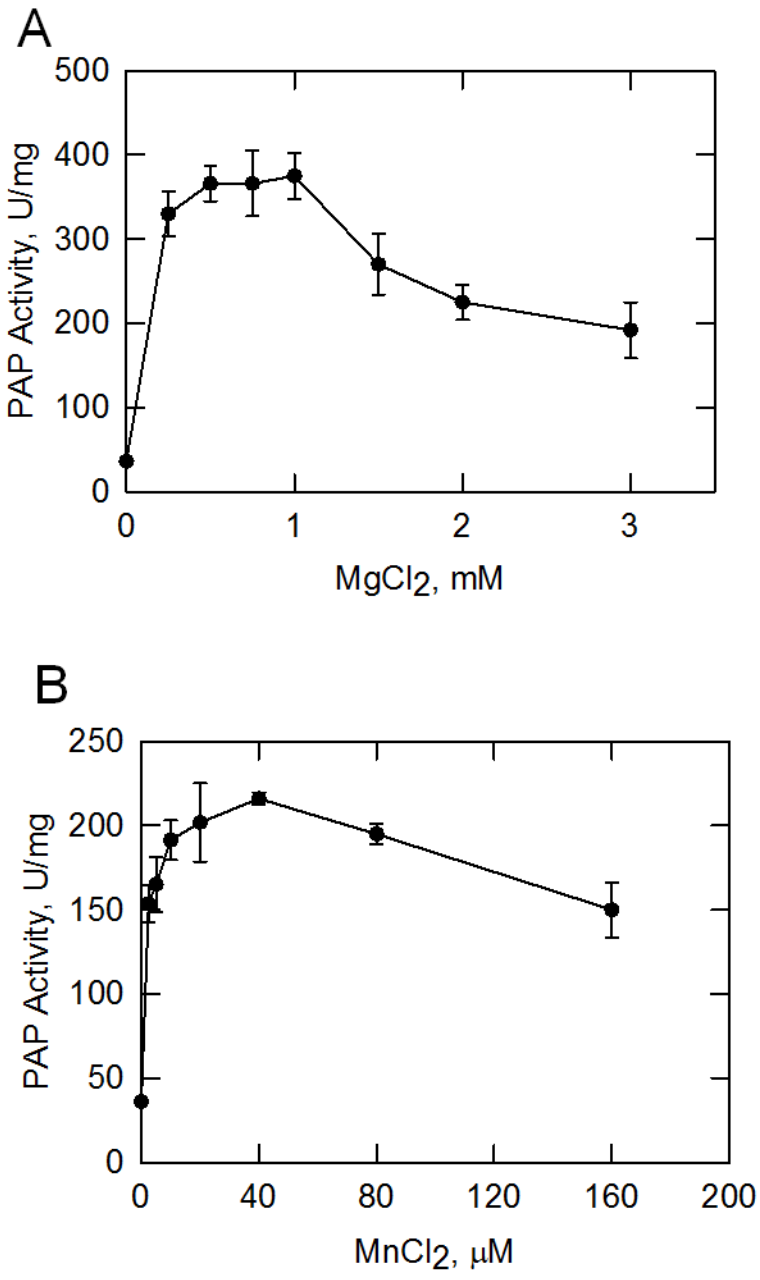
A
500
400
300
200
100
0
PAP Activity, U/mg
0
1
2
3
MgCl2, mM
B
250
200
150
100
50
0
PAP Activity, U/mg
0
40
80
120
160
200
MnCl2, μM

FIGURE 16. **Effects of Divalent Cations on App1p PAP Activity.** PAP activity was measured in the presence of the indicated concentration of $CaCl_2$, $MnCl_2$ and $ZnCl_2$. The data shown are means ± S.D. from triplicate enzyme determinations.

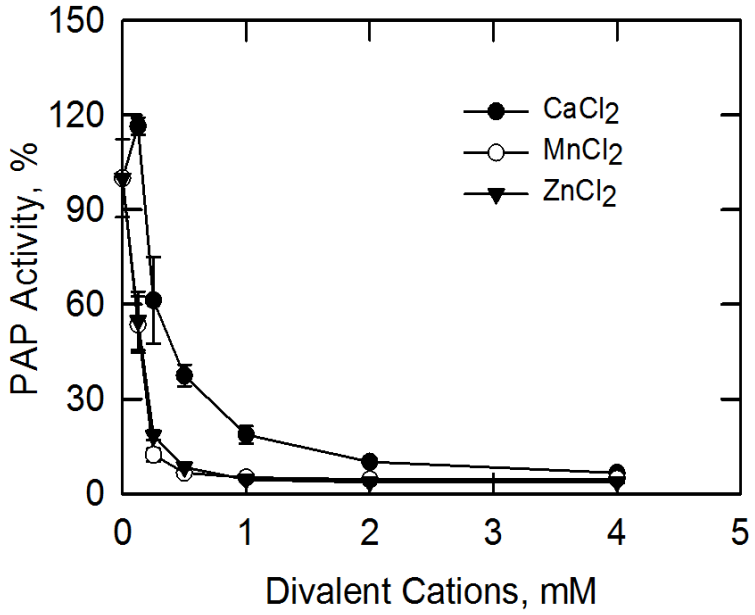
150
120
90
60
30
0
PAP Activity, %
0
1
2
3
4
5
Divalent Cations, mM
CaCl2
MnCl2
ZnCl2

FIGURE 17. **Equilibrium Constant of the App1p PAP Reaction.** The equilibrium constant for the App1p PAP reaction was determined using 2 mM PA. The formation of DAG was measured at indicated time point. The data shown are means ± S.D. from triplicate enzyme determinations.

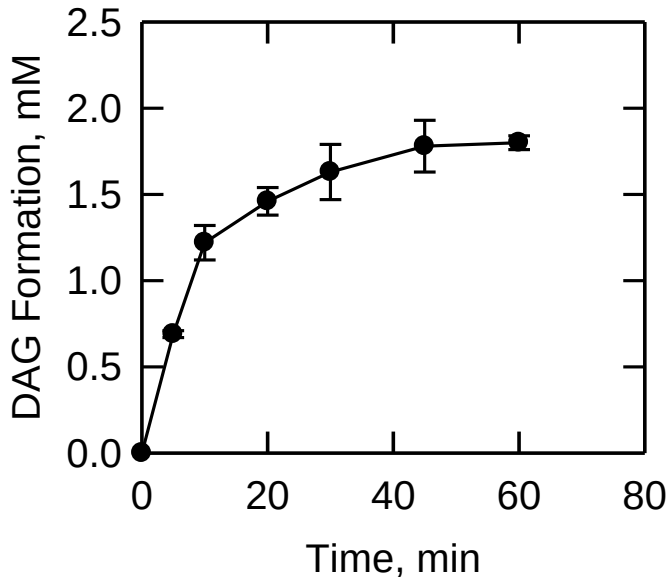
DAG Formation, mM
2.5
2.0
1.5
1.0
0.5
0.0
0
20
40
60
80
Time, min

FIGURE 18. **Effects of NEM and β-ME on App1p PAP Activity.** PAP activity was measured in the presence of the indicated concentration of NEM (*A*) or β-ME (*B*). In A, β-MEwas not present. The data shown are means ± S.D. from triplicate enzyme determinations.

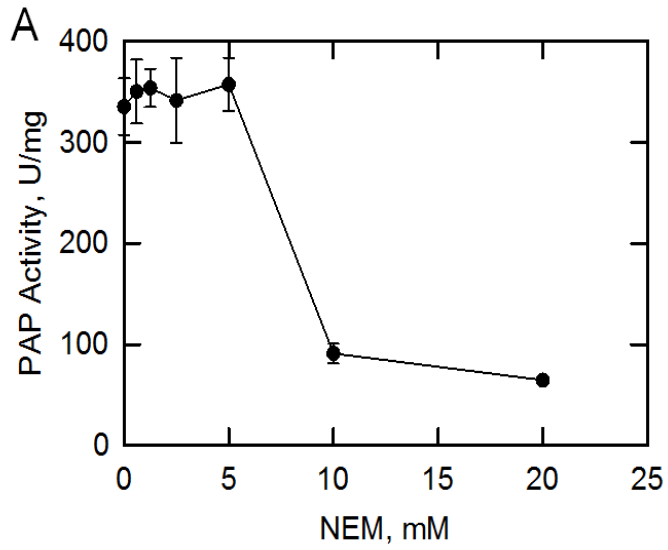
A
400
300
200
100
0
PAP Activity, U/mg
0
5
10
15
20
25
NEM, mM

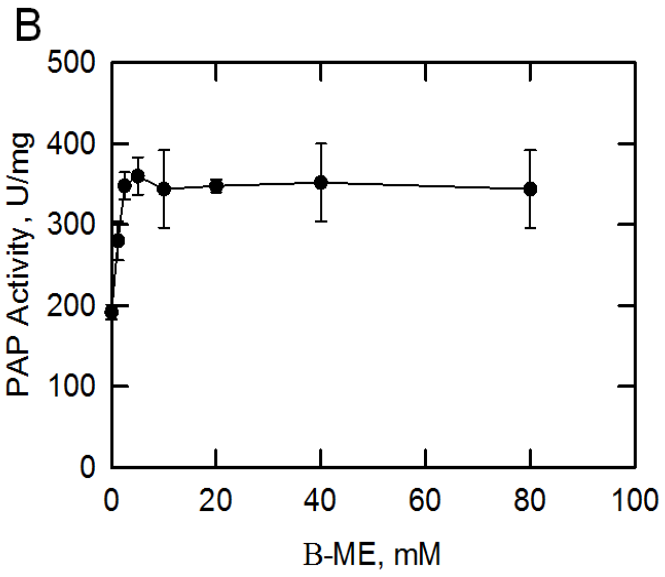
B
500
400
300
200
100
0
PAP Activity, U/mg
0
20
40
60
80
100
B-ME, mM

FIGURE 19. **Effect of Phenylglyoxal and ProPr on App1p PAP Activity.** PAP activity was measured in the presence of the indicated concentration of phenylglyoxal (*A*) and proPr (*B*). The enzyme samples were incubated for 50 min at 30 ^{0}C with the indicated concentration of phenlyglyoxal (*A*) and proPr (*B*) in the standard reaction mixture minus substrate. Following incubation, [γ-^{32}P] labeled substrate was added to the reaction mixtures and PAP activity was measured for 20 min in a 30 ^{0}C. 100 % activity is 370 U/mg.

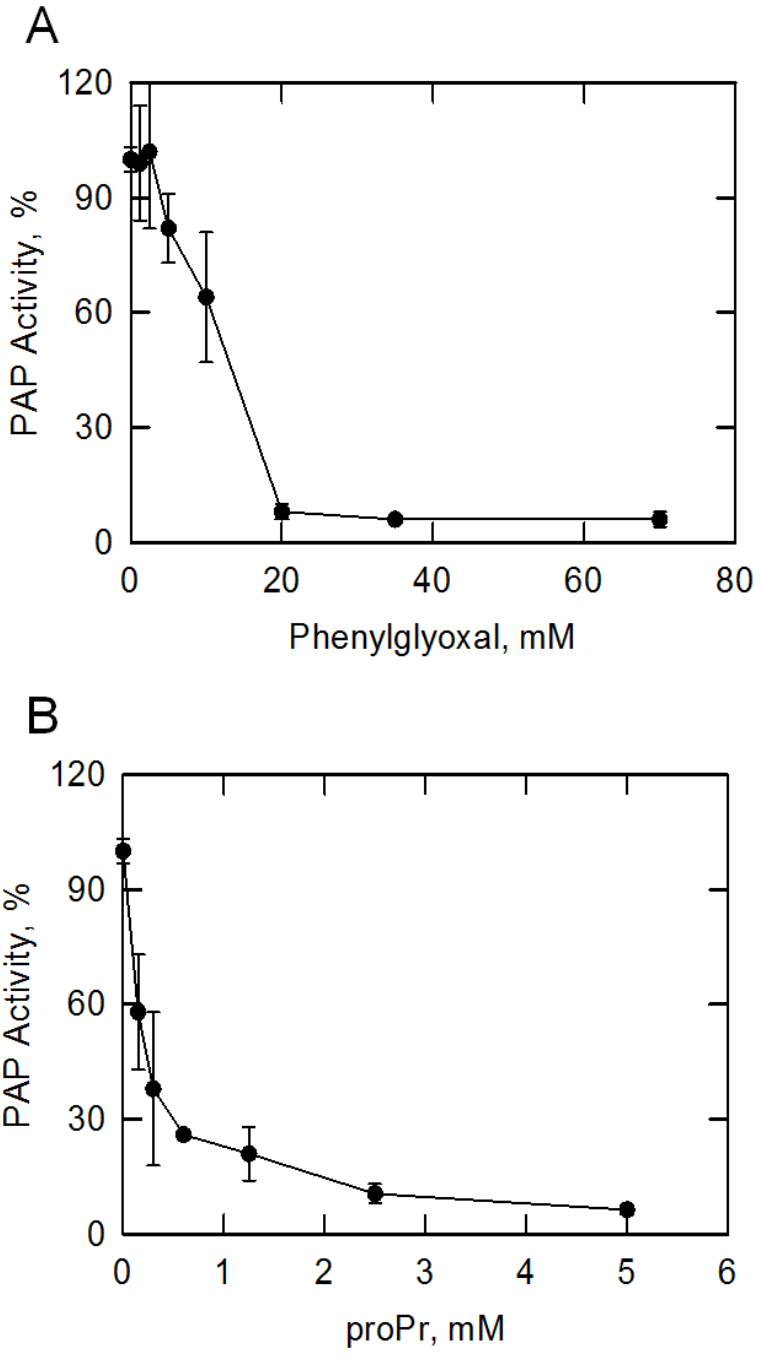
A
120
90
60
30
0
PAP Activity, %
0
20
40
60
80
Phenylglyoxal, mM
B
120
90
60
30
0
PAP Activity, %
0
1
2
3
4
5
6
proPr, mM

Effect of Temperature on App1p PAP

The effect of temperature on the App1p PAP activity was examined. Maximum activity was observed at 30 ^{0}C and was essentially inactive at 50 ^{0}C (Fig. 20A). Arrhenius plots of the data from 0 to 30 ^{0}C were constructed and the energy of activation was calculated to be 16.5 kcal/mol (Fig. 20B). The App1p PAP was examined for its thermal stabilities by preincubation at temperatures ranging from 0 to 70 ^{0}C for 20 min (Fig. 21). Following the preincubation, the enzyme samples were cooled on ice for renaturation and then measured for PAP activity at 30 ^{0}C. A loss of the PAP activity of the App1p PAP was minor after preinculation at 30 ^{0}C, whereas 83% of the activity was lost at 40 ^{0}C (Fig. 21).

Kinetic Properties of App1p PAP

The kinetics analysis of the App1p PAP was performed using Triton X-100/PA mixed micelles. This micelle system permitted the analysis of the PAP activity in an environment that mimics the surface of the cellular membrane (116, 174). To examine an enzyme according to surface dilution kinetics, activity is measured as a function of the bulk concentration of PA at a series of set surface concentrations of PA. Activity was dependent on the bulk concentration of PA. As the mol % of PA of the mixed micelle decreased, there was a decrease in the apparent V_{max} (Fig. 22A). A double-reciprocal plot of the results showed that PAP exhibited saturation kinetics when the bulk concentration of substrate was varied at each fixed mol % of PA (Fig. 22B). The equation predicts that a replot of the *1/V* intercepts *versus 1/B* from Fig. 14B should be linear and the intercept of the *1/V* intercept axis is $1/V_{max}$ and the intercept of the *1/B* axis is $-1/xK_m^B$ (Fig. 22C). A replot of the data was linear and the V_{max} and xK_m^B were calculated to be 557 µmol/min/mg and 4.2 mol %. The equation also predicts that a replot of the slopes versus *1/B* from should be linear and pass through the origin. The slope of the replot is equal to nK_s^A

FIGURE 20. **Effects of Temperature on App1p PAP Activity.** *A*, PAP was measured at the indicated temperatures for 20 min in a temperature controlled water bath. *B*, the data in *A* from 0 to 30 ^{0}C were plotted as log PAP activity *versus* the reciprocal of the absolute temperature (1/^{0}K). The curves drawn were a result of a least squares analysis of the data. The data shown are means ± S.D. from triplicate enzyme determinations.

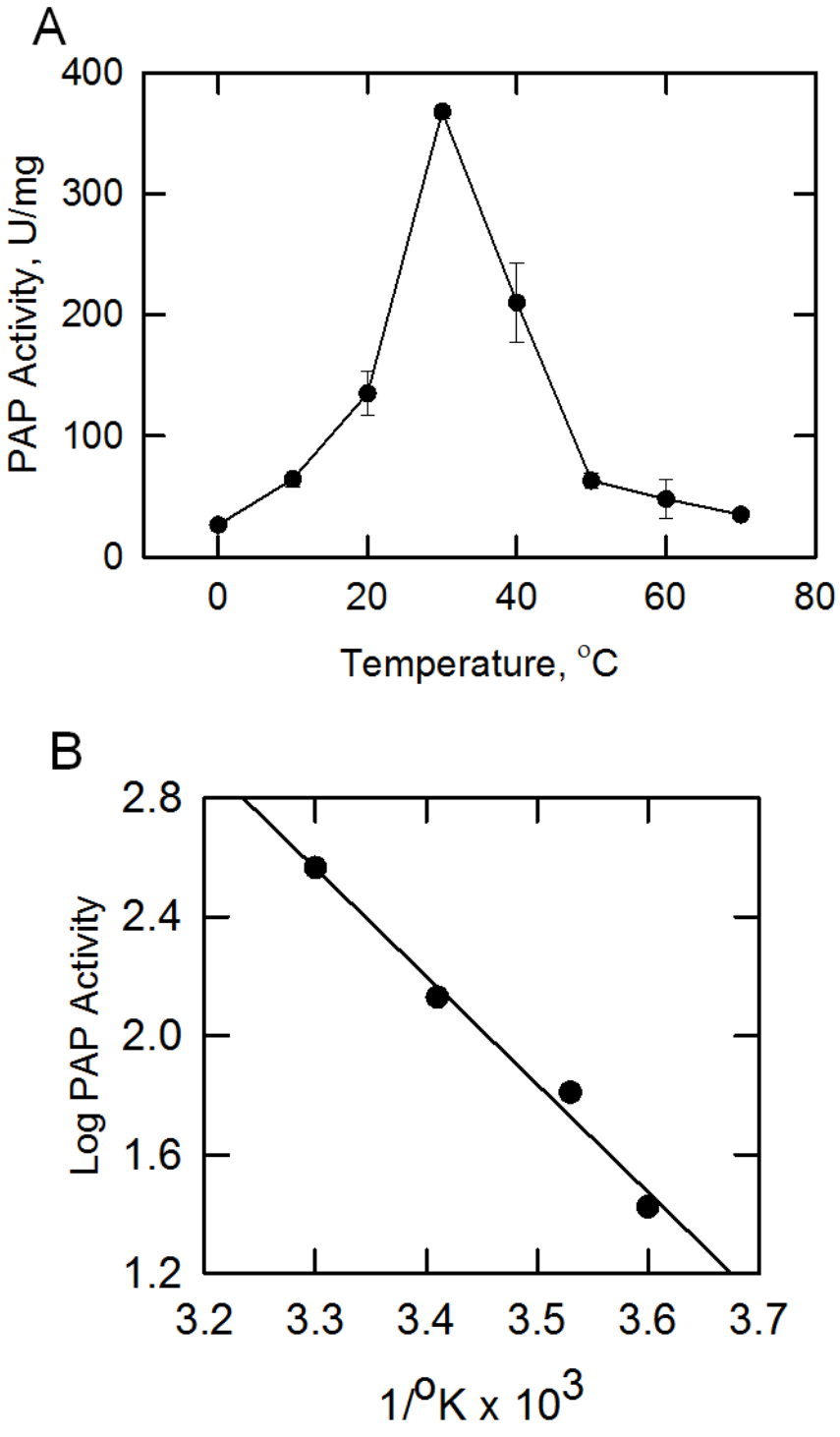
A
400
300
200
100
0
PAP Activity, U/mg
0
20
40
60
80
Temperature, °C
B
2.8
2.4
2.0
1.6
1.2
Log PAP Activity
3.2
3.3
3.4
3.5
3.6
3.7
1/°K x 10^3

FIGURE 21. **Effects of Temperature on the Stability of App1p PAP Activity.** The enzyme samples were first incubated for 20 min at the indicated temperatures. After incubation, the samples were cooled in an ice bath for 10 min allow for enzyme renaturation, and PAP was measured for 20 min in a 30 ^{0}C. The data shown are means ± S.D. from triplicate enzyme determinations.

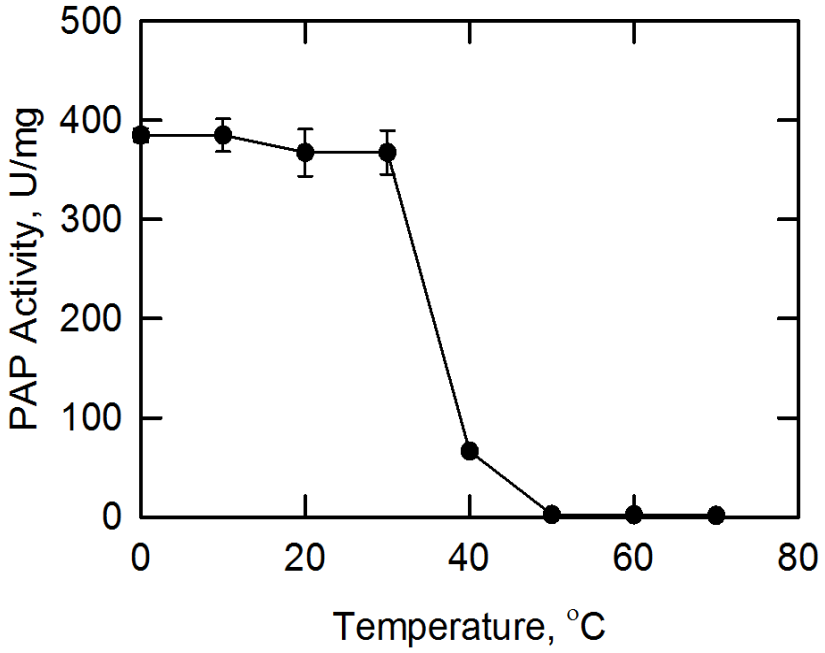
500
400
300
200
100
0
PAP Activity, U/mg
0
20
40
60
80
Temperature, °C

FIGURE 22. **Activity of PAP toward PA in Mixed Micelles with Triton X-100.** *A,* PAP activity was measured as a function of the sum of the molar concentrations of Triton X-100 (*TX*) plus PA at set mol % of PA: ●, 9.1; ◆, 4.5; ▲, 3.3; and ■, 2.0. *B,* reciprocal plot of the data in *A. C*. replot of *1/V* intercepts obtained in B *versus* the mol % of PA. *D,* replot of slopes obtained in *B versus* the mol % of PA. The lines drawn are a result of a least squares analysis of the data.

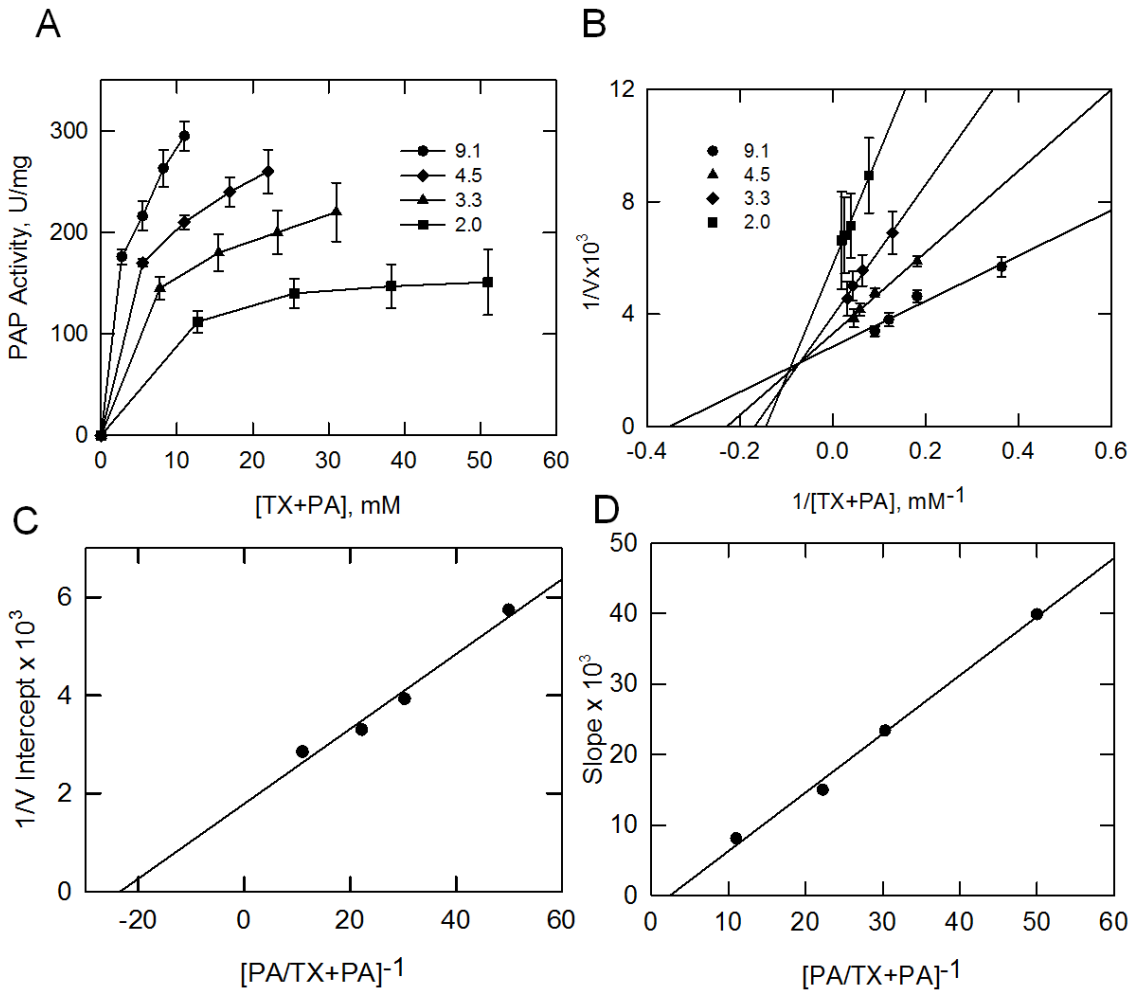
A
PAP Activity, U/mg
[TX+PA], mM
9.1
4.5
3.3
2.0
B
1/Vx10^3
1/[TX+PA], mM^-1
C
1/V Intercept x 10^3
[PA/TX+PA]^-1
D
Slope x 10^3
[PA/TX+PA]^-1

$xK_m^B/x/V_{max}$. Fig. 25D shows that such a replot was linear and pass through the origin. The nK_s^A was calculated to 11 mM.

Since the enzyme follows surface dilution kinetics, we performed a more simple analysis to vary molar at only one mol % of PA and surface at only one molar concentration of PA. In the first set of kinetics experiments, the activity was measured as a function of the molar concentration of PA by maintaining the molar ratio of Triton X-100 to PA in the micelle at 10:1 (i.e. 9.1 mol %). Under these conditions, the enzyme followed Michaelis-Menton kinetics (Fig. 23A). Analysis of the data according to the Michaelis-Menton kinetics showed that V_{max} and K_m were 463 µmol/min/mg and 0.52 mM, respectively. In the second set of kinetic experiments, the enzyme activity was measured as a function of the surface concentration (mol %) of PA in the micelle by maintaining the molar concentration of PA at 2mM (Fig. 23B). Under these conditions, the activity was independent of the PA molar concentration, and they followed positive cooperative kinetics with respect to the surface concentration of PA. The maximum activity was observed at 9.1 mol %. Analysis of the data according to the Hill equation showed that K_m and Hill value for PA surface concentration are 2.0 mol % and 2.3, respectively. Under optimum assay conditions, the specific activity of App1p PAP was 400 µmol/min/mg.

Substrate specificity of the App1p was examined using lipid phosphate molecules, such as LPA, DGPP, sphinganine 1-phosphate, sphingosine 1-phosphate, and ceramide 1-phosphate. The App1p exhibited DGPP phosphatase and LPA phosphatase activities which were measured as a function of the surface concentration (mol %) of DGPP and LPA, respectively, in the micelle by maintaining the molar concentration of DGPP and LPA at 2 mM (Fig. 24). Analysis of the data according to the Hill equation yielded a V_{max} for DGPP and LPA of 143 and 139 µmol/min/mg, respectively, a K_m for DGPP and LPA of 2.9 and 4.8 mol %, respectively, and a Hill value for DGPP and LPA of 3.3 and 3.4, respectively (Table 4). The specificity constants

FIGURE 23. **Dependence of App1p PAP Activity on the Molar and Surface Concentrations of PA.** PAP activity was measured as a function of the indicated molar concentrations of PA (*A*) and as a function of the indicated surface concentration of PA (*B*). For the experiment shown in *A*, the molar ratio of Triton X-100 to PA was maintained at 10:1 (9.1 mol % PA). For the experiment shown in *B*, the molar concentration was varied to obtain the indicated surface concentrations. The data shown are means ± S.D. from triplicate enzyme determinations. The best fit curves were derived from the kinetic analysis of the data.

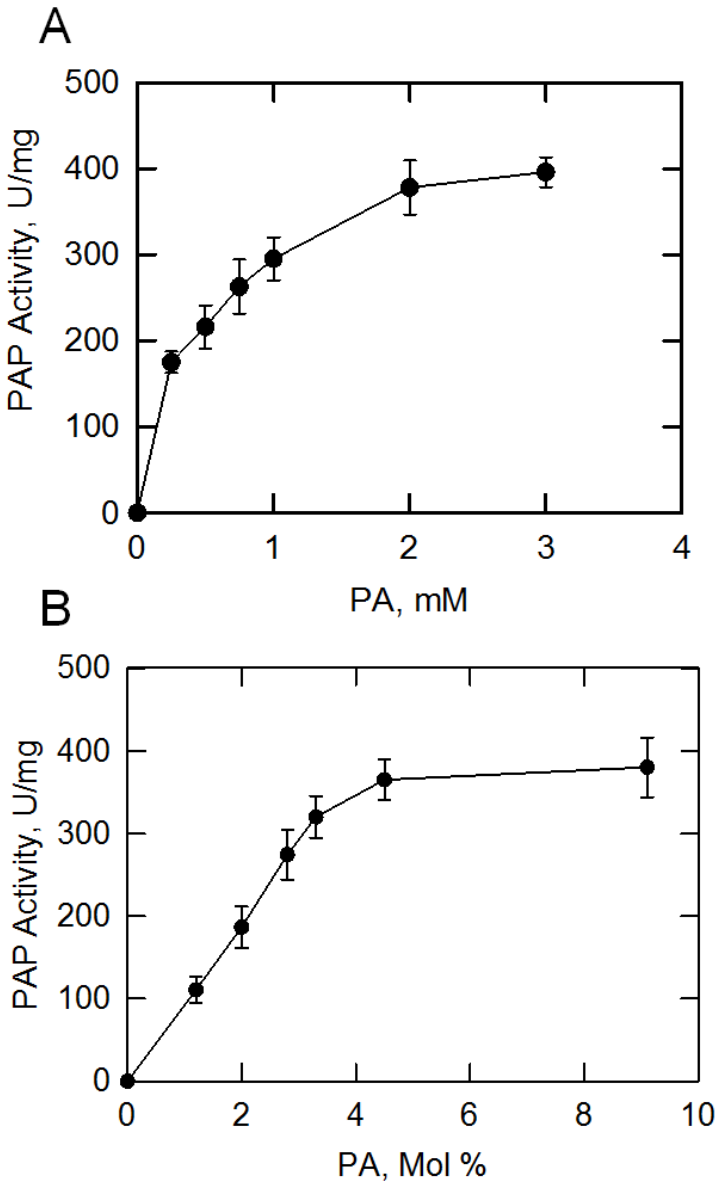
A
500
400
300
200
100
0
PAP Activity, U/mg
0
1
2
3
4
PA, mM
B
500
400
300
200
100
0
PAP Activity, U/mg
0
2
4
6
8
10
PA, Mol %

FIGURE 24. **App1p Utilized PA, LPA and DGPP as Substrates and the Activities Were Dependent on Surface Concentration of PA, LPA, and DGPP.** PA, LPA and DGPP phosphatase activities was measured as a function of the indicated surface concentration of PA, LPA and DGPP, respectively. The bulk concentration was maintained in 2mM for PA, LPA and DGPP, respectively. The data shown are means ± S.D. from triplicate enzyme determinations.

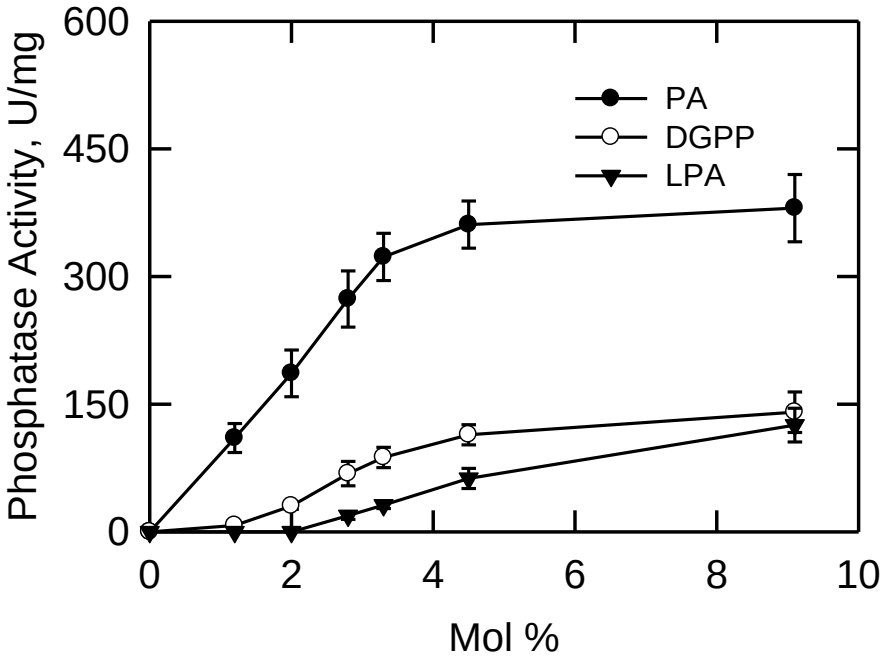
600
450
300
150
0
Phosphatase Activity, U/mg
0
2
4
6
8
10
Mol %
PA
DGPP
LPA

TABLE 4. Kinetic Constants for the App1p PAP of Its Substrates

Substrate	V_{max}	K_m	V_{max}/K_m	Hill no.
	Units/mg	*Mol %*		
PA	400	2.0	200	2.3
DGPP	143	2.9	49	3.3
LPA	139	4.8	29	3.4

(V_{max}/K_m) of PAP showed 4- and 7- fold higher than DGPP phosphatase and LPA phosphatase, respectively, suggesting that PA was the best substrate for App1p phosphatase.

Effect of Nucleotides and Lipids on App1p PAP

The effect of nucleotides on the activity of the App1p PAP was examined. PAP was inhibited by ATP (IC_{50} 3.1 mM), GTP (IC_{50} 3.8 mM), CTP (IC_{50} 3.3 mM), TTP (IC_{50} 5.5 mM) and UTP (IC_{50} 3.8 mM) in a dose-dependent manner (Fig 25). ATP and CTP were the most potent inhibitors of the enzyme. It was suggested that the mechanism of enzyme inhibition by nucleotides was the chelation of Mg^{2+} ion (120) because the mechanism of nucleotide inhibition with respect to Mg^{2+} ions was competitive.

The effect of phospholipids, neutral lipids, and sphingolipids on the activity of the App1p PAP was examined (Fig. 26 and Fig. 27). To better observe the stimulatory or inhibitory effects of lipids on the enzyme, the activity was measured with a subsaturating concentration of PA (2.5 mol % at 0.2 mM PA) and various concentrations of the lipid effectors. The activity was inhibited by phospholipids DAG, PE, PC, and sphingoid bases sphinganine, while phospholipids, LPA, CL, PG, PS, TAG, DGPP, CDP-DAG, and sphingoid base, sphingosine and sphingosine 1-phosphate, stimulate the activities. In particular, at concentration of 7.5 mol %, the sphinganine, DAG and PC inhibit the activity by 90, 61 and 57 %, respectively.

Effects of the *app1*Δ, *pah1*Δ, *dpp1*Δ, *lpp1*Δ Mutations on Lipid Composition

The PAP deletion mutants were used to determine the contribution of *APP1*, *PAH1*, *DPP1*, and *LPP1* to lipid composition. In the first set of experiments, wild type and mutants cells were labeled to steady state with [2-^{14}C] acetate to analyze DAG, TAG, and total phospholipids**.** Cells were grown to the stationary phase (the growth phase where DAG and TAG are most affected (86)), lipids were extracted, and then analyzed by one-dimensional TLC. The *app1*Δ and

FIGURE 25. **Effect of Nucleotides on App1p PAP Activity.** PAP activity was measured in the presence of the indicated concentration of nucleotides. The surface concentration of PA was 2.5 mol % (bulk concentration of 0.2 mM PA). The data shown are means ± S.D. from triplicate enzyme determinations. 100 % activity is 70 U/mg.

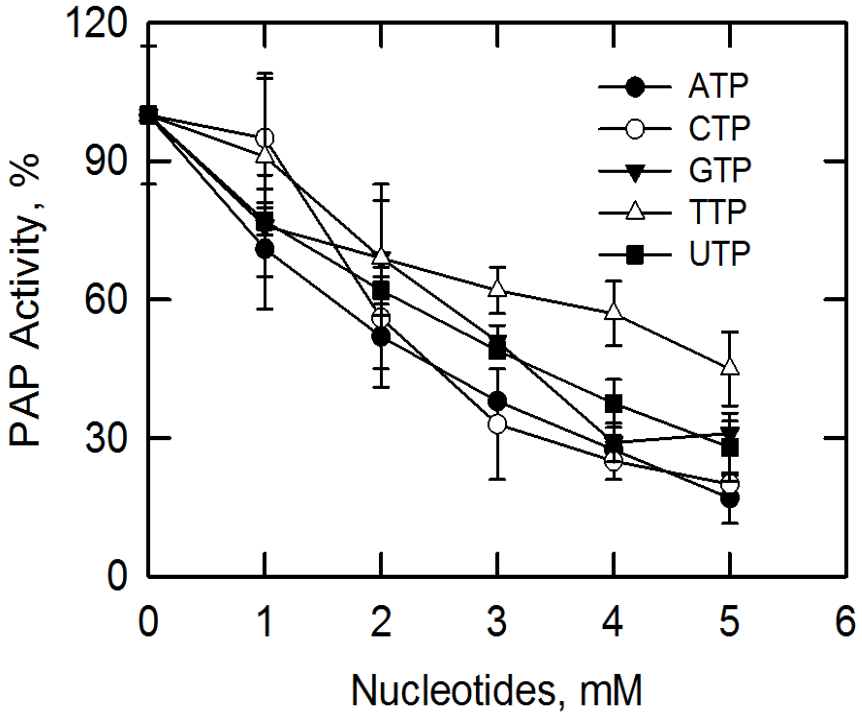
120
90
60
30
0
PAP Activity, %
0
1
2
3
4
5
6
Nucleotides, mM
ATP
CTP
GTP
TTP
UTP

FIGURE 23. **Effect of Phospholipids and Neutral Lipids on App1p PAP Activity.** PAP activity was measured in the presence of the indicated concentration of phospholipids or neutral lipids. The surface concentration of PA was 2.5 mol % (bulk concentration of 0.2 mM PA). The data shown are means ± S.D. from triplicate enzyme determinations. 100 % activity is 76 U/mg.

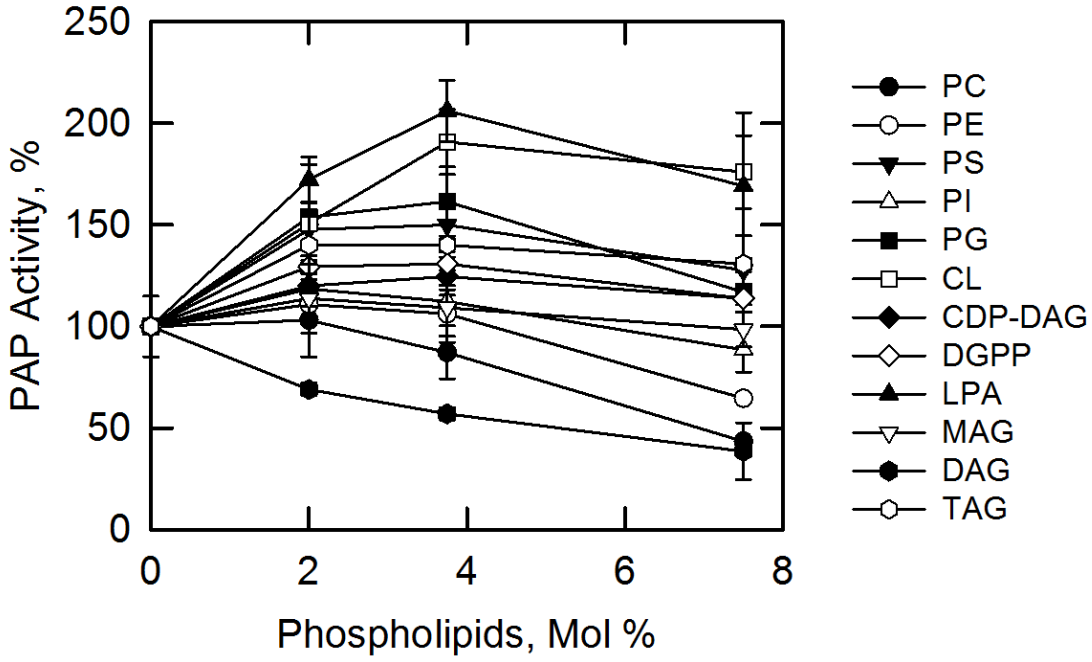
250
200
150
100
50
0
PAP Activity, %
0
2
4
6
8
Phospholipids, Mol %
PC
PE
PS
PI
PG
CL
CDP-DAG
DGPP
LPA
MAG
DAG
TAG

FIGURE 24. **Effect of Sphingolipids on App1p PAP Activity.** PAP activity was measured in the presence of the indicated concentration of sphingolipids. The surface concentration of PA was 2.5 mol % (bulk concentration of 0.2 mM PA). The data shown are means ± S.D. from triplicate enzyme determinations. 100 % activity is 72 U/mg.

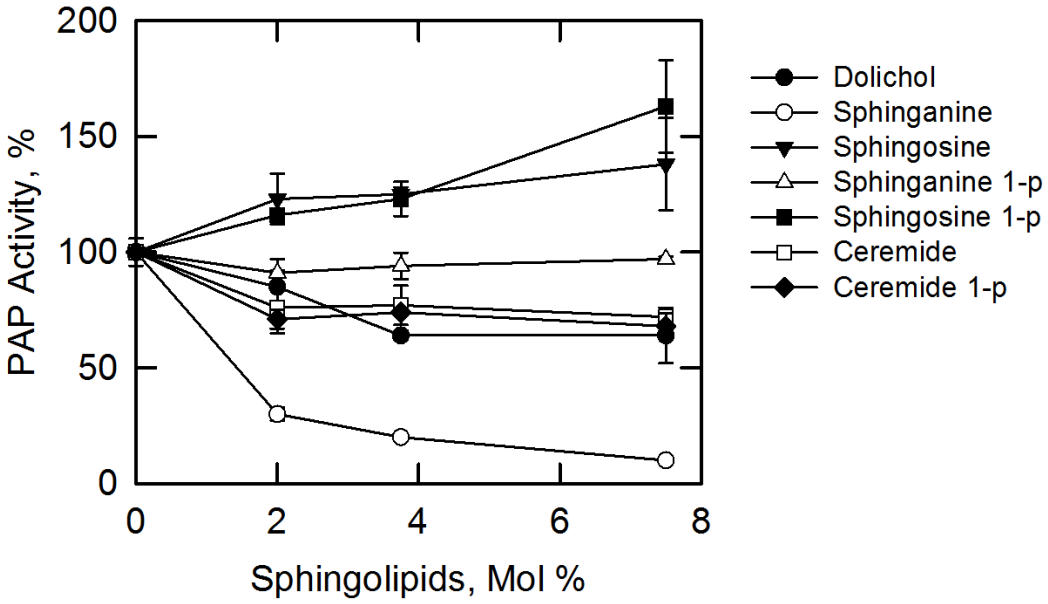
200
150
100
50
0
PAP Activity, %
0
2
4
6
8
Sphingolipids, Mol %
Dolichol
Sphinganine
Sphingosine
Sphinganine 1-p
Sphingosine 1-p
Ceremide
Ceremide 1-p

*dpp1*Δ *lpp1*Δ mutations did not have a significant effect on the relative amounts of DAG, TAG, and total phospholipids (Fig. 28). This analysis did show however, that of all the genes that encode PAP activity in yeast, *PAH1* was responsible for the synthesis of TAG and regulated the relative amounts of TAG and total phospholipids (Fig. 28). Moreover, alterations in lipid composition observed in the double, triple and quadruple mutants of which *pah1Δ* was included could be attributed to the *pah1Δ* mutation (Fig. 28). In the second set of experiments, the wild type and mutant cells were labeled to steady state with $^{32}P_i$ to analyze the composition of individual phospholipids. The phospholipids were extracted from exponential phase cells (the growth phase were phospholipid composition is most affected (86)) and analyzed by two-dimensional TLC. The relative amounts of the major phospholipids PC, PE, PI, PS, and the precursor PA were not affected by the *app1Δ* and *dpp1Δ lpp1Δ* mutations (Fig. 29). The relative amounts of these phospholipids, however, were affected by the *pah1Δ* mutation alone, and in combination with the *app1Δ* and *dpp1Δ lpp1Δ* mutations (Fig. 29). As described previously (86), the *pah1Δ* mutation caused decreases in the amounts of PC (37 %) and PS (33 %), and increases in the amounts of PE (108 %), PI (42 %), and PA (86 %). Interestingly, when combined with the *pah1Δ dpp1Δ lpp1Δ* mutations, the *app1Δ* mutation reversed the effects of the *pah1Δ* mutation on phospholipid composition. The reason for this observation is unclear.

FIGURE 28. **Effects of the *app1*Δ, *pah1*Δ, *dpp1*Δ, *lpp1*Δ Mutations on DAG, TAG, and Total Phospholipids.** The indicated cells were grown to the stationary phase of growth in the presence of [2-^{14}C]acetate (1 μCi/ml). Lipids were extracted, separated by one-dimensional TLC, and the images were subjected to ImageQuant analysis. The percentages shown for the individual lipids were normalized to the total ^{14}C-labeled chloroform-soluble fraction, which also contained sterols, fatty acids, and unidentified neutral lipids. Each data point represents the average of three experiments ± S.D. (*error bars*). PL, phospholipids. These experiments were performed by Gil-Soo Han.

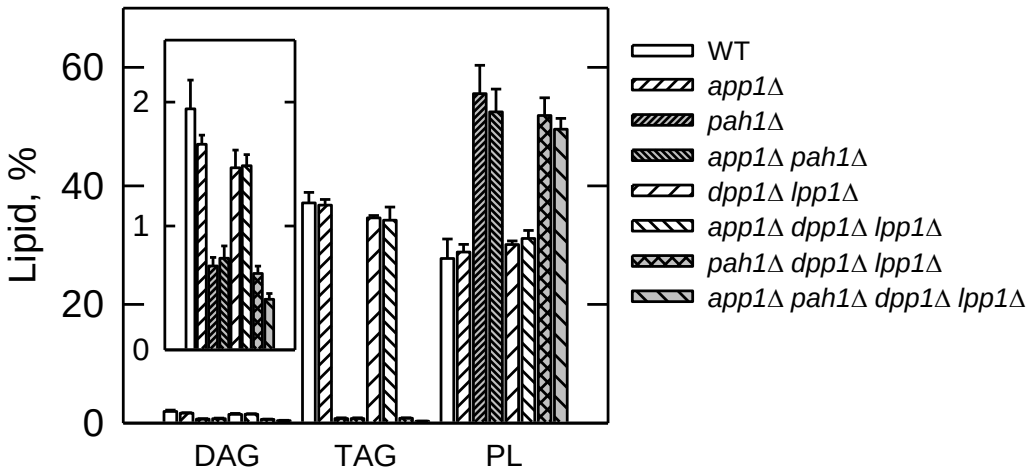
Lipid, %
60
40
20
0
2
1
0
DAG
TAG
PL
WT
app1Δ
pah1Δ
app1Δ pah1Δ
dpp1Δ lpp1Δ
app1Δ dpp1Δ lpp1Δ
pah1Δ dpp1Δ lpp1Δ
app1Δ pah1Δ dpp1Δ lpp1Δ

FIGURE 29. **Effects of the *app1*Δ, *pah1*Δ, *dpp1*Δ, *lpp1*Δ Mutations on Phospholipid Composition.** The indicated cells were grown to the exponential phase of growth in the presence of $^{32}P_i$ (10 μCi/ml). Phospholipids were extracted, separated by two-dimensional TLC, and the images were subjected to ImageQuant analysis. The percentages shown for the individual phospholipids were normalized to the total ^{32}P-labeled chloroform-soluble fraction that included sphingolipids and unidentified phospholipids. Each data point represents the average of three experiments ± S.D. (*error bars*). These experiments were performed by Gil-Soo Han.

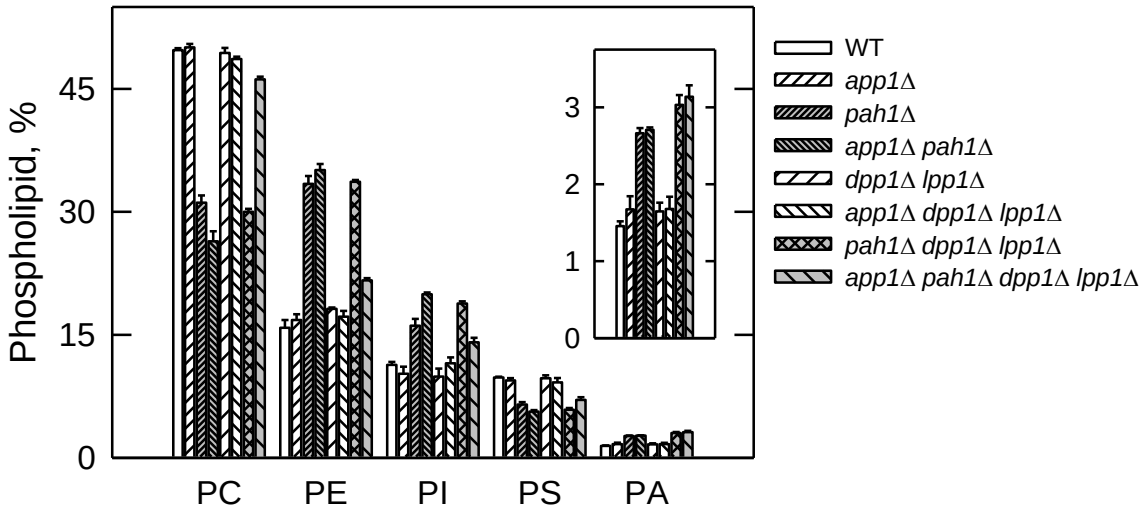
Phospholipid, %
0
15
30
45
PC
PE
PI
PS
PA
0
1
2
3
WT
app1Δ
pah1Δ
app1Δ pah1Δ
dpp1Δ lpp1Δ
app1Δ dpp1Δ lpp1Δ
pah1Δ dpp1Δ lpp1Δ
app1Δ pah1Δ dpp1Δ lpp1Δ

DISCUSSION

It has been recognized that three genes *PAH1*, *DPP1*, and *LPP1* encode PAP enzys mein *S. cerevisiae* (80, 81, 86). One of the genes, *PAH1* encodes a Mg^{2+}- dependent soluble 95-kDa protein with a HAD-like domain with a catalytic D*X*D*X*T motif (86, 89). The Pah1p PAP has been shown to play a central role in the *de novo* synthesis of TAG and phospholipids (via the Kennedy pathway) in *S. cerevisiae*. The *pah1*Δ shows elevated levels of PA and decreased levels of DAG and TAG (86). Additionally, the amounts of phospholipids, fatty acids, and sterol esters are also elevated in response to the *pah1*Δ mutation (86). Unlike *PAH1*, *DPP1* and *LPP1* are Mg^{2+}-independent PAP enzymes with a three-domain lipid phosphatase motif comprised of the consensus sequences K*XXXXXX*RP(I), PSGH(II), and SR*XXXXX*H*XXX*D (III) (81, 96). Dpp1p is a Zn^{2+}-regulated seven transmembrane domains PAP localized to the vacuole, and acts on DAG pyrophosphate and PA (43). Lpp1p is a polytopic PAP localized to Golgi puncta and dephosphorylates PA, LPA, and DGPP (80). The *pah1*Δ *dppl1*Δ *lpp1*Δ triple mutant still shows residual activity in a Mg^{2+}-dependent PAP that is sensitive to inhibition by NEM (86).

APP1 was identified through a reverse genetics approach using protein sequence information derived from the PAP enzyme purified from the *pah1*Δ *dpp1*Δ *lpp1*Δ triple mutant. The PAP activity was labile in the absence of high salt, which comprised the effectiveness of some chromatography steps. While the developed eight-step purification scheme resulted in a 2,143-fold enrichment in PAP specific activity, it did not result in a homogenous enzyme preparation that could be used for unequivocal protein sequence determination. In addition, the advanced liquid chromatography/tandem mass spectrometry technology used to obtain sequence information from the protein band enriched for PAP activity yielded very complex sequence information. Moreover, the reduced activity in the *app1*Δ mutant from the yeast deletion strain collection was only 30%, which did not provide much confidence that *APP1* encoded a PAP.

Nonetheless, the collective data (e.g., reduction of PAP activity in the *app1*Δ mutant, the *APP1*-directed overexpression of PAP activity in the *app1*Δ *pah1*Δ *dpp1*Δ *lpp1*Δ quadruple mutant, and the heterologous expression of App1p PAP activity in *E. coli)* provided a conclusive level of evidence that *APP1* is the structural gene encoding a PAP enzyme in *S. cerevisiae*.

Efforts to identify *APP1* by informatics and by genetic approaches were unsuccessful. For example, a protein blast search using Pah1p as the query did not identify App1p or any other homologs in the *Saccharomyces* genome database. A blast search against higher eukar yotic organism databases identified mammalian lipin proteins, but this was expected since a blast search with mouse lipin-1 as the query identifies yeast Pah1p (133) Likewise, a blast search using App1p as the query does not identify Pah1p or the mammalian lipins. Instead, this blast identifies homologous proteins that are only found in fungi. A synthetic genetic array screen using the *pah1*Δ mutant in combination with the *cho2*Δ and *opi3*Δ mutations defective in the PE methylation steps of PC synthesis via the CDP-DAG pathway (175, 176) has also been performed. The rationale being that a gene might be identified encoding a PAP enzyme that could bypass the loss of Pah1p and produce DAG for PC synthesis via the Kennedy pathway (66, 175). This genetic screen, however, did not lead to the identification of *APP1*, indicating that the molecular functions of App1p and Pah1p are not overlapping with respect to lipid synthesis. This assertion was further supported by the fact that *APP1* did not complement the temperature sensitive phenotype exhibited by the *pah1*Δ mutant, and that the analysis of cells possessing the *app1*Δ mutation alone and in combination with mutations for all the known PAP genes showed that only Pah1p PAP was involved in *de novo* lipid synthesis.

While there is essentially no protein sequence homology between App1p and Pah1p, both enzymes possess the canonical D*X*D*X*(T/V) catalytic motif that is typical of Mg^{2+}-dependent phosphatase enzymes (95). For Pah1p, its DIDGT catalytic sequence is contained within the HAD-like domain similar to that found in the mammalian lipin PAP enzyme (51, 134, 177).

However, the HAD-like domain is not found in App1p, but instead, it contains a conserved domain found in fungi that has some sequence similarity to the HAD-like domain found in Pah1p and lipin (178). It is within this domain that the App1p DIDDT catalytic sequence is found (Fig. 26), and indeed, the D281E mutation abolished PAP activity confirming this to be the catalytic sequence.

PAP activities have been isolated from *S. cerevisiae* that have molecular masses of 91 kDa (12), 75 kDa (84), 45 kDa (85), and 34 kDa (79). Protein sequence information has confirmed that the 91-kDa enzyme is a proteolysis product of Pah1p (86), and that the 34-kDa enzyme is Dpp1p (80). Lpp1p PAP was identified based on its sequence homology with Dpp1p (81). The identity of the genes encoding the 75- and 45-kDa forms of PAP activity has been an enigma. While the basic enzymological properties of these enzymes are similar, the 75-kDa enzyme is soluble whereas the 45-kDa enzyme is associated with mitochondria (84, 85). Because of the differences in size and location, it has been assumed that the 75- and 45-kDa PAP activities are encoded by different genes. Based on the fact that no detectable PAP activity was present in the *app1*Δ *pah1*Δ *dpp1*Δ *lpp1*Δ quadruple mutant, we hypothesize that the 75-kDa PAP was the soluble form of App1p and that the 45-kDa PAP was a proteolytic fragment of App1p bound to mitochondrial membranes. Unfortunately, this hypothesis cannot be addressed because preparations of the 75- and 45-kDa PAP enzymes are no longer available.

The identification of *APP1* as the gene encoding PAP allows us to express, purify, and characterize this new enzyme. App1p predicted to have a subunit molecular mass of ~66 kDa was migrated to be ~68 kDa upon SDS-PAGE. The molecular mass was also calculated to be ~66 kDa by gel filtration, suggesting its monomer properties. Early studies have provided useful information (*e.g.* pH optimum, Mg^{2+} ion requirement, and sensitivity to modifying chemicals like NEM) about the basic enzymological properties of PAP from yeast (84-86). However, the data derived from this work are difficult to interpret in a definitive way because they have been

derived from studies using impure enzymes. The work reported here on the App1p PAP did not contain competing and/or modifying enzymes or molecules that inhibit or stimulate activity. This work also reported the fact that Mn^{2+} could partially substitute for the Mg^{2+} dependences of the activity. However, Mg^{2+} and especially Mn^{2+} were inhibitory to the PAP activity at concentrations higher than their optimum levels. In addition, the purified enzyme was potently inhibited by Ca^{2+} and Zn^{2+}.

The availability of the purified App1p PAP permitted defined kinetic studies using Triton X-100/PA-mixed micelles. Indeed, the App1p PAP followed surface dilution kinetics because their PAP activities were dependent on both the molar (*e.g.* number of micelles containing PA) and the surface (*e.g.* number of PA molecules on a micelle surface) concentrations of PA. The K_m values for the molar concentration of PA reflected the interactions of the enzymes with the micelle surface, whereas the K_m values for the surface concentration of PA reflected the interactions with PA within the surface. These kinetic properties may reflect the *in vivo* condition, where soluble PAP binds to the mixed micelle surface before binding to its substrate and catalysis occurs (132). Specific constants (V_{max}/K_m , µmol/min/mg/mol %) of App1p, Pah1p, Dpp1p and Lpp1p PAP showed 200, 1.3 (126), 32 (42), and 4.2 (42), respectively. The App1p PAP activity exhibits the highest specific constant among all known PAP enzymes, indicating the best efficiency on dephosphorylation of PA.

The App1p PAP also shows LPAP and DGPP phosphatase activities. The V_{max} for PA has 3- fold higher than the V_{max} for DGPP and LPA, whereas K_m for PA has 2.4- and 1.5- fold lower than the K_m for DGPP and LPA, respectively. Thus, the specificity constant was in the order of PA> DGPP> LPA. The cooperative nature (Hill number ~2) of the activities with respect to the PA surface concentration may reflect cooperative interactions with the PA substrate, suggesting that the enzyme interacts with one PA molecule before it dephosphorylates another PA molecule (116). Like App1p enzyme, Dpp1p and Lpp1p enzymes have broad substrate specificity (PA,

LPA, and DGPP) (42, 79, 81). The order of substrate preference of *DPP1* gene products was DGPP> LPA> PA (79), whereas the order of *LPP1* gene products was PA> DGPP> LPA (81). The broad substrate specificity of App1p elucidates its important roles in lipid signaling like Dpp1p and Lpp1p .

Interestingly, LPA another substrate for App1p phosphatase simulated PAP activity. We expected LPA inhibits the PAP activity because PA and LPA were competitor for enzyme but otherwise LPA activated PAP activity. This activation can be explained by change in surface charge density of the micelle. Mosior and McLauglin (179) report cooperative binding of peptides and proteins to membrane bilayers is induced by the additional electrostatic term in the binding energy as well as the reduced dimensionality. PAP activation by CL, CDP-DAG, and PI is previously reported and the activation by anionic phospholipids may be physiologically relevant (118). The activation of App1p PAP activity by CL and PG both of which are anionic phospholipids might be due to change in the surface charge density. The App1p PAP activities were inhibited by phospholipids DAG, PC and PE, which may be explained by downstream product inhibition or overall charge change of the micelle surface by zwitterionic phospholipids (PC and PE), which is consistent with a previous report PE and PC had a slight inhibitory effect on PAP (118). Sphingoid bases sphinganine was potently inhibitor of the App1p PAP. Sphinganine is a precursor of phytosphingosine in *S. cerevisiae* (180, 181) and sphingsosine and phytosphingosine in mammalian cells (182). It is reported that sphinganine, a positively charged sphingoid base, inhibits the PAP activity and antagonizes the activation of the enzyme by CL and PI (118, 119). This inhibition provides the interrelationship between PA metabolism and sphingolipid signaling.

The PAP enzymes in *S. cerevisiae* are found in different cellular locations and play diverse roles in cell physiology (173). Pah1p is a cytoplasmic enzyme that associates with and functions at the nuclear/ER membrane to regulate the synthesis of TAG and membrane

phospholipids (33, 51, 86, 173, 183). Dpp1p and Lpp1p PAP are thought to control the signaling functions of PA, DGPP and LPA in the vacuole and Golgi membranes, respectively, the organelles for which these enzymes reside (79- 81, 33, 50, 43, 173, 184, 185). Like Pah1p, App1p is a cytoplasmic protein (185) that associates with membranes, but the role this PAP plays in cell physiology is not yet clear. An important clue as to its cellular function might come from the fact that it interacts with endocytic proteins at cortical actin patches (165-172).

The formation of endocytic vesicles in *S. cerevisiae* involves a series of processes that include actin patch assembly, actin polymerization, and changes in membrane structure and curvature (170, 186). These processes involve numerous endocytic proteins, and App1p physically interacts with many of them (165-172) (Fig. 30). While these interactions have yet to be studied in great detail, the presence of proline-rich regions (P*XX*P motifs) in App1p suggests interactions with SH3 domains of Abp1p, Ysc84p, Sla1p, Bbc1p, Bzz1p, and Rvs167p (198, 199). App1p interactions with proteins that do not possess SH3 domains (e.g., Las17p, Sla2p, Cof1p, Crn1p, and Rvs161) must occur through other mechanisms yet to be defined. In any event, the position of App1p at cortical actin patches (186) raises the suggestion that its PAP activity controls the local concentrations of PA and DAG. These lipids are known to control membrane fission/fusion events in model systems (60, 176, 187-190) and they are also known to interact with and regulate enzymes (e.g., protein kinase C, protein kinase D) that play important roles in vesicular trafficking (52, 53, 56). For example, in mammalian cells, the proPr-mediated inhibition of PAP activity attenuates protein kinase D recruitment to Golgi membranes blocking vesicle bud formation and protein transport to the cell surface (56). We speculate that in yeast App1p PAP activity plays a role in vesicle formation through its recruitment from the cytoplasm to cortical actin patches via endocytic proteins. These proteins may simply serve as a scaffold to attract App1p to actin patches and/or may serve to regulate PAP activity to control the relative

FIGURE 30. **Motifs in App1p and Interacting Endocytic Cortical Actin Patch Proteins.** *A*, **t**he diagram shows a linear representation of App1p with the approximate positions of the region that has similarity to an HAD-like domain (183), the D*X*D*X*(T/V) catalytic motif, and the P*XX*P motif for SH3 binding. *B*, the diagram shows that App1p interacts with the endocytic proteins Abp1p (167-169, 171, 172), Bbc1p (171, 172), Bzz1p (171-173), Cof1p (168), Crn1p (166), Las17p (170), Rvs161p (165, 166, 171-173), Rvs167p (165, 166, 171-173), Sla1p (166, 172), Sla2p (166), and Ysc84p (171-172). The proteins that possess SH3 binding domains are indicated by the *parentheses* after the name.

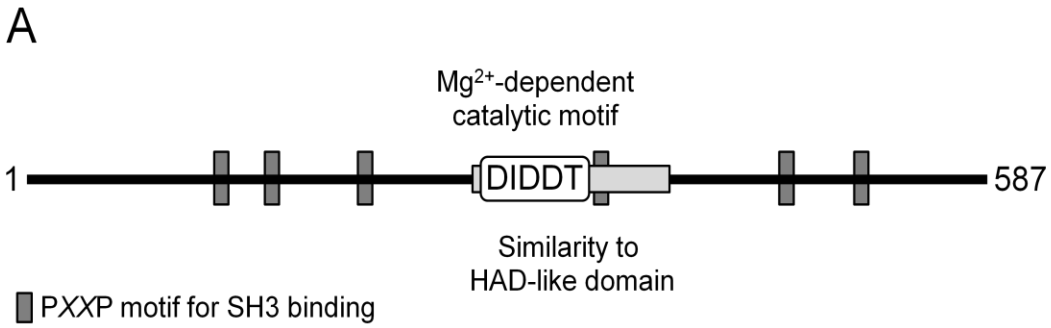
A
Mg2+-dependent
catalytic motif
1
DIDDT
587
Similarity to
HAD-like domain
PXXP motif for SH3 binding

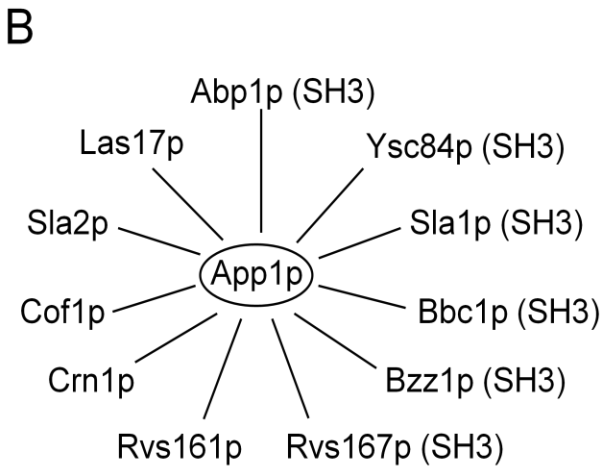
B
Abp1p (SH3)
Las17p
Ysc84p (SH3)
Sla2p
Sla1p (SH3)
App1p
Cof1p
Bbc1p (SH3)
Crn1p
Bzz1p (SH3)
Rvs161p
Rvs167p (SH3)

amounts of PA and DAG, which in turn, may control vesicle formation directly and/or indirectly. The work reported here provides the impetus to address these questions.

App1p was first known as an actin patch protein becase of its interaction with Rvs161p and Rvs167p, which form a heterodimer through their BAR (Bin Amphiphysin Rvs) domains (191). In budding yeast, Rvs161p and Rvs167p (192) are the only BAR domain proteins and members of the BAR domain superfamily play important roles in membrane remodeling processes (193). Rvs161p consists solely of a BAR domain, whereas Rvs167p is composed of a BAR domain followed by a region rich in glycine, proline, and alanine (GPA), and an SH3 (Src-homology 3) domain at its C-terminus (194). The *rvs* defects results in polarizing the actin cytoskeleton, endocytosis, growth on salt, and sporulation (192, 195). In growing yeast cells, Rvs161p and Rvs167p localize to cortical actin patches, which are sites of endocytosis, and plays important roles in vesicle-scission step (195-198). A significant fraction of the endocytic patches begin to be internalized and move inward from the cell surface but are then retracted toward the cortex in *rvs161*Δ, *rvs167*Δ and *rvs161*Δ *rvs167*Δ mutants (198). We speculate the biochemical mechanism by which Rvs161p-Rvs167p promoting scission may be mediated by interaction with App1p.

For the future study, the effect of App1p on the endoscytosis should be examined. Morphology of endocytosis could be monitored under an electron microscopy in *app*1Δ and *APP1* overexpression strains. Besides, the mechanism of interaction of App1p with endocytic cortical actin patch proteins should be examined. The interaction can be mediated through P*XX*P motif for SH3 binding (Abp1p, Ysc84p, Sla1p, Bbc1p, Bzz1p, and Rvs167p) or other mechanisms (Las17p, Sla2p, Cof1p, Crn1p, and Rvs1). We speculate the interaction with those actin patch proteins may regulate the App1p PAP activity because the App1p PAP purified from yeast shows much higher specific acitivity (400 μmol/min/mg) than that in cell extracts (1 nmol/min/mg). PAP activities in mutants lacking actin patch proteins interacting with App1p

should be measured to test this hypothesis. If the mutants show any changes in PAP acitivity, the proteins deleted in the mutants could be purified to test the effect of them on the App1p PAP activity and to determine the mechanism of interactions by defining the binding mode of the actin patch proteins with App1p. Furthermore, mutants with the actin patch proteins in combination with App1p should be constructed to see defects in endocytosis. Finally, while an App1p homolog does not exist in higher eukaryotes, the mammalian lipins do catalyze the PAP reaction (86, 199, 200), and as indicated above, PAP activity has been implicated in vesicular trafficking in mammalian cells.

REFERENCES

1. Schlame, M. and Greenberg, M. L. (1997) Cardiolipin Synthase from Yeast. *Biochim. Biophys. Acta Lipids Lipid Metabolism.* **1348**, 201-206.

2. Alberts, B., Johnson, A., Lewis, J., Raff, M., Roberts, K., Walter, P. (2002) *Molecular Biology of the Cell*: Fourth Ed. Garland Science, New York.

3. Nelson, D. L. and Cox, M. M. (2000) *Lehninger Principles of Biochemistry*: Third Ed. Worth Publishers, New York.

4. Ichimura, Y., Kirisako, T., Takao, T., Satomi, Y., Shimonishi, Y., Ishihara, N., Mizushima, N., Tanida, I., Kominami, E., Ohsumi, M., Noda, T., and Ohsumi, Y. (2000) A Ubiquitin-like System Mediates Protein Lipidation. *Nature* **408**, 488-492.

5. Carman, G. M. (1989) Phosphatidylcholine Metabolism in *Saccharomyces cerevisiae*. In *Phosphatidylcholine Metabolism*. D. E. Vance, Ed. CRC Press Inc., Boca Raton.

6. Paltauf, F., Kohlwein, S. D., and Henry, S. A. (1992) Regulation and Compartmentalization of Lipid Synthesis in Yeast. In *The Molecular and Cellular Biology of the Yeast Saccharomyces: Gene Expression*. Broach, J. R., E. W. Jones and J. R. Pringle, Eds. Cold Spring Harbor Laboratory, New York; pp. 415-500.

7. Lin, Y.-P. and Carman, G. M.. (1989) Purification and Characterization of Phosphatidate Phosphatase from *Saccharomyces cerevisiae*. *J. Biol. Chem.* **264**, 8641-8645.

8. Goffeau, A., Barrell, B. G., Bussey, H., Davis, R. W., Dujon, B., Feldmann, H., Galibert, F., Hoheisel, J. D., Jacq, C., Johnston, M., Louis, E. J., Mewes, H. W., Murakami, Y., Philippsen, P., Tettelin, H., and Oliver, S. G. (1996) Life with 6000 Genes. *Science* **274**, 546-547.

9. Gaspar, M. L., Aregullin, M. A., Jesch, S. A., Nuñez, L. R., Villa-García, M., and Henry, S. A. (2007) The Emergence of Yeast Lipidomics. *Biochim. Biophys. Acta.* **1771**, 241-254.

10. Henry, S. A. and Patton-Vogt, J. L. (1998) Genetic Regulation of Phospholipid Metabolism: Yeast as a Model Eukaryote. *Prog. Nucleic Acid Res.* **61**, 133-179.

11. Majumder, A. L., Johnson, M. D., and Henry, S. A. (1997) 1L-*myo*-Inositol-1-Phosphate Synthase. *Biochim. Biophys. Acta Lipids Lipid Metabolism* **1348**, 245-256.

12. Carman, G. M. and Henry, S. A. (1989) Phospholipid Biosynthesis in Yeast. *Annu. Rev. Biochem*. **58**, 635-669.

13. Carman, G. M. and Zeimetz, G. M. (1996) Regulation of Phospholipid Biosynthesis in the Yeast *Saccharomyces cerevisiae*. *J. Biol. Chem.* **271**, 13293-13296.

14. Carman, G. M. and Henry, S. A. (1999) Phospholipid Biosynthesis in the Yeast *Saccharomyces cerevisiae* and Interrelationship with other Metabolic Processes. *Prog. Lipid Res.* **38**, 361-399.

15. Li, G., Chen, S., Thompson, M. N., and Greenberg, M. L. (2007) New Insights into the Regulation of Cardiolipin Biosynthesis in Yeast: Implications for Barth Syndrome. *Biochim. Biophys. Acta.* **1771**, 432-441.

16. Kanfer, J. N. and Kennedy, E. P. (1964) Metabolism and Function of Bacterial Lipids II. Biosynthesis of Phospholipids in *Escherichia coli*. *J. Biol. Chem.* **239**, 1720-1726.

17. Kiyono, K., Miura, K., Kushima, Y., Hijiki, T., Fukushima, M., Shibuya, I., and Ohta, A. (1987) Primary Structure and Product Characterization of the *Saccharomyces cerevisiae CHO1* Gene that Encodes Phosphatidylserine Synthase. *J. Biol. Chem.* **102**, 1089-1100.

18. Letts, V. A., Klig, L. S., Bae-Lee, M., Carman, G. M., and Henry, S. A. (1983) Isolation of the Yeast Structural Gene for the Membrane-Associated Enzyme Phosphatidylserine Synthase. *Proc. Natl. Acad. Sci. USA* **80**, 7279-7283.

19. Nikawa, J., Tsukagoshi, Y., Kodaki, T., and Yamashita, S. (1987) Nucleotide Sequence and Characterization of the Yeast *PSS* Gene Encoding Phosphatidylserine Synthase. *Eur. J. Biochem.* **167**, 7-12.

20. Clancey, C. J., Chang, S.-C., and Dowhan, W. (1993) Cloning of a Gene (*PSD1*) Encoding Phosphatidylserine Decarboxylase from *Saccharomyces cerevisiae* by Complementation of an *Escherichia coli* Mutant. *J. Biol. Chem.* **268**, 24580-24590.

21. Trotter, P. J., Pedretti, J., and Voelker, D. R. (1993) Phosphatidylserine decarboxylases from *Saccharomyces cerevisiae*. Isolation of Mutants, Cloning of the Gene, and Creation of a Null Allelle. *J. Biol. Chem.* **268**, 21416-21424.

22. Trotter, P. J., Pedretti, J., Yates, R., and Voelker, D. R. (1995) Phosphatidylserine decarboxylases 2 of *Saccharomyces cerevisiae*. Cloning and Mapping of the Gene, Heterologous Expression, and Creation of the Null Allelle. *J. Biol. Chem.* **270**, 6071-6080.

23. Trotter, P. J. and Voelker, D. R. (1995) Identification of a Non-Mitochondrial Phosphatidylserine Decarboxylase Activity (*PSD2*) in the Yeast *Saccharomyces cerevisiae*. *J. Biol. Chem.* **270**, 6062-6070.

24. Bremer, J. and Greenberg, D. M. (1961) Methyl Transferring Enzyme System of Microsomes in the Biosynthesis of Lecithin (Phosphatidylcholine). *Biochim. Biophys. Acta.* **46**, 205-216.

25. Kodaki, T. and Yamashita, S. (1987) Yeast Phosphatidylethanolamine Methylation Pathway: Cloning and Characterizat6ion of Two Distinct Methyltransferase Genes. *J. Biol. Chem.* **262**, 15428-15435.

26. McGraw, P. and Henry, S. A. (1989) Mutations in the *Saccharomyces cerevisiae OPI3* Gene: Effects on Phospholipid Methylation, Growth, and Cross-Pathway Regulation of

Phospholipid Synthesis. *Genetics.* **122**, 317-330.

27. Summers, E. F., Letts, V. A., McGraw, P., and Henry, S. A. (1988) *Saccharomyces cerevisiae cho2* Mutants are Deficient in Phospholipid Methylation and Cross-Pathway Regulation of Inositol Synthesis. *Genetics* **120**, 909-922.

28. Hosaka, K., Kodaki, T., and Yamashita, A. (1989) Cloning and Characterization of the yeast *CKI1* Gene Encoding Choline Kinase and its Expression in *Escherichia coli*. *J. Biol. Chem.* **264**, 2053-2059.

29. Kim, K., Kim, K.-H., Storey, M. K., Voelker, D. R., and Carman, G. M. (1999) Isolation and Characterization of the *Saccharomyces cerevisiae EKI1* Gene Encoding Ethanolamine Kinase. *J. Biol. Chem.* **274**, 14857-14866.

30. Min-Seok, R., Kawamata, Y., Nakamura, H., Ohta, A., and Tagaki, M. (1996) Isolation and Characterization of the *ECT1* Gene Encoding CTP:Phosphoethanolamine Cytidyltransferase of *Saccharomyces cerevisiae*. *J. Biol. Chem.* **120**, 1040-1047.

31. Tsukagoshi, Y., Nikawa, J., and Yamashita, S. (1987) Molecular Cloning and Characterization of the Gene Encoding Cholinephosphate Cytidyltransferase in *Saccharomyces cerevisiae*. *Eur. J. Biochem.* **169**, 477-486.

32. Vance, D. E. Glycerolipid Biosynthesis in Eukaryotes. In: *Biochemistry of Lipids, Lipoproteins and* Membranes. Vance, D. E. and J. Vance, Eds. Elsevier Science, Amsterdam: pp. 153-181

33. Carman, G. M. and Han, G.-S. (2009) Regulation of Phospholipid Synthesis in Yeast. *J. Lipid Res.* **50**, S69-S73

34. McMaster, C. R. and Bell, R. M. (1994) Phosphatidylcholine Biosynthesis in *Saccharomyces cerevisiae*. Regulatory Insights from Studies Employing Null and Chimeric *sn*-1,2-diacylglycerol Choline- and Ethanolaminephosphotransferases. *J. Biol. Chem.* **269**, 28010-28016

35. Patton-Vogt, J. L., Griac, P., Sreenivas, A., Bruno, V., Dowd, S., Swede, M. J., and Henry, S. A. (1997) Role of the Yeast Phosphatidylinositol/Phosphatidylcholine Transfer Protein (Sec14p) in Phosphatidylcholine Turnover and *INO1* Regulation. *J. Biol. Chem.* **272**, 20873-20883.

36. Rajakumari, S., Grillitsch, K., and Daum, G. 2008. Synthesis and Turnover of Non-Polar Lipids in Yeast. *Prog. Lipid Res.* **47**, 157-171.

37. Xie, Z., Fang, M., Rivas, M. P., Faulkner, A. J., Sternweis, P. C., Engebrecht, J., and Bankaitis, V. A. (1998) Phospholipase D Activity is Required for Suppression of Yeast Phosphatidylinositol Transfer Protein Defects. *Proc. Natl. Acad. Sci. USA* **95**, 12346-12351.

38. Atkinson, K., Fogel, S., and Henry, S. A. (1980) Yeast Mutant Defective in Phosphatidylserine Synthesis. *J. Biol. Chem.* **255**, 6653-6661.

39. Morash, S. C., McMaster, C. R., Hjelmstad, R. H., and Bell, R. M. (1994) Studies Employing *Saccharomyces cerevisiae cpt1* and *ept1* Null Mutants Implicate the *CPT1* Gene in Coordinate Regulation of Phospholipid Biosynthesis. *J. Biol. Chem.* **269**, 28769-28776.

40. Murray, M. and Greenberg, M. L. (2000) Expression of Yeast *INM1* Encoding Inositol Monophosphatase is Regulated by Inositol, Carbon Source and Growth Stage and is Decreased by Lithium and Valproate. *Mol. Microbiol.* **36**, 651-661.

41. Dean-Johnson, M. and Henry, S. A. (1989) Biosynthesis of Inositol in Yeast. Primary Structure of *myo*-Inositol-1-Phosphaste Synthase (EC 5.5.1.4) and Functional Analysis of its Structural Gene, the *INO1* Locus. *J. Biol. Chem.* **264**, 1274-1283.

42. Furneisen, J. M. and Carman, G. M. (2000). Enzymological properties of the *Lpp1*-encoded lipid phosphatase from *Saccharomyces cerevisiae*. *Biochim. Biophys. Acta* **1484**, 71-82.

43. Klig, L. S. and Henry, S. A. (1984) Isolation of the Yeast *INO1* Gene: Located on an Autonomously Replicating Plasmid, the Gene is Fully Regulated. *Proc. Natl. Acad. Sci. USA* **81**, 3816-3820.

44. Minskoff, S. A. and Greenberg, M. L. (1997) Phosphatidylglycerophosphate Synthase from Yeast. *Biochim. Biophys. Acta. Lipids Lipid Metabolism.* **1348**, 187-191.

45. Carman, G. M. and Belunis, C. J. (1983) Phosphatidylglycerophosphate Synthase Activity in *Saccharomyces cerevisiae*. *Can. J. Microbiol.* **29**, 1452-1457.

46. Brindley, D. N. (1984) Intracellular Translocation of Phosphatidate Phosphohydrolase and its Possible Role in the Control of Glycerolipid Synthesis. *Prog. Lipid Res.* **23**, 115-133.

47. Kennedy, E. P. (1986) In *Lipids and Membranes: Past, Present and Future.* Op den Kamp, J. A. F., B. Roelofsen, and K. W. A. Wirtz, Eds. Elsevier Science, Amsterdam: pp. 171-206.

48. Stryer,L. (1995) Biochemistry, fourth ed., W.H. Freeman and Company, New York.

49. Brindley, D. N. (2004) Lipid Phosphate Phosphatases and Related Proteins: Signaling Functions in Development, Cell Division, and Cancer. *J. Cell Biochem.* **92**, 900-912.

50. Carman, G. M. and Han, G.-S. (2008) Phosphatidic Acid Phosphatase, a Key Enzyme in the Regulation of Lipid Synthesis. *J. Biol. Chem.* **284**: 2593-2597.

51. Carman, G. M. and Han, G.-S. (2006) Roles of Phosphatidate Phosphatase Enzymes in Lipid Metabolism. *Trends Biochem. Sci.* **31**, 694-699.

52. Sciorra, V.A., and Morris, A.J. (2002) Roles for Lipid Phosphate Phosphatase in Regulation of Cellular Signaling. *Biochim Biophys Acta.* **1582**, 45-51.

53. Testerink, C. and Munnik, T. (2005) Phosphatidic Acid: a Multifunctional Stress

Signaling Lipid in Plants. *Trends Plant Sci.* **10**, 368-375.

54. Wang, X., Devaiah, S. P., Zhang, W., and Welti, R. (2006) Signaling Functions of Phosphatidic Acid. *Prog. Lipid Res.* **45**, 250-278.

55. Cai J, Abramovici H, Gee SH, and Topham MK. (2009) Diacylglycerol Kinases as Sources of Phosphatidic Acid. *Biochem Biophys Acta.* **1791**, 942-8.

56. Baron, C. L., and Malhotra, V. (2002) Role of diacylglycerol in PKD recruitment to the TGN and protein transport to the plasma membrane. *Science* **295**, 325–328.

57. Lehel, C., Olah, Z., Jakab, G., Szallasi, Z., Petrovics, G., Harta, G., Blumberg, P. M., and Anderson, W. B. (1995) Protein kinase C epsilon subcellular localization domains and proteolytic degradation sites. A model for protein kinase C conformational changes. *J. Biol. Chem.* **270**, 19651–19658.

58. Maissel, A., Marom, M., Shtutman, M., Shahaf, G., and Livneh, E. (2006) PKCeta is localized in the Golgi, ER and nuclear envelope and translocates to the nuclear envelope upon PMA activation and serum-starvation: C1b domain and the pseudosubstrate containing fragment target PKCeta to the Golgi and the nuclear envelope. *Cell Signal.* **18**, 1127–1139.

59. Wang, Q. J., Bhattacharyya, D., Garfield, S., Nacro, K., Marquez, V. E., and Blumberg, P. M. (1999) Differential localization of protein kinase C delta by phorbol esters and related compounds using a fusion protein with green fluorescent protein. *J. Biol. Chem.* **274**, 37233–37239.

60. Shemesh, T., Luini, A., Malhotra, V., Burger, K. N., and Kozlov, M. M. (2003) Prefission constriction of Golgi tubular carriers driven by local lipid metabolism: a theoretical model. *Biophys. J.* **85**, 3813–3827.

61. Chernomordik, L., Kozlov, M. M., and Zimmerberg, J. (1995) Lipids in biological membrane fusion. *J. Membr. Biol.* **146**, 1–14.

62. Kooijman, E. E., Chupin, V., de Kruijff, B., and Burger, K. N. (2003) Modulation of membrane curvature by phosphatidic acid and lysophosphatidic acid. *Traffic* **4**, 162–174.

63. Kooijman, E. E., Tieleman, D. P., Testerink, C., Munnik, T., Rijkers, D. T., Burger, K.N., and de Kruijff, B. (2007) An electrostatic/hydrogen bond switch as basis for the specific interaction of phosphatidic acid with proteins. *J. Biol. Chem.* **282**, 11356–11364.

64. Carman, G. M. and Henry, S. A. (2007) Phosphatidic Acid Plays a Central Role in the Transcriptional Regulation of Glycerophospholipid Synthesis in *Saccharomyces cerevisiae*. *J.Biol.Chem.* **282**, 37293-37297.

65. Finck, B.N., Gropler, M.C., Chen, Z., Leone, T.C., Croce, M.A., Harris, T.E., Jr. Lawrence, J.C., and Kelly, D.P. (2006) Lipin 1 is an inducible amplifier of the hepatic PGC-1a /PPARa regulator pathway. *cell metab*. **4**, 199 -210.

66. Henry, S. A., Kohlwein, S., and Carman, G. M. (2012). Metabolism and regulation of glycerolipids in the yeast *Saccharomyces cerevisiae*. *Genetics* **190**, 317-349.

67. Bachhawat, N., Ouyang, Q., and Henry, S. A. (1995) Functional Characterization of an Inositol-Sensitive Upstream Activation Sequence in Yeast. *J. Biol. Chem.* **270**, 25807-25095

68. Chi, A., Huttenhower, C., Geer, L. Y., Coon, J. J., Syka, J. E., Bai, D. L., Shabanowitz, J., Burke, D. J., Troyanskaya, O. G., and Hunt, D. F. (2007) Analysis of Phosphorylation Sites on Proteins from *Saccharomyces cerevisiae* by Electron Transfer Dissociation (ETD) Mass Spectrometry. *Proc. Natl. Acad. Sci. USA.* **104**, 2193-2198.

69. Ambroziak, J. and Henry, S. A. (1994) *INO2* and *INO4* Gene Products, Positive Regulators of Phospholipid Biosynthesis in *Saccharomyces cerevisiae*, Form a Complex that Binds to the *INO1* Promoter. *J. Biol. Chem.* **269**, 15344-15349.

70. Nikoloff, D. M. and Henry, S. A. (1994) Functional Characterization of the *INO2* Gene of *Saccharomyces cerevisiae*. A Positive Regulator of Phospholipid Biosynthesis. *J. Biol. Chem.* **269**, 7402-7411

71. Loewen, C. J. R. and Levine, T. P. (2005) A Highly Conserved Binding Site in Vesicle-Associated Membrane Protein-Associated Protein (VAP) for the FFAT Motif of Lipid-Binding Proteins. *J. Biol. Chem.* **280**, 14097-14104.

72. Loewen, C. J. R., Roy, A., and Levine, T. P. (2003) A Conserved ER Targeting Motif in Three Families of Lipid Binding Proteins and in Opi1p Binds VAP. *EMBO J.* **22**, 2025-2035.

73. Loewen, C. J. R., Gaspar, M. L., Jesch, S. A., Delon, C., Ktistakis, N. T., Henry, S. A., and Levine, T. P. (2004) Phospholipid Metabolism Regulated by a Transcription Factor Sensing Phosphatidic Acid. *Science.* **304**, 1644-1647.

74. Homann, M. J., M. A. Poole, P. M. Gaynor, C.-T. Ho, and G. M. Carman. (1987) Effect of Growth Phase on Phospholipid Biosynthesis in *Saccharomyces cerevisiae*. *J. Bacteriol.* **169**: 533-539.

75. Taylor, F. R. and Parks, L. W. (1979) Triacylglycerol Metabolism in *Saccharomyces cerevisiae* Relation to Phospholipid Synthesis. *Biochim. Biophys. Acta* **575**, 204-214.

76. Kelley, M. J., Bailis, A. M., Henry, S. A., and Carman, G. M. (1988) Regulation of Phospholipid Biosynthesis in *Saccharomyces cerevisiae* by Inositol. Inositol is an Inhibitor of Phosphatidylserine Synthase Activity. *J. Biol. Chem.* **263**, 18078-18085.

77. Han, S.-H., Han, G.-S., Iwanyshyn, W. M., and Carman, G. M. (2005) Regulation of the *PIS1*-encoded Phosphatidylinositol Synthase in *Saccharomyces cerevisiae* by Zinc. *J. Biol. Chem.* **280**, 29017-29024

78. Smith, S.W., Weiss, S.B., and Kennedy, E.P. (1957). The enzymatic dephosphorylation of phosphoatidic acids. *J. Biol. Chem.* **228,** 915-92

79. Wu, W.I., Liu, Y., Riedel, B., Wissing, J.B., Fischl, A.S. and Carman, G.M. (1996) Purification and characterization of diacylglycerol pyrophosphate phosphatase from *Saccharomyces cerevisiae*. *J. Biol. Chem.* **271**: 1868-1876.

80. Toke, D. A., Bennett, W. L., Dillon, D. A., Chen, X., Oshiro, J., Ostrander, D. B., Wu, W.-I., Cremesti, A., Voelker, D. R., Fischl, A. S., and Carman, G. M. (1998) Isolation and Characterization of the *Saccharomyces cerevisiae DPP1* Gene Encoding for Diacylglycerol Pyrophosphate Phosphatase. *J. Biol. Chem.* **273**, 3278-3284.

81. Toke, D. A., Bennett, W. L., Oshiro, J., W,-I Wu, Voelker, D. R., and Carman, G. M. (1999) Isolation and Characterization of the *Saccharomyces cerevisiae LPP1* Gene Encoding a Mg^{2+}-Independent Phosphatidate Phosphatase. *J. Biol. Chem.* **273**, 14331-14338.

82. Faulkner, A. J., Chen, X., Rush, J., Horazdovsky, B., Waechter, C. J., Carman, G. M., and Sternweis, P. C. (1999) The *LPP1* and *DPP1* Gene Products Account for Most of the Isoprenoid Phosphatase Activities in *Saccharomyces cerevisiae*. *J. Biol. Chem.* **274**, 14831-14837.

83. Brindley, D.N., English, D., Pilquil, C., Buri, K., Ling, Z.C. (2002) Lipid phosphate phosphatases regulate signal transduction through glycerolipids and sphingolipids. *Biochim Biophys Acta*. **1582**, 33-44.

84. Hosaka, K. and Yamashita, S. (1984) Partial purification and properties of phosphatidate phosphatase in Saccharomyces cerevisiae. *Biochim. Biophys. Acta* **796**, 110-117.

85. Morlock, K. R., McLaughlin, J. J., Lin, Y.-P., and Carman, G. M. (1991) Phosphatidate phosphatase from Saccharomyces cerevisiae. .*J. Biol. Chem.* **266,** 3586 3593

86. Han, G.-S., Wu, W.-I., and Carman, G. M. (2006) The *Saccharomyces cerevisiae* Lipin Homolog is a Mg^{2+}-dependent Phosphatidate Phosphatase Enzyme. *J. Biol. Chem.* **281**, 9210-9218.

87. Irie, K., Takase, M., Araki, H., and Oshima, Y. (1993) A gene, *SMP2*, involved in plasmid maintenance and respiration in *Saccharomyces cerevisiae* encodes a highly charged protein. *Mol.Gen.Genet.* **236,** 283-288.

88. Santos-Rosa, H., Leung, J., Grimsey, N., Peak-Chew, S., and Siniossoglou, S. (2005) The Yeast Lipin Smp2 Couples Phospholipid Biosynthesis to Nuclear Membrane Growth. *EMBO J.* **24**, 1931-1941.

89. Han, G. S., Siniossoglou, S., and Carman, G. M. (2007) The Cellular Functions of the Yeast Lipin Homolog Pah1p are Dependent on its Phosphatidate Phosphatase Activity. *J. Biol. Chem.* **282**, 37026-37035.

90. Adeyo, O., Horn, P.J., Lee, S., Binns, D.D., Chandrahas, A., Chapman, K.D., and Goodman, J.M. (2011) The yeast lipin orthologue Pah1p is important for biogenesis of lipid droplets. *J. Cell Biol.* **192**, 1043–1055.

91. Fei, W., Shui, G., Zhang, Y., Krahmer, N., Ferguson, C., Kapterian, T.S., Lin, R.C., Dawes, I.W., Brown, A.J., Li, P., Huang, X., Parton, R.G., Wenk, M.R., Walther, T.C., Yang, H. (2011) A role for phosphatidic acid in the formation of "supersized" lipid droplets, *PLoS Genet*. **7,** e1002201.

92. Sasser, T., Qiu, Q.S., Karunakaran, S., Padolina, M., Reyes, A., Flood, B., Smith, S., Gonzales, C. and Fratti, R.A. (2011) The yeast lipin 1 orthologue Pah1p regulates vacuole homeostasis and membrane fusion. *J. Biol. Chem.* **287**, 2221–2236.

93. Fakas, S., Qiu, Y., Dixon, J.L., Han, G.S., Ruggles, K.V., Garbarino, J., Sturley, S.L., and Carman, G.M. (2011) Phosphatidate phosphatase activity plays a key role in protection against fatty acid-induced toxicity in yeast. *J. Biol. Chem.* **286**, 29074–29085.

94. Koonin, E. V., and Tatusov, R. L. (1994) Computer Analysis of Bacterial Haloacid Dehalogenases Defines a Large Superfamily of Hydrolases with Diverse Specificity: Application of an Iterative Approach to Database Search. *J. Mol. Biol.* **244**, 125-132.

95. Madera, M., Vogel, C., Kummerfeld, S. K., Chothia, C., and Gough, J. (2004) The SUPERFAMILY Database in 2004: Additions and Improvements. *Nucleic Acids Res.* **32**, D235-D239.

96. Stukey, J. and Carman, G. M. (1997) Identification of a novel phosphatase sequence motif. *Protein Science*. **6**, 469-472.

97. Toke, D. A., McClintick, M. L., and Carman, G. M. (1999) Mutagenesis of the phosphatase sequence motif in diacylglycerol pyrophosphate phosphatase from *Saccharomyces cerevisiae*. *Biochemistry*. **38**, 14606-14613

98. Soto-Cardalda, A., Fakas, S., Pascual, F., Choi, H.S., and Carman, G.M. (2011) Phosphatidate phosphatase plays role in zinc-mediated regulation of phospholipid synthesis in yeast. *J. Biol. Chem.* **287**, 968–977.

99. Vallee, B.L. and Falchuk, K.H. (1993) The biochemical basis of zinc physiology, *Physiol. Rev.* **73**, 79–118.

100. Eide, D.J. (2009) Homeostatic and adaptive responses to zinc deficiency in *Saccharomyces cerevisiae*, *J. Biol. Chem.* **284**, 18565–18569.

101. Schwabe, J.W. and Klug, A. (1994) Zinc mining for protein domains. *Nat. Struct. Biol.* **1**, 345–349.

102. Eide, D.J. (2003) Multiple regulatory mechanisms maintain zinc homeostasis in *Saccharomyces cerevisiae. J. Nutr*. **133**, 1532S–1535S

103. Devirgiliis, C., Murgia, C., Danscher, G., and Perozzi, G. (2004) Exchangeable zinc ions transiently accumulate in a vesicular compartment in the yeast *Saccharomyces cerevisiae*, *Biochem. Biophys. Res. Commun.* **323**, 58–64.

104. Ellis, C.D., MacDiarmid, C.W., and Eide, D.J. (2005) Heteromeric protein complexes mediate zinc transport into the secretory pathway of eukaryotic cells, *J. Biol. Chem.* **280**, 28811–28818.

105. Ellis, C.D., Wang, F., MacDiarmid, C.W., Clark, S., Lyons, T., and Eide, D.J. (2004) Zinc and the Msc2 zinc transporter protein are required for endoplasmic reticulum function. *J. Cell Biol.* **166**, 325–335.

106. MacDiarmid, C.W., Gaither, L.A. and Eide, D. (2000) Zinc transporters that regulate vacuolar zinc storage in *Saccharomyces cerevisiae. EMBO J*. **19**, 2845–2855.

107. MacDiarmid, C.W., Milanick, M.A. and Eide, D.J. (2003) Induction of the ZRC1 metal tolerance gene in zinc-limited yeast confers resistance to zinc shock. *J. Biol. Chem*. **278**, 15065–15072.

108. Miyabe, S., Izawa, S. and Inoue, Y. (2001) The Zrc1 is involved in zinc transport system between vacuole and cytosol in *Saccharomyces cerevisiae*. *Biochem. Biophys. Res. Commun.* **282**,79–83.

109. Muhlenhoff, U., Stadler, J.A., Richhardt, N., Seubert, A., Eickhorst, T., Schweyen, R.J., Lill, R. and Wiesenberger, G. (2003) A specific role of the yeast mitochondrial carriersMRS3/4p in mitochondrial iron acquisition under iron-limiting conditions. *J. Biol. Chem.* **278**, 40612–40620.

110. Waters, B.M. and Eide, D.J. (2002) Combinatorial control of yeast FET4 gene expression by iron, zinc, and oxygen *J. Biol. Chem.* **277**, 33749–33757.

111. Zhao, H. and Eide, D. (1996) The yeast ZRT1 gene encodes the zinc transporter protein of a high-affinity uptake system induced by zinc limitation, *Proc. Natl. Acad. Sci. U. S.A.* **93**, 2454–2458.

112. Zhao, H. and Eide, D. (1996) The ZRT2 gene encodes the low affinity zinc transporter in *Saccharomyces cerevisiae*. *J. Biol. Chem.* **271**, 23203–23210.

113. Han, G.-S., Johnston, C.N., Chen, X., Athenstaedt, K., Daum, G., and Carman, G.M. (2001) Regulation of the Saccharomyces cerevisiae *Dpp1p* diacylglycerol pyro-phosphate phosphatase by zinc. *J. Biol. Chem.* **276**, 10126–10133.

114. Kersting, M.C. and Carman, G.M. (2006) Regulation of the *Saccharomyces cerevisiae EKI1*-encoded ethanolamine kinase by zinc depletion. *J. Biol. Chem.* **281**, 13110–13116.

115. Soto, A. and Carman, G.M. (2008) Regulation of the *Saccharomyces cerevisiae CKI1*-encoded choline kinase by zinc depletion. *J. Biol. Chem.* **283**, 10079–10088.

116. Carman, G. M., Deems, R. A and Dennis, E. A. (1995) Lipid Signaling Enzymes and Surface Dilution Kinetics. *J. Biol. Chem.* **270**, 18711-18714.

117. Lin, Y.-P. and Carman, G. M. 1990. Kinetic Analysis of Yeast Phosphatidate Phosphatase toward Triton X-100/Phosphatidate Mixed Micelles. *J. Biol. Chem.* **265**, 166-170

118. Wu WI, and Carman GM. (1996) Regulation of phosphatidate phosphatase activity from the yeast Saccharomyces cerevisiae by phospholipids. *Biochemistry.* **35**,3790-6.

119. Wu, W.-I., Lin, Y.-P., Wang, E., Merrill, Jr., A. H. and Carman G. M. (1993) Regulation of Phosphatidate Phosphatase Activity from the Yeast *Saccharomyces cerevisiae* by Sphingoid Bases. *J. Biol. Chem.* **268**, 13830-13837.

120. Wu, W.I, and Carman, G.M. (1994) Regulation of phosphatidate phosphatase activity from the yeast *Saccharomyces cerevisiae* by nucleotides. *J. Bio. Chem.* **269**, 29495-29501

121. Ostrander, D. B., O'Brien, D. J., Gorman, J. A., and Carman, G. M. (1998) Effect of CTP Synthetase Regulation by CTP on Phospholipid Synthesis in *Saccharomyces cerevisiae*. *J. Biol. Chem.* **273**, 18992-19001.

122. Burnett, G. and Kennedy, E.P. (1954) The enzymatic phosphorylation of proteins. *J Biol.Chem.* **211,** 969-980.

123. Carman, G. M. and Kersting, M. C. (2004) Phospholipid Synthesis in Yeast: Regulation by Phosphorylation. *Biochem. Cell. Biol.* **82**, 62-70.

124. Karin, M. and Hunter, T. (1995) Transcriptional control by protein phosphorylation: signal transmission from the cell surface to the nucleus. *Curr. Biol.* **5**, 747-57.

125. Komeili, A., and O'Shea, E.K. (1999) Roles of phosphorylation sites in regulating activity of the transcription factor Pho4. *Science.* **284**, 977-80.

126. Xue, Li, Scott, A.G., Adam, D.R., Sean A., A.B., Wilhelm, H., Judit, V., Joshua, E.E. and Steve, P.G. (2007) Large-scale phosphorylation analysis of alpha-factor-arrested Saccharomyces cerevisiae, *J Proteome Res*. **6**, 1190-1197

127. O'Hara, L., Han, G.-S., Peak-Chew, S., Grimsey, N., Carman, G. M. and Siniossoglou, S. (2006) Control of Phospholipid Synthesis by Phosphorylation of the Yeast Lipin Pah1p/Smp2p Mg^{2+}-dependent Phosphatidate Phosphatase. *J. Biol. Chem.* **281**, 34537-34548.

128. Choi, H.-S., Su, W.M., Han, G.S., Plote, D., Xu, Z., and Carman, G.M. (2012) Pho85p–Pho80p phosphorylation of yeast Pah1p phosphatidate phosphatase regulates its activity, location, abundance, and function in lipid metabolism. *J. Biol. Chem.* **287**, 11290–11301

129. Choi, H.S., Su, W.M., Morgan, J.M., Han, G.S., Xu, Z., Karanasios, E., Siniossoglou, S. and Carman, G. M. (2011) Phosphorylation of phosphatidate phosphatase regulates its membrane association and physiological functions in Saccharomyces cerevisiae: identification of SER^{602}, THR^{723}, and SER^{744} as the sites phosphorylated by *CDC28* (*CDK1*)-encoded cyclin-dependent kinase. *J. Biol. Chem.* **286**, 1486-98.

130. Su,W.-M., Han, G.-S., Casciano, J., and Carman, G.M. Protein kinase A-mediated phosphorylation of Pah1p phosphatidate phosphatase functions in conjunction with the Pho85p–Pho80p and Cdc28p-cyclin B kinases to regulate lipid synthesis in yeast, *J. Biol. Chem.* 287 (in press)

131. Phan, J. and Reue, K. (2005) Lipin, a Lipodystrophy and Obesity Gene. *Cell Metab.* **1**, 73-83.

132. Langner, C. A., Birkenmeier, E. H., Roth, K. A., Bronson, R. T. and Gordon, J. L. (1991) Characterization of the Peripheral Neuropathy in Neonatal and Adult Mice that are Homozygous for the Fatty Liver Dystrophy (*fld*) Mutation. *J. Biol. Chem.* **266**, 1955-11964.

133. Peterfy, M., Phan, J., Xu, P. and Reue, K. (2001) Lipodystrophy in the *fld* Mouse Results from Mutation of a New Gene Encoding a Nuclear Protein, Lipin. *Nat. Genet.* **27**, 121-124.

134. Peterfy, M., Phan, J., and Reue, K. (2005) Alternatively Spliced Lipin Isoforms Exhibit Distinct Expression Pattern, Subcellular Localization, and Role in Adipogenesis. *J. Biol. Chem.* **280,** 32883-32889.

135. Langner, C. A., Birkenmeier, E. H., Ben-Zeev, O., Schotz, M. C., Sweet, H. O., Davisson, M. T., Gordon, and J. I. (1989) The Fatty Liver Dystrophy (*fld*) Mutation. A New Mutant Mouse with a Developmental Abnormality in Triglyceride Metabolism and Associated Tissue-Specific Defects in Lipoprotein Lipase and Hepatic Lipase Activities. *J. Biol. Chem.* **264**, 7994-8003.

136. Nadra, K., De Preux Charles, A.-S., Medard, J.-J., Hendriks, W. T., Han, G.-S., Gres, S., Carman, G. M., Saulnier-Blache, J.-S., Verheijen, M. H. G., and Chrast, R. (2008) Phosphatidic Acid Mediates Demyelination in *Lpin1* mutant mice. *Genes Dev.* **22**, 1647-1661.

137. Zeharia, A., Shaag, A., Houtkooper, R. H., de L, T., Hindi, P., Erez, G., Hubert, L., de K, A., Saada, Y., Eshel, G., Vaz, F. M., Pines., O., and Elpeleg, O. (2008) Mutations in *LPIN1* Cause Recurrent Acute Myoglobinuria in Childhood. *Am. J. Hum. Genet.* **83**, 489-494.

138. Grimsey, N., Han, G.-S., O'Hara, M L., Rochford, J. J., Carman, G. M., and Siniossoglou, S. (2008) Temporal and Spatial Regulation of the Phosphatidate Phosphatases Lipin 1 and 2. *J. Biol. Chem.* **283**, 29166-29174.

139. Mammontri, B., Sariahmetoglu, M., Donkor, J., Bou, K. M., Sundaram, M., Yao, Z., Reue, K., Lehner, R., and Brindley, D. N. (2008) Glucocorticoids and Cyclic AMP Selectively Increase Hepatic Lipin-1 Expression, and Insulin Acts Antagonistically. *J. Lipid. Res.* **49**, 1056-1067.

140. Zhang, P., O'Loughlin, L., Brindley, D. N., and Reue, K. (2008) Regulation of Lipin-1 Gene Expression by Glucocorticoids during Adipogenesis. *J. Lipid Res.* **49**, 1519-1528.

141. Huffman TA, Mothe-Satney, I., and JR Lawrence, JC. (2002) Insulin-stimulated phosphorylation of lipin mediated by the mammalian target of rapamycin. *Proc Natl Acad Sci.* **99,** 1047-1052.

142. Harris, T. E., Huffman, T.A., Chi, A., Shabanowitz, J., Hunt, D.F., Kumar, A., and JR.

Lawrence, J.C. (2007) Insulin controls subcellular localization and multisite phosphorylation of the phosphatidic acid phosphatase, lipin 1. *J. Bio. Chem.* **282**, 277-286.

143. Rose, M. D., Winston, F., and Heiter, P. (1990). Methods in Yeast Genetics: A Laboratory Course Manual. (Cold Spring Harbor, N.Y.: Cold Spring Harbor Laboratory Press).

144. Sambrook, J., Fritsch, E. F., and Maniatis, T. (1989). *Molecular Cloning, A Laboratory Manual*. (Cold Spring Harbor, N.Y.: Cold Spring Harbor Laboratory).

145. Ito, H., Yasuki, F., Murata, K., and Kimura, A. (1983). Transformation of intact yeast cells treated with alkali cations. *J. Bacteriol*. **153**, 163-168.

146. Innis, M.A. and Gelfand, D.H. (1990). Optimization of PCRs. In PCR Protocols. A Guide to Methods and Applications, M.A.Innis, D.H.Gelfand, J.J.Sninsky, and T.J.White, eds. (San Diego: Academic Press, Inc.), pp. 3-12.

147. Brachmann,C.B., Davies, A., Cost, G.J., Caputo, E., Li, J., Hieter, P., and Boeke, J.D. (1998). Designer deletion strains derived from *Saccharomyces cerevisiae* S288C: a useful set of strains and plasmids for PCR-mediated gene disruption and other applications. *Yeast* **14**, 115-132.

148. Thomas, B. and Rothstein, R. (1989). Elevated recombination rates in transcriptionally active DNA. *Cell* **56**, 619-630.

149. Hill, J. E., Myers, A. M., Koerner, T. J., and Tzagoloff, A. (1986). Yeast/*E. coli* shuttle vectors with multiple unique restriction sites. *Yeast* **2**, 163-167.

150. Fischl, A. S. and Carman, G. M. (1983). Phosphatidylinositol biosynthesis in *Saccharomyces cerevisiae*: purification and properties of microsome-associated phosphatidylinositol synthase. *J. Bacteriol.* **154**, 304-311.

151. Belendiuk, G., Mangnall, D., Tung, B., Westley, J., and Getz, G. S. (1978). CTP-phosphatidic acid cytidyltransferase from *Saccharomyces cerevisiae*:partial purification, characterization, and kinetic behavior. *J. Biol. Chem.* **253**, 4555-4565.

152. Carman, G.M. and Lin, Y.P. (1991) Phosphatidate phosphatase from yeast. *Methods Enzymol*. **197**, 548-553.

153. Noguchi, K., Kokubu, A., Kitanaka, C., Ichijo, H., and Kuchino, Y. (2001). ASK1-signaling promotes c-Myc protein stability during apoptosis. Biochem. *Biophys. Res. Commun.* **281**, 1313-1320.

154. Robson, R. J. and Dennis, E. A. (1977). The size, shape, and hydration of nonionic surfactant micelles. Triton X-100. *J. Phys. Chem.* **81**, 1075-1078.

155. Lichtenberg, D., Robson, R. J., and Dennis, E. A. (1983). Solubilization of phospholipids by detergents: structural and kinetic aspects. *Biochim. Biophys. Acta.* **737**, 285-304.

156. Bradford, M. M. (1976). A rapid and sensitive method for the quantitation of microgram quantities of protein utilizing the principle of protein-dye binding. *Anal. Biochem.* **72**, 248-254.

157. Laemmli, U. K. (1970) Cleavage of structural proteins during the assembly of the head of bacteriophage T4. *Nature (London)*. **227**, 680-685

158. Burnette, W. (1981). Western blotting: Electrophoretic transfer of proteins from sodium dodecyl sulfate-polyacrylamide gels to unmodified nitrocellulose and radiographic detection with antibody and radioiodinated protein A. *Anal. Biochem.* **112**, 195-203.

159. Haid, A. and Suissa, M. (1983). Immunochemical identification of membrane proteins after sodium dodecyl sulfate-polyacrylamide gel electrophoresis. *Methods Enzymol.* **96**, 192-205.

160. Das, A., Li, H., Liu, T., and Bellofatto, V. (2006). Biochemical characterization of *Trypanosoma brucei* RNA polymerase II. *Mol. Biochem. Parasitol.* **150**, 201-210.

161. Jain, M. R., Li, Q., Liu, T., Rinaggio, J., Ketkar, A., Tournier, V., Madura, K., Elkabes, S., and Li, H. (2012). Proteomic identification of immunoproteasome accumulation in formalin-fixed rodent spinal cords with experimental autoimmune encephalomyelitis. *J. Proteome. Res.* **11**, 1791-1803.

162. Bligh, E. G. and Dyer, W. J. (1959) A rapid method for total lipid extraction and purification. *Can. J. Biochem. Physiol.* **37,** 911-917

163. Esko, J. D. and Raetz, C. R. H. (1980) A Chinese hamster ovary cell (CHO) mutant (strain 58), defective in CDP-choline synthetase (cholinephosphate cytidylyltransferase; CTP:cholinephosphate cytidylyltransferase, EC 2.7.7.15), is temperature sensitive for growth and contains less than half of the normal amount of phosphatidylcholine under nonpermissive conditions. *J. Biol. Chem.* **255,** 4474-4480

164. Henderson, R. J. and Tocher, D. R. (1992) Thin-layer chromatography. In Hamilton, R. J. and Hamilton, S., editors. *Lipid Analysis*, IRL Press, New York

165. Bon, E., Recordon-Navarro, P., Durrens, P., Iwase, M., Toh, E., and Aigle, M. (2000). A network of proteins around Rvs167p and Rvs161p, two proteins related to the yeast actin cytoskeleton. *Yeast* **16**, 1229-1241.

166. Drees, B. L., Sundin, B., Brazeau, E., Caviston, J. P., Chen, G. C., Guo, W., Kozminski, K. G., Lau, M. W., Moskow, J. J., Tong, A., Schenkman, L. R., McKenzie, A., III, Brennwald, P., Longtine, M., Bi ,E., Chan, C., Novick, P., Boone, C., Pringle, J.R., Davis, T.N., Fields, S., and Drubin, D.G. (2001). A protein interaction map for cell polarity development. *J. Cell Biol.* **154**, 549-571.

167. Fazi, B., Cope, M. J., Douangamath, A., Ferracuti, S., Schirwitz, K., Zucconi, A., Drubin, D. G., Wilmanns, M., Cesareni, G., and Castagnoli, L. (2002). Unusual binding properties of the SH3 domain of the yeast actin-binding protein Abp1: structural and functional analysis. *J. Biol. Chem.* **277**, 5290-5298.

168. Ho, Y., Gruhler, A., Heilbut, A., Bader, G. D., Moore, L., Adams, S. L., Millar, A., Taylor, P., Bennett, K., Boutilier, K., Yang, L., Wolting, C., Donaldson, I., Schandorff, S., Shewnarane, J., Vo, M., Taggart, J., Goudreault, M., Muskat, B., Alfarano, C., Dewar, D., Lin, Z., Michalickova, K., Willems, A.R., Sassi, H., Nielsen, P. A., Rasmussen, K. J., Andersen, J. R., Johansen, L. E., Hansen, L. H., Jespersen, H., Podtelejnikov, A., Nielsen, E., Crawford, J., Poulsen, V., Sorensen, B. D., Matthiesen, J., Hendrickson, R. C., Gleeson, F., Pawson, T., Moran, M. F., Durocher, D., Mann, M., Hogue, C. W., Figeys, D., and Tyers, M. (2002). Systematic identification of protein complexes in *Saccharomyces cerevisiae* by mass spectrometry. *Nature* **415**, 180-183.

169. Landgraf, C., Panni, S., Montecchi-Palazzi, L., Castagnoli, L., Schneider-Mergener, J., Volkmer-Engert, R., and Cesareni, G. (2004). Protein interaction networks by proteome peptide scanning. *PLoS. Biol.* **2**, E14.

170. Michelot, A., Costanzo, M., Sarkeshik, A., Boone, C., Yates, J.R., III, and Drubin, D.G. (2010). Reconstitution and protein composition analysis of endocytic actin patches. *Curr. Biol.* **20**, 1890-1899.

171. Tong, A. H., Drees, B., Nardelli, G., Bader, G. D., Brannetti, B., Castagnoli, L., Evangelista, M., Ferracuti, S., Nelson, B., Paoluzi, S., Quondam, M., Zucconi, A., Hogue, C. W., Fields, S., Boone, C., and Cesareni, G. (2002). A combined experimental and computational strategy to define protein interaction networks for peptide recognition modules. *Science* **295**, 321-324.

172. Tonikian, R., Xin, X., Toret, C. P., Gfeller, D., Landgraf, C., Panni, S., Paoluzi, S., Castagnoli, L., Currell, B., Seshagiri, S., Yu, H., Winsor, B., Vidal, M., Gerstein, M. B., Bader, G. D., Volkmer, R., Cesareni, G., Drubin, D. G., Kim, P. M., Sidhu, S. S., and Boone, C. (2009). Bayesian modeling of the yeast SH3 domain interactome predicts spatiotemporal dynamics of endocytosis proteins. *PLoS. Biol.* **7**, e1000218.

173. Yu, H., Braun, P., Yildirim, M.A., Lemmens, I., Venkatesan, K., Sahalie, J., Hirozane-Kishikawa, T., Gebreab, F., Li, N., Simonis, N., Hao, T., Rual, J.F., Dricot, A., Vazquez, A., Murray, R.R., Simon, C., Tardivo, L., Tam, S., Svrzikapa, N., Fan, C., de Smet, A.S., Motyl, A., Hudson, M.E., Park, J., Xin, X., Cusick, M.E., Moore, T., Boone, C., Snyder, M., Roth, F.P., Barabasi, A.L., Tavernier, J., Hill, D.E., and Vidal, M. (2008). High-quality binary protein interaction map of the yeast interactome network. *Science* **322**, 104-110.

174. Dennis, E.A. (1983). Phospholipases. In The enzymes, P.D.Boyer, ed. (New York: Academic Press), pp. 307-353.

175. Carman, G. M. and Han, G.-S. (2011). Regulation of phospholipid synthesis in the yeast *Saccharomyces cerevisiae*. *Ann. Rev. Biochem.* **80**, 859-883.

176. Goni, F. M. and Alonso, A. (1999). Structure and functional properties of diacylglycerols in membranes. *Prog. Lipid Res.* **38**, 1-48.

177. Csaki, L. S. and Reue, K. (2010). Lipins: multifunctional lipid metabolism proteins. *Annu. Rev. Nutr.* **30**, 257-272.

178. Punta, M., Coggill, P. C., Eberhardt, R. Y., Mistry, J., Tate, J., Boursnell, C., Pang, N., Forslund ,K., Ceric, G., Clements, J., Heger, A., Holm, L., Sonnhammer, E. L., Eddy, S. R., Bateman, A., and Finn, R. D. (2012). The Pfam protein families database. *Nucleic Acids Res.* **40**, D290-D301.

179. Mosior, M. and McLaughlin, S. (1992) Binding of basic peptides to acidic lipids in membranes: effects of inserting alanine(s) between the basic residues. Biochemistry **31**,1767-73.

180. Wells, G.B. and Lester, R.L. (1983) The isolation and characterization of a mutant strain of *Saccharomyces cerevisiae* that requires a long chain base for growth and for synthesis of phosphosphingolipids. *J Biol Chem* **258**,10200-3

181. Pinto, W.J., Wells, G.W., and Lester, R.L. (1992) Characterization of enzymatic synthesis of sphingolipid long-chain bases in Saccharomyces cerevisiae: mutant strains exhibiting long-chain-base auxotrophy are deficient in serine palmitoyltransferase activity. *J Bacteriol.* 174, 2575-81.

182. Merrill, A.H. and Jr, Jones, D.D. (1990) An update of the enzymology and regulation of sphingomyelin metabolism. *Biochim Biophys Acta.***1044**, 1-12.

183. Karanasios, E., Han, G.-S., Xu, Z., Carman, G. M., and Siniossoglou, S. (2010). A phosphorylation-regulated amphipathic helix controls the membrane translocation and function of the yeast phosphatidate phosphatase. *Proc. Natl. Acad. Sci. U. S. A.* **107**, 17539-17544.

184. Huh, W .K ., Falvo, J. V., Gerke, L. C., Carroll, A. S., Howson, R. W., Weissman, J. S., and O'Shea, E. K. (2003). Global analysis of protein localization in budding yeast. *Nature* **425**, 686-691.

185. Friesen H, Humphries C, Ho Y, Schub O, Colwill K, Andrews B. **(2005)** Interaction of the Saccharomyces cerevisiae cortical actin patch protein Rvs167p with proteins involved in ER to Golgi vesicle trafficking. *Genetics* **170**, :555-68

186. Weinberg,J. and Drubin,D.G. (2012). Clathrin-mediated endocytosis in budding yeast. Trends Cell Biol. 2*2*, 1-13.

187. Blackwood, R.A., Smolen, J. E., Transue, A., Hessler, R. J., Harsh, D. M., Brower, R. C., and French, S. (1997). Phospholipase D activity facilitates Ca2+-induced aggregation and fu sion of complex liposomes. *Am. J. Physiol* **272**, C1279-C1285.

188. Koter, M., de, K. B., and van Deenen, L. L. (1978). Calcium-induced aggregation and fusion of mixed phosphatidylcholine-phosphatidic acid vesicles as studied by 31P NMR. *Biochim. Biophys. Acta* **514**, 255-263.

189. Liao, M. J. and Prestegard, J. H. (1979). Fusion of phosphatidic acid-phosphatidylcholine mixed lipid vesicles. *Biochim. Biophys. Acta* **550**, 157-173.

190. Weigert, R., Silletta, M. G., Spano, S., Turacchio, G., Cericola, C., Colanzi, A., Senatore, S., Mancini, R., Polishchuk, E.V., Salmona, M., Facchiano, F., Burger, K. N., Mironov,

A., Luini, A., and Corda, D. (1999). CtBP/BARS induces fission of Golgi membranes by acylating lysophosphatidic acid. *Nature* **402**, 429-433.

191. Ren, G., Vajjhala, P., Lee, J. S., Winsor, B., and Munn, A. L. (2006) The BAR domain proteins: molding membranes in fission, fusion, and phagy. *Microbiol. Mol. Biol. Rev.* **70**, 37–120.

192. Sivadon, P., Crouzet, M., and Aigle, M. (1997) Functional assessment of the yeast *Rvs161* and *Rvs167* protein domains. *FEBS Lett*. **417**, 21–27.

193. Dawson J. C., Legg J. A., and Machesky L. M. (2006) Bar domain proteins: a role in tubulation, scission and actin assembly in clathrin-mediated endocytosis. *Trends Cell Biol* **16**, 493–498

194. Bauer, F., Urdaci, M., Aigle, M., and Crouzet, M. (1993) Alteration of a yeast SH3 protein leads to conditional viability with defects in cytoskeletal and budding patterns. *Mol Cell Biol* **13**, 5070–5084.

195. Colwill, K., Field, D., Moore, L., Friesen, J., and Andrews, B. (1999) In vivo analysis of the domains of yeast Rvs167p suggests Rvs167p function is mediated through multiple protein interaction. *Genetics* **152**, 881 893.

196. Brizzio, V., Gammie, A.E., Rose, M.D. (1998) Rvs161p interacts withFus2p to promote cell fusion in *Saccharomyces cerevisiae*. *J Cell Biol* **141**, 567–584.

197. Balguerie, A., Sivadon, P., Bonneu, M., and Aigle, M. (1999) Rvs167p, the budding yeast homolog of amphiphysin, colocalises with actin patches. *J Cell Sci* **112**, 2529–2537.

198. Kaksonen, M., Toret, C. P., and Drubin, D. G. (2005). A modular design for the clathrin- and actin mediated endocytosis machinery. *Cell* **123**, 305–320.

199. Donkor, J., Sariahmetoglu, M., Dewald, J., Brindley, D. N., and Reue, K. (2007) Three Mammalian Lipins Act as Phosphatidate Phosphatases with Distinct Tissue Expression Patterns. *J. Biol.Chem.* **282**, 3450-3457.

200. Han, G.-S. and Carman, G. M. (2010). Characterization of the human *LPIN1*-encoded phosphatidate phosphatase isoforms. *J. Biol. Chem.* **285**, 14628-14638.

VITA

Minjung Chae

Education

2005 B.S., in Food and Nutrition, and Biological Science, Seoul National University, Seoul, Korea

2007 M.S., in Food Science and Technology, Oregon State University, Corvallis, Oregon

2013 Ph.D., in Food Science, Rutgers University, New Brunswick, New Jersey

Publication

Chae, M. and Su, Y. C. (2009) Temperature effects on the depuration of *Vibrio parahaemolyticus* and *Vibrio vulnificus* from the American oyster (*Crassostrea virginica*). *J Food Sci.* 74:M62-M66

Chae, M., Han, G.S., and Carman, G.M. (2012) The *Saccharomyces cerevisiae* Actin Patch Protein App1p is a Phosphatidate Phosphatase Enzyme, *J Bio Chem.* (Accepted)

Chae, M. and Carman, G.M. Characterization of App1p PAP in *Saccharomyces cerevisiae*. (In Preparation)